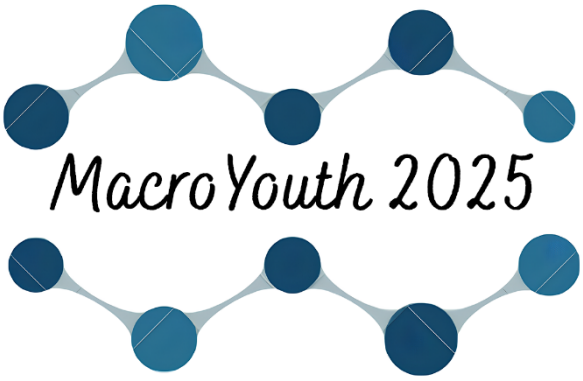

OPEN DOOR TO THE FUTURE SCIENTIFIC COMMUNICATIONS OF YOUNG RESEARCHERS

6th Edition

Marking the Romanian Researcher's Day

Dedicated to the 105th anniversary of
Acad. Cristofor I. Simionescu (1920-2007)

Program & Book of Abstracts

ICMPP – Petru Poni Institute of Macromolecular Chemistry
Iasi | Romania | November 19, 2025
https://icmpp.ro/macroyouth2025

Edited by

Marcela MIHAI
Marius-Mihai ZAHARIA
Bianca-Iustina ANDREICA

Cover by

Diana SCHWAB

Welcome to the

OPEN DOOR TO THE FUTURE

Scientific Communications of Young Researchers with international participation,

MacroYouth 2025

It is a great pleasure to welcome you in Iasi, on 19.11.2025, on the occasion of the 6th Edition OPEN DOOR TO THE FUTURE Scientific Communications of Young Researchers with international participation, MacroYouth 2025. The scientific communications event with international participation is organized by the Doctoral School of Chemical Sciences of the School of Advanced Studies of Romanian Academy, through Petru Poni Institute of Macromolecular Chemistry - ICMPP, and the Romanian Chemical Society, with to mark the Romanian Researcher's Day, and offers the opportunity for the doctoral students and young scientists (maximum 3 years from thesis defense) to present the results of their studies. The scientific program includes various topics in organic and macromolecular chemistry and physics.

Best wishes for a professionally rewarding scientific meeting!

Dr. Valeria HARABAGIU and Dr. Marcela MIHAI

Chairpersons of MacroYouth 2025

CHAIRPERSONS of MacroYouth 2025

Dr. Valeria HARABAGIU and Dr. Marcela MIHAI

ROMANIAN SCIENTIFIC BOARD

- Acad. Maria ZAHARESCU (Romanian Academy)
- Acad. Marius ANDRUH (Romanian Academy, ICOS Bucharest)
- Dr. Maria CAZACU (ICMPP Iasi)
- Dr. Liliana CSEH (ICHT Timisoara)
- Dr. Sergiu COSERI (ICMPP Iasi)
- Dr. Mariana Dana DAMACEANU (ICMPP Iasi)
- Dr. Gheorghe FUNDUEANU (ICMPP Iasi)
- Dr. Gabriela IONITA (ICF Bucharest)
- Dr. Luminita MARIN (ICMPP Iasi)
- Dr. Mariana PINTEALA (ICMPP Iasi)

ORGANIZING BOARD

Program

- Dr. Petrisor SAMOILA
- Dr. Florin BUCATARIU
- Dr. Corneliu COJOCARU

Editorial

- Dr. Marius-Mihai ZAHARIA
- Dr. Bianca-Iustina ANDREICA

Executive

- Dr. Narcisa Laura MARANGOCI
- Dr. Florica DOROFTEI
- Dr. Daniela PAMFIL
- Dr. Bogdan-Constantin CONDURACHE
- Dr. Dumitru POPOVICI
- Catalin BUZDUGAN – IT support

CONTENT

POSTERS

PROGRAM

ICMPP Conference Hall

https://us06web.zoom.us/j/83698688230

08^{30} – 09^{00}	**Registration of Participants**

09^{00} – 10^{45}
Session 1
Chairs: Dr. Adina COROABA and Codrin TUGUI

09^{00}– 09^{15}	**Opening Ceremony** Dr. Valeria HARABAGIU and Dr. Marcela MIHAI *Petru Poni Institute of Macromolecular Chemistry, Iasi, Romanian Academy, Romania*
09^{15}– 09^{45}	**CL1. Modern aspects of polymer melt rheology** Paul LAZAR *Laboratorium SRL Bucharest, Romania*
09^{45}– 10^{00}	**OC1. New multi-stimuli responsive hydrogels** Adina FERARIU*, Irina POPESCU, Sanda BUCATARIU, Marieta CONSTANTIN, Gheorghe FUNDUEANU *Petru Poni Institute of Macromolecular Chemistry, Romanian Academy, Iasi, Romania*
10^{00}– 10^{15}	**OC2. Radiation-mediated synthesis of silver nanoparticles in silica-based drug delivery systems with antimicrobial properties** Andreea-Simona BALTAC[1,2*], Irina ATKINSON[1], Daniela CULITA[1], Simona IONITA[1], Andreea Elena SERBAN[2], Paul MEREUTA[2], Daniel NEGUT[2], Mioara ALEXANDRU[2], Raul Augustin MITRAN[1] [1]*"Ilie Murgulescu" Institute of Physical Chemistry, Romanian Academy, Bucharest, Romania* [2]*"Horia Hulubei" National Institute of Physics and Nuclear Engineering, Romanian Academy, Magurele, Romania*
10^{15}– 10^{30}	**OC3. Cinnamon oil and cinnamaldehyde: mic testing for applications in bovine endometritis** Paula LORENT (CUCU)[1,2]*, Mihai MARES[1], Iuliana SPIRIDON[2] [1]*Faculty of Veterinary Medicine, "Ion Ionescu de la Brad" University of Life Sciences, Iasi, Romania* [2]*Petru Poni Institute of Macromolecular Chemistry, Romanian Academy, Iasi, Romania*
10^{30}– 10^{45}	**OC4. Heat transfer analysis inside a supercritical water reactor for process optimization of metal oxide synthesis** Mihail-Calin LICU*, Florentina MAXIM, Speranta TANASESCU *Institute of Physical Chemistry-Ilie Murgulescu, Romanian Academy, Bucharest, Romania*
10^{45}– 11^{15}	**Coffee break & POSTER SESSION**

11^{15} – 13^{15}

Session 2

Chairs: Dr. Bianca ANDREICA and Andrei DASCALU

11^{15}– 11^{30}	**OC5. Unveiling the role or urocanic acid in the formation of skin cancer**
	Petru TIRNOVAN[1]*, Dragos Lucian ISAC[1], Mihaela SILION[1], Adina COROABA[1], Aatto LAAKSONEN[1], Mariana PINTEALA[1] [1]*Petru Poni Institute of Macromolecular Chemistry, Romanian Academy, Iasi, Romania* [2]*Division of Physical Chemistry, Department of Materials and Environmental Chemistry, Arrhenius Laboratory, Stockholm University, Stockholm, Sweden*
11^{30}– 11^{45}	**OC6. Metabolomic biomarkers in phenylketonuria (PKU)**
	Dan-Cristian USURELU[1,2]*, Chiril BOICIUC[2], Daniela BLANITA[2], Ecaterina PAVLOVSCHI[1], Natalia USURELU[2], Alina NICOLESCU[3], Calin DELEANU[3] [1]*IMSP Institute of Mother and Child, Chisinau, Republic of Moldova* [2] *Departmen of Biochemistry and Clinical Biochemistry Chisinau, USMF "Nicolae Testemițanu", Republic of Moldova* [3]*Petru Poni Institute of Macromolecular Chemistry, Romanian Academy, Iasi, Romania*
11^{45}– 12^{00}	**OC7. Functionalized starch flocculant for the recovery of water produced by petroleum industry**
	Melinda-Maria BAZARGHIDEANU[1]*, Paulo Cristiano SILVA da ROCHA[2], Letícia DIAS da SILVA[2], Rita de Cassia PESSANHA NUNES[2], Diana-Felicia LOGHIN[1], Marcela MIHAI[1], Elizabete FERNANDES LUCAS[2,3] [1]*Petru Poni Institute of Macromolecular Chemistry, Romanian Academy, Iasi, Romania* [2]*Universidade Federal do Rio de Janeiro, Instituto de Macromoléculas/LMCP, Rio de Janeiro, Brazil* [3]*Universidade Federal do Rio de Janeiro, Programa de Engenharia Metalúrgica e de Materiais/COPPE/LADPOL, Rio de Janeiro, Brazil*
12^{00}– 12^{15}	**OC8. New Schiff base ligands for 3*d*, 3*d*-4*f*, 4*f*, and 4*f*-4*f* ' complexes**
	Diana-Ioana EFTEMIE[1,2]*, Teodora MOCANU[3], Sergiu SHOVA[4], Diana DRAGANCEA[2], Mihai RĂDUCA[1,2], Marius ANDRUH[1,2] [1] *Faculty of Chemistry, Department of Inorganic Chemistry, Organic Chemistry, Biochemistry and Catalysis, University of Bucharest, Bucharest, Romania* [2]*"C. D. Nenitzescu" Institute of Organic and Supramolecular Chemistry, Romanian Academy, Bucharest, Romania* [3]*Petru Poni Institute of Macromolecular Chemistry, Romanian Academy, Iasi, Romania*
12^{15}– 12^{45}	**CL2. Shape of Flavor: Tea Leaf Characterization Using Dynamic Image Analysis**
	Miklós ATTILA *Anton Paar GmbH*
12^{45}– 13^{15}	**ED. Equipment demonstration**
	Miklós ATTILA *Anton Paar GmbH*
13^{15}– 14^{30}	**Lunch break - ICMPP Library**

14^{30} – 16^{30}
Session 3
Chairs: Dr. Cristina STANCIU and Dr. Alexandru ANISIEI

14^{30}– 14^{45}	**OC9. Targeted removal of phenolic pollutants from water using metal-organic frameworks impregnated with ionic liquids**
	Marcela IOSIVONI[1]*, Nicoleta PLESU[1], Bianca MARANESCU[2], Lavinia LUPA[3], Aurelia VISA[1] *[1]"Coriolan Dragulescu" Institute of Chemistry, Romanian Academy, Timisoara, Romania* *[2]Faculty of Chemistry, Biology, Geography, West University of Timisoara, Timisoara, Romania* *[3]Faculty of Industrial Chemistry and Environmental Engineering, Politehnica University, Timisoara, Romania*
14^{45}– 15^{00}	**OC10. Guar/gelatin matrix as platform for *Vaccinium Vittis- Idaea* extract release**
	Irina APOSTOL*, Narcis ANGHEL, Iuliana SPIRIDON *Petru Poni Institute of Macromolecular Chemistry, Romanian Academy, Iasi, Romania*
15^{00}– 15^{15}	**OC11. Polymer/Sand composites with fast sorption toward soluble organic pollutants**
	Timeea-Anastasia CIOBANU*, Florin BUCATARIU, Larisa-Maria PETRILA, Marius-Mihai ZAHARIA, Marcela MIHAI *Petru Poni Institute of Macromolecular Chemistry, Romanian Academy, Iasi, Romania*
15^{15}– 15^{30}	**OC12. Host–guest interactions between functionalized nitroxide radicals with β- and γ-cyclodextrins studied by EPR spectroscopy**
	Muhammed ALKALI[1]*, Alexandru Gabriel BUCUR[1], Jean-Patrick JOLY[2], Gabriela IONITA[1] *[1]Institute of Physical Chemistry – Ilie Murgulescu, Romanian Academy, Bucharest, Romania.* *[2]Aix Marseille University, ICR (UMR 7273), Marseille, France.*
15^{30}– 15^{45}	**OC13. Tunable substituted imidazolium and benzimidazolium precursors for ionic liquid design**
	Rares-Georgian MOCANU*, Alina NICOLESCU, Sergiu SHOVA, Irina ROSCA, Narcisa MARANGOCI, Mariana PINTEALA, Dana BEJAN *Petru Poni Institute of Macromolecular Chemistry, Romanian Academy, Iasi, Romania*
15^{45}– 16^{00}	**OC14. Electrochemical methods for studying the host-guest interaction of cyclodextrins with nitronyl-nitroxide radicals derivatives**
	Andreea Iuliana FTODIEV[1,2]*, Mihai Marian RADU[1], Loredana PREDA[1], Alexandru Vincentiu Florian NECULAE[1], Alexandru Gabriel BUCUR[1,2], Gabriela IONITA[1] *[1]''Ilie Murgulescu'' Institute of Physical Chemistry, Romanian Academy, Bucharest, Romania* *[2]Department of Analytical Chemistry and Physical Chemistry, Faculty of Chemistry, University of Bucharest, Romania*

16^{00}– 16^{15}	**OC15. Sensitive coatings based on *ortho*-phenanthroline polymer for detection of 2-methyl-1-butanol vapours** Maria-Daniela SECMAN*, Loredana VACAREANU, Mariana-Dana DAMACEANU *Petru Poni Institute of Macromolecular Chemistry, Romanian Academy, Iasi, Romania*
16^{15}– 16^{30}	**OC16. Synthesis of 1,2,3-triazole-1,4-disubstituted derivatives *via* Cu(I)-catalyzed huisgen azide-alkyne cycloaddition** Camelia-Georgiana MARANDIS[1,2,*], Dorina AMARIUCAI-MANTU[1], Vasilichia ANTOCI[1], Catalina-Ionica CIOBANU[3], Ionel I. MANGALAGIU[1], Marcela MIHAI[2] [1] *Faculty of Chemistry, "Alexandru Ioan Cuza" University of Iasi, Iasi, Romania* [2]*Petru Poni Institute of Macromolecular Chemistry, Romanian Academy, Iasi, Romania* [3]*ICI-CERNESIM, "Alexandru Ioan Cuza" University of Iasi, Iasi, Romania*
16^{30}– 17^{00}	**Coffee break & POSTER SESSION**
	17^{00} – 18^{15} **Session 1** Chairs: Dr. Marcela MIHAI
17^{00}– 17^{45}	**INVITED LECTURE** **Immobilized enzymes for agro-resources valorization** Prof. Rénato FROIDEVAUX *Lille University, France*
17^{45}– 18^{15}	**AWARDING AND CLOSING CEREMONY**
18^{15}– 20^{00}	**Dinner – ICMPP Library**

IL – Invited lecture, **CL** – Course lecture, **OC** – Oral communication, **ED** – Equipment demonstration

POSTERS LIST

Chairs: Dr. Daniela PAMFIL and Dr. Bogdan-Constantin CONDURACHE

PP1 **PHENANTHRIDINIUM MONOQUATERNARY SALTS: SYNTHESIS, STRUCTURAL INSIGHTS, AND ANTIMICROBIAL ACTIVITY**
Ashraf AL-MATARNEH[1,2]*, Florentina Gabriela LAZAR[2], Irina ROSCA[2], Alina NICOLESCU[2], Cristina Maria AL-MATARNEH[2], Ionel I. MANGALAGIU[1]
[1]Faculty of Chemistry, "Alexandru Ioan Cuza" University of Iasi, Iasi, Romania
[2]Petru Poni Institute of Macromolecular Chemistry, Romanian Academy, Iasi, Romania

PP2 **FLUOROSULFONYL-FUNCTIONALIZED NITROGEN HETEROCYCLES: SYNTHESIS AND CHARACTERIZATION**
Florentina-Gabriela LAZAR*, Cristina AL-MATARNEH, Mariana PINTEALA
Petru Poni Institute of Macromolecular Chemistry, Romanian Academy, Iasi, Romania

PP3 **DEEP LEARNING-BASED COMPUTER VISION SYSTEM FOR INTELLIGENT PLASTIC WASTE SORTING IN THE CIRCULAR ECONOMY**
Madalina-Maria ENACHE*, Carmen TEODOSIU
"Cristofor Simionescu" Faculty of Chemical Engineering and Environmental Protection, "Gheorghe Asachi" Technical University of Iasi, Iasi, Romania

PP4 **CHARACTERIZATION OF WATER RETENTION PVA/CASEIN/LIGNIN NANOPARTILESC HYDROGELS FOR SUSTAINABLE AGRICULTURE**
Cosmina-Maria BOGZA*, Maria-Cristina POPESCU, Carmen-Mihaela POPESCU
Petru Poni Institute of Macromolecular Chemistry, Romanian Academy, Iasi, Romania

PP5 **HETEROSTRUCTURES OF METAL NANOPARTICLES AND LAYERED DOUBLE HYDROXIDES AS ACTIVE SOLAR RESPONSIVE CATALYSTS FOR POLLUTANTS REMOVAL**
Oleg TIHON*, Sofronia BOUARIU, Gabriela CARJA
"Cristofor Simionescu" Faculty of Chemical Engineering and Environmental Protection, "Gheorghe Asachi" Technical University of Iasi, Iasi, Romania

PP6 **POLYMERIC MICROPARTICLES FOR CONTROLLED RELEASE OF NORFLOXACIN: PREPARATION AND EVALUATION**
Alexandru-Mihail SERBAN*, Alexandra VIERU, Irina ROSCA, Alina-Gabriela RUSU, Loredana Elena NITA
Petru Poni Institute of Macromolecular Chemistry, Romanian Academy, Iasi, Romania

PP7 **SYNTHESIS OF NITRONYL-NITROXIDE HALOGENATED DERIVATIVES AND COMPLEXATION WITH CYCLODEXTRINS**
Mihaela-Lavinia CIUTU*, Alexandru Vincentiu Florian NECULAE, Carla-Cezarina PADURETU, Alexandru Gabriel BUCUR, Georgiana-Alexandra SANDA, Elena-Gabriela IONITA
Institute of Physical Chemistry - Ilie Murgulescu, Romanian Academy, Bucharest, Romania

PP8 **NEW SYNTHETIC ROUTE TO HETERICYCLIC SCHIFF BASES AS PRECURSORS FOR BIOACTIVE CU(II) COMPLEXES**
Alexandra BIRZU*, Mihaela DASCALU, Gheorghe ROMAN, Vladimir ARION, Maria CAZACU
Petru Poni Institute of Macromolecular Chemistry, Romanian Academy, Iasi, Romania

PP9 **FUNCTIONALIZED INDOLIZINES AS POTENTIAL ANTICANCER AGENTS**

Roxana CIORTEANU[1,2*], Catalina CIOBANU[3], Ionel I. MANGALAGIU[2], Ramona DANAC[2]

[1"]ICI - RECENT AIR Center, "Alexandru Ioan Cuza" University of Iasi, Iasi, Romania
[2]Faculty of Chemistry, "Alexandru Ioan Cuza" University of Iasi, Iasi, Romania
[3]Institute of Interdisciplinary Research - CERNESIM Centre, "Alexandru Ioan Cuza" University of Iasi, Iasi, Romania

PP10 **SORPTION OF NATURAL POLYSACCHARIDES ON ION EXCHANGE RESINS**

Alina-Petronela MORARU*, Marius-Mihai ZAHARIA, Florin BUCATARIU, Marcela MIHAI

Petru Poni Institute of Macromolecular Chemistry, Romanian Academy, Iasi, Romania

PP11 **HOST-GUEST INTERACTIONS IN CYCLODEXTRIN-GRAFTED POLYACRYLATES**

Georgiana- Alexandra SANDA[1,2]*, Ludmila ARICOV[1], Mihaela- Lavinia CIUTU[1], Gabriela IONITA

[1]Institute of Physical Chemistry – Ilie Murgulescu, Romanian Academy, Bucharest, Romania
[2] Faculty of Chemistry, University of Bucharest, Bucharest, Romania

PP12 **MISCIBILITY STUDY OF HYDROXYPROPYL CELLULOSE AND POLY(N-VINYLPYRROLIDONE) MIXTURES IN DILUTE SOLUTION**

Alexandra LUPU*, Ioana-Alexandra PLUGARIU, Luiza Madalina GRADINARU, Maria BERCEA

Petru Poni Institute of Macromolecular Chemistry, Romanian Academy, Iasi, Romania

PP13 **FATE OF PET MICROPLASTICS IN SOIL AND THEIR IMPACT ON SOIL PROPERTIES**

Eliška KAMENÍKOVÁ[1]*, Adéla HRUŠKOVÁ[1], Martin BRTNICKÝ[2], Lucie ŠUDOMOVÁ[3], Jiří KUČERÍK[2]

[1]Institute of Chemistry and Technology of Environmental Protection, Faculty of Chemistry, Brno University of Technology, Brno, Czech Republic
[2] Department of Agrochemistry, Soil Science, Microbiology and Plant Nutrition, Mendel University in Brno, Czech Republic

PP14 **HOW DOES MICROFLUIDICS ENABLE THE PRECISE AND REPRODUCIBLE FORMATION OF LIPOSOMES?**

Razvan GHIARASIM

Petru Poni Institute of Macromolecular Chemistry, Romanian Academy, Iasi, Romania

PP15 **OPTICAL AND STRUCTURAL CHARACTERIZATION OF Fe_3O_4 AEROMATERIAL**

Catalin CRECIUNEL[1,]*, Tatiana GALATONOVA[1], Vadim MORARI[2], Florica DOROFTEI[3], Andrei DASCALU[3], Laura URSU[3], Vladimir CIOBANU[1]

[1]National Center for Materials Study and Testing, Technical University of Moldova, Chisinau, Republic of Moldova
[2]Institute of Electronic Engineering and Nanotechnologies "D. Ghitu", Technical University of Moldova, Chisinau, Republic of Moldova
[3]Petru Poni Institute of Macromolecular Chemistry, Romanian Academy, Iasi, Romania

PP16 **TAILORING PULLULAN REACTIVITY THROUGH MULTI-ROUTE OXIDATION APPROACHES**

Ioana-Sabina TRIFAN*, Raluca Ioana BARON, Gabriela BILIUTA, Gabriela Liliana AILIESEI, Sergiu COSERI

Petru Poni Institute of Macromolecular Chemistry, Romanian Academy, Iasi, Romania

PP17 **NOVEL PHTHALAZINO-ACETOPHENONE HYBRIDS: DESIGN, SYNTHESIS, AND STRUCTURAL CHARACTERIZATION**

Marius SAVU[1], Vasilichia ANTOCI[1], Dorina AMARIUCAI-MANTU[1], Ramona DANAC[1], Dumitrela DIACONU[1,2], Catalina CIOBANU[3], Ionel I. MANGALAGIU[1,3]

[1]Faculty of Chemistry,"Alexandru Ioan Cuza" University of Iasi, Iasi, Romania

[2]RECENT AIR Center,"Alexandru Ioan Cuza" University of Iasi, Iasi, Romania

[3]Institute of Interdisciplinary Research- CERNESIM, "Alexandru Ioan Cuza" University of Iasi, Iasi, Romania

PP18 **MODIFIED POLYHEDRAL OLIGOMERIC SILSESQUIOXANE: SYNTHESIS, CHARACTERIZATION AND POSSIBLE APPLICATIONS**

Maria MEDRIHAN[1]*, Bogdan-Constantin CONDURACHE[1], Maria IGNAT[1,2], Valeria HARABAGIU[1]

[1]Petru Poni" Institute of Macromolecular Chemistry, Romanian Academy, Iasi, Romania

[2] Faculty of Chemistry, "Alexandru Ioan Cuza University of Iasi", Iasi, Romania

PP19 **PREPARATION OF DEXTRAN–GUANOSINE–GOLD HYBRID MAGNETIC NANOPARTICLES AS SUBSTRATES FOR SURFACE-ENHANCED RAMAN SCATTERING**

Tecla DULGHERIU*, Laura URSU, Razvan GHIARASIM, Alexandru ROTARU, Mariana PINTEALA

Petru Poni Institute of Macromolecular Chemistry, Romanian Academy, Iasi, Romania

Invited lectures

INVITED LECTURE

Prof. Rénato FROIDEVAUX is full professor of biocatalysis at Lille University in France. He

is heading the team « Biotransformation, biocatalysis and enzyme » in the BioEcoAgro Joint Cross-Border Research Unit. His research concerns enzymatic biocatalysis (homogeneous and heterogeneous) applied to hydrolysis of agro-food proteins for obtaining bioactive peptides, enzymatic biocatalysis applied to the valorization of lignin for obtaining biobased aromatics. More recently, he developed the concept of "hybrid catalysis" which consists of combining chemical catalysis and enzymatic biocatalysis for biomass valorization. This interdisciplinary concept involves the search for new enzymes, the search for compatible reaction conditions between (bio)catalysts and the development of different types of reactors (one-pot one step, two-pots one-step) and Multi Catalytic Hybrid Materials (also called MMCH) for heterogeneous (bio)catalysis. Author and co-author of more than 50 articles mostly in JCR, 3 book chapters and 3 patents. Total citations almost 800 (WoS), H Index 16. He is a project leader and participant of more than 15 national and international research projects. He is responsible of an Industrial Chair called « Charles Viollette », financed by the European Metropole of Lille and the University of Lille. This chair brings together academic partners from Lille and Canada (INAF in Quebec) and industrial partners in the development of co-products from the agricultural and agro-food industries by biotechnological tools for the production of bioactive molecules for animal, human nutrition and plant health. He was a lecturer in enzyme biocatalysis from 2004 to 2009 in the Franco-Romanian Master's "Bioprocesses in the Agrifood field" between Al. I. Cuza University of Iasi and Lille University, then director of this master's until 2013. Currently, he works with the Technical University Gheorghe Asachi of Iasi (Dr Alexandra BLAGA) for the implementation of a double master ‘degree in (bio)chemical engineering.

IL. IMMOBILZED ENZYMES FOR AGRO-RESOURCES VALORIZATION

Rénato Froidevaux[1]*, Cédric Decarpigny[1], Muriel Bigan[1], Nicolas Chaussard[2], Clémence Nikitine[2], David Rouzineau[3], Michel Meyer[3], Pascal Fongarland[2]

[1]UMRT BioEcoAgro 1158, Equipe Biotransformation/Enzymes et Biocatalyse, Univ. Lille, INRAE, Univ. Liège, UPJV, JUNIA, Univ. Artois, Univ. Littoral Côte d'Opale, ICV – Institut Charles Viollette, F-59000 Lille, France

[2]CP2M, UMR 5128, Université Claude Bernard Lyon 1, CNRS, CPE Lyon, Villeurbanne, France

[3]LGC, UMR 5503 Université de Toulouse, CNRS, INPT, UPS, Toulouse, France

**renato.froidevaux@univ-lille.fr*

Introduction. The current context of enzyme immobilization is marked by rapid innovation and interdisciplinary convergence, driven by the need for more robust, sustainable, and efficient biocatalytic processes. The key trends and advances are the development of novel carrier materials (covalent organic frameworks, nanoparticles...), advanced immobilization approaches such as carrier-free methods (CLEAs) and entrapment methods, sustainable immobilization using renewable materials, the enhancement of process efficiency and enzyme stability. In summary, enzyme immobilization is evolving from a niche technique to a mainstream, transformative tool in biocatalysis, with a strong emphasis on sustainability, precision, and industrial scalability. Among all enzymes, lipases are known to be very effective in transesterification reactions, and tends to be more stable by being immobilized by entrapment over adsorbed lipases, and avoids deactivation from covalent binding.[1] Besides, lipases have the ability to esterify free fatty acids (FFA) to biodiesel. Several lipases may be applied in transesterification of oils into biodiesel, and some show the best catalytic activity, like *Thermomyces lanuginosus* [2-4] or *Candida antarctica* [5-7].

My presentation will focus on general informations about enzyme immobilization, the principal methods of immobilization and their main advantages/disadvantages. I will also present examples developed in UMRtBioEcoAgro concerning enzyme immobilization approaches for agro-resources valorization with lipases. In this work, lipase from *Candida antarctica* (CALB) was used to transform triglyceride substrates into biodiesel, virgin oil, and waste cooking oil (WCO), WCO having a higher quantity of impurities. Entrapment technique is applied to immobilize the lipase, and a xerogel is prepared by polycondensation of a combination of tetramethyl orthosilicate (TMOS) and trimethoxymethylsilane (MTMS). The focus was on the composition of the xerogel to optimize gel quality and give CALB the best environment to maintain its stability and activity, the parameters of the reaction for biodiesel production will not be studied. Another important part of this work was to synthetize biocatalyst that can be reused for several cycles [8,9].

Experimental. Xerogel was developed by the combination of TMOS and MTMS for polycondensation in sol-gel reaction. Then the second step consisted to water hydrolysis in sol-gel reaction, in presence of ammonia as catalyst of the reaction, and PEG 400 as an additive, then, CALB was added. After sol-gel reaction with lipase, nearly 5 g of xerogel with immobilized CalB were obtained. For transesterification of oils, sunflower virgin oil or WCO, 2 mL of oil was placed in a flask, and heated at 40°C, 1 g of immobilized CALB was added followed by ethanol at a ratio of 36:1 per gram of oil. The reaction took place for 48 hours and was stirred magnetically at 300 RPM. To recover the CALB, the mixture was centrifuged at 13,400 RPM for 5 minutes. The separation gave three phases: the aqueous phase containing the ethanol and glycerol, the organic phase containing the fatty acid ethyl esters (FAEE), the FFA, and glycerides, and the bottom phase, the immobilized enzyme. The liquid phases were separated from the solid immobilized enzyme, and the lipase was reused with no further treatment for another run in the same flask. Two milliliters of new oil were added, and the reaction took place in the same conditions as the first run. The same steps were reproduced for every run.

Results and discussion. This method allows the immobilization of the CALB by entrapment into the silica gel network. Two stock solutions are prepared, one organic (solution A), containing the silica precursors, and one aqueous (solution B), with the catalyst and the CALB immobilized (**Table 1**).

Table 1. Initial composition of the xerogel.

	Component	Concentration
Solution A	Methanol	41.0% (v/v)
	Tetramethyl orthosilicate (TMOS)	7.5% (v/v)
	Trimethoxymethylsilane (MTMS)	28.9% (v/v)
Solution B	Water	15.5% (v/v)
	CALB	5.9% (w/v)
	Ammonia	0.4% (v/v)
	PEG 400	0.8% (w/v)

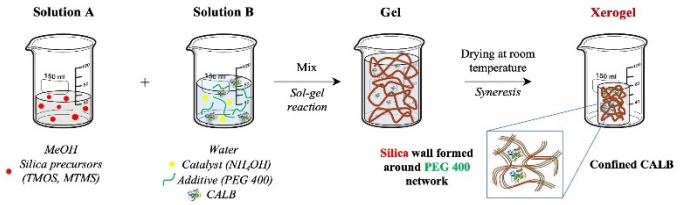

Scheme 1. Schematic illustration of the preparation procedure of the confinement of lipase CALB into the xerogel.

As the TMOS/MTMS ratios increases, gelation times do not vary at first for the three catalysts, as the gels remains cloudy and heterogeneous. Then, for a ratio around 0.70, the gelation times decreases suddenly, reaching less than 10 minutes of gel formation. As the times decreases, the gels become clearer and homogeneous, giving better-quality gels, as shown in **Figure 1**, for instance, with ammonia catalyst. Those observations tend to favor a higher TMOS/MTMS ratio for improving the gel quality and the gelation time.

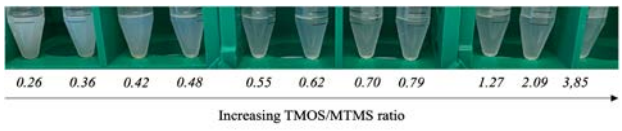

Figure 1. Gels quality with ammonia catalyst depending on

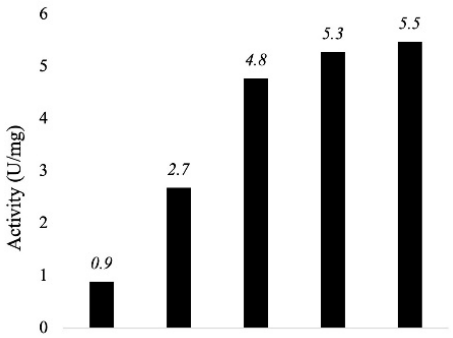

Figure 2. Activity of immobilized CALB depending on its amount

Activity measurements were then made and exposed in **Figure 2.** As expected, the activity grows with the increasing of the amount of CALB incorporated into the xerogel, the major observation is a slowdown of the activity from an amount of CALB of 0.3% (w/v) at 5.3 U/mg, for an amount of 0.4% (w/v). The activity does not evolve much, to reach a value of 5.5 U/mg. A saturation of the xerogel is reached from an amount of CALB of 0.3% (w/v), decision has been taken to choose an amount of CALB of 0.3% (w/v) and not 0.4% (w/v), because from this value, the xerogel quality starts to decrease.

Figure 3 shows results of the different tests made. First observation is the difference of efficiency between the free and immobilized CALB, the entrapment of the CALB allow a protection of the enzyme and gives better yield to reach 45.9 and 46.1% with sunflower oil and WCO respectively, whereas the yield of biodiesel with free CALB reaches 29.7 and 15.1% with sunflower oil and WCO respectively. These results also show the influence of the oil and the type of oil on the lipase as proved by the difference in yields between sunflower oil and WCO, biodiesel yield with WCO decreases by half, because of high level of impurities in WCO like soap, water, ashes. Clearly, immobilized CALB does not show any influence of the oil or type of oil. **Figure 3b** proved that entrapped CALB in xerogel can be reused for five full runs, the slight decreases of the yield can be explained by very small loss of catalyst during the recovery method. Although no washing step is applied to the catalyst between each run, the xerogel also protect the CALB from glycerine, which can have an inhibitive effect.

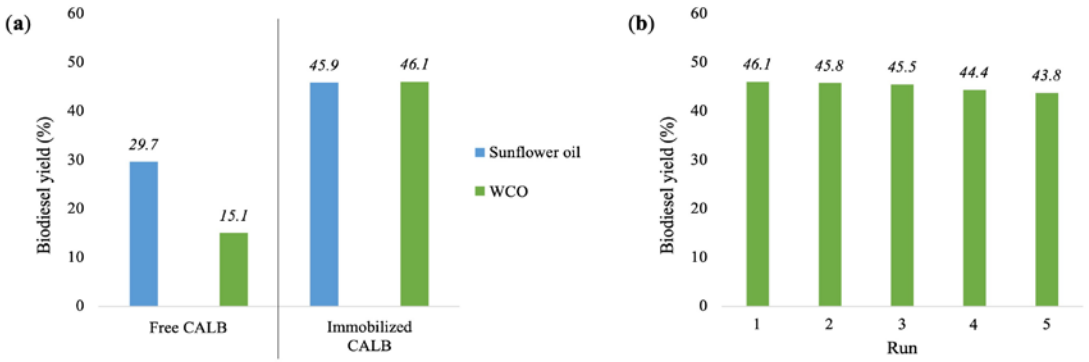

Figure 3. Biodiesel yields obtained from: (a) the comparison of free and immobilized CALB on sunflower oil and WCO; (b) number of runs made with the immobilized CALB on WCO.

References

[1] C.M. Schwartz, MS Thesis, University of Nebraska-Lincoln, 2014.
[2] N.S. Abdul Manab, H. Veny, A. Gusniah, S. Sulaiman, N. Aziz, ASEAN *J. Chem. Eng.* 2021, 21, 19-26.
[3] F. Yagiz, D. Kazan, A.N. Akin, *Chem. Eng. J.* 2007, 134, 262-267.
[4] I.B.B. Romdhane, Z.B. Romdhane, M. Bouzid, A. Gargouri, H. Belghith, *Appl. Biochem. Biotechnol.* 2013, 171, 1986-2002.
[5] S.F.A. Halim, A.H. Kamaruddin, *Process Biochem.* 2008, 43, 1436-1439.
[6] R. Macreiras, M. Vega, C. Costa, P. Ramos, M.C. Márquez, *Fuel.* 2009, 88, 2130-2134.
[7] K.F. Haigh, S.Z. Abidin, G.T. Vladisavljević, B. Saha, *Fuel.* 2013, 111, 186-193.
[8] C. Decarpigny, A. Aljawish, C. His, B. Fertin, M. Bigan, P. Dhulster, M. Millares, R. Froidevaux, *Energies* 2022, 15, 3381.
[9] C. Decarpigny, M. Bigan, R. Froidevaux, *ChemBioChem* 2025, 26(4), e202400327.

Acknowledgment: The authors thank the ANR (CENDHRE project) for its fundings in this project. The authors are also grateful for the financial support from Hauts-de-France council to develop the CPER BIHautEcodeFrance project and Industrial Chair Charles Viollette. Ministère de l'Enseignement Supérieur, de la Recherche et de l'Innovation and FEDER are acknowledged for supporting and funding partially this work.

CL1. MODERN ASPECTS OF POLYMER MELT RHEOLOGY

Paul Lazar
Laboratorium S.R.L., Bucharest, Romania
**paul.lazar@laboratorium.ro*

Rheological properties of matter are crucial in many manufacturing processes like food industry, production of personal care products, cement industry, production of paints, glues, inks, laundry and surface cleaning liquids, polymer processing. Shear viscosity (Pa·s) is the ratio of the shear stress (Pa) to shear rate (s^{-1}). For common liquids, viscosity may vary over many orders of magnitude, e.g. 3 x 10^{-4} Pa·s for petrol to 10^{9} Pa·s for bitumen. For all simple liquids, viscosity decreases with increase in temperature according to Andrade equation: $\log_{10}\eta = A + B/T$ [2]. A Newtonian fluid is a fluid whose viscosity remains constant upon variation of shear stress or shear rate. Non-Newtonian fluids may be of different types like shear-thinning (pseudoplastic) or shear-thickening (dilatant). Materials with time-dependent viscosity can be rheopectic (apparent viscosity increases with duration of stress) or thixotropic (apparent viscosity decreases with duration of stress). Bingham plastic are fluids with linear relationship between shear stress and shear rate but require a finite yield stress before they begin to flow. Bingham pseudoplastic fluids are similar, but with a non-linear dependence between shear stress and shear rate. There are many different instruments and geometries that can be used in measuring the viscosity of a sample: rotational viscometers with geometries like narrow-gap concentric-cylinder or small-angle cone-and-plate, straight circular pipes, spheres falling in liquids [2]. Rheometers are high-precision instruments that measure flow and deformation by applying a force to a sample and measuring the resulting stress or strain, allowing for measurement of viscosity and modulus. Rheological measurements are typically performed using a rheometer to obtain critical material parameters such as viscosity and modulus. With a rheometer, viscosity measurements extend far beyond the limits of a traditional viscometer, characterizing non-Newtonian behaviors like shear thinning, thixotropy, and yield stress of complex fluids (emulsions, suspensions, paints, inks, coatings, slurries). Oscillatory rheology measures viscoelasticity (Storage Modulus, Loss Modulus, Tan Delta) of materials ranging from low-viscosity fluids to stiff solids in DMA mode (Dynamic Mechanical Analysis) [3].

The working principle of rotational rheometer is presented in detail. There are two main types of such rheometers: the simpler, stress-controlled, CMT (Combined Motor and Transducer) and the more complex, strain-controlled, SMT (Separate Motor and Transducer). Such rheometers mainly measure two parameters: torque and angular displacement. By combining the two parameters with the shape and dimension of the geometry used, one can calculate all the relevant experimental parameters like shear rate and shear stress. For best performance, these instruments should be characterized by very low friction and inertia. All the necessary calibrations (instrument inertia, geometry inertia, bearing friction, rotational mapping) are discussed and explained. The temperature of the sample is controlled using systems like Peltier Plate (-40°C to 200°C), Peltier Concentric Cylinder (-20°C to 150°C), Electrically Heated Concentric Cylinder (up to 300°C), Electrically Heated Plates (-70°C to 400°C), Dual Stage Peltier Plate (-45°C to 200°C), Upper Peltier Plate (-40°C to 200°C), Environmental Test Chamber (-160°C to 600°C). For cooling, some temperature systems use liquid nitrogen or air chiller systems.

Adding to the experimental set-up modules like Optical Plate Accessory, Modular Microscope Accessory, Small Angle Light Scattering, Rheo-Raman Accessory, one can gather different complementary information, synchronized with the rheological data. Electro-Rheology and Magneto-Rheology experiments can be performed using the appropriate accessories [4]. Shear Rheometry and Dynamic Mechanical Analysis (DMA) are some of the most important tools for characterization of polymers. A typical characteristic of a polymer melts is that they are non-Newtonian fluids with viscosity decreasing with increasing shear rate. Viscosity measurements can be performed either through direct flow measurements or through oscillation measurements over a range of frequencies. This is important from the standpoint of processing ease, and for determining processing energy needs. The dynamic measurement also provides a simultaneous measure of melt elasticity, the main determinant of viscoelastic melt behavior, and the cause of such phenomena as die swell. Measuring the viscoelastic properties as function of strain rate (frequency), strain amplitude and temperature offers valuable information regarding molecular structure (molecular weight, molecular weight distribution, chain branching and cross-linking, interaction of fillers with matrix polymer, single or multi-phase structure).The most important types rheological experiments (Flow/Steady Shear, Oscillation/Dynamic, Creep and Recovery) used for characterization of polymers are described and commented. Dynamic stress or strain sweep at constant frequency and temperature are used to determine the linear viscoelastic range (LVR). Dynamic time sweep is used for time-dependent thixotropy, cure studies, stability against thermal degradation and solvent evaporation/drying. Frequency sweep experiments at constant strain amplitude and temperature are used to find out the time-dependent behavior of a polymer in the non-destructive deformation range (LVR).

A series of different polymer rheograms a presented and discussed. They cover the influence of molecular weight and molecular weight distribution on viscosity, G’ and G’’. The G’ and G’’ moduli of a typical polymer melt cross over between 1 and 100 rad/s. The position on the frequency axis and the absolute value of the cross over modulus correlate with Mw and the width of molecular weight distribution. The effect of branching is also visible in a frequency sweep experiment: long chain branches increase the melt viscosity compared with linear polymers with the same Mw. The viscosity of long branched polymers is more shear dependent and the elasticity is higher. For filled systems, a dramatic increase in viscosity at low shear rate is observed due to interaction between filler and filler-matrix.

For polymer blends, properties like melt viscosity, glass transition temperature combines according to the following equation: $P_{mix} = (1 - x_B)P_A + x_BP_B + I\,P_AP_B$ where x_B is the fraction of B in the mix and the last term denotes the interaction between the two polymers. An increase of the elastic contribution at low frequencies in a polymer blend can be explained by energy storage at the interface [1].

References

[1] Baiardo M. TA Instruments, 2008. https://waterscorp.sharepoint.com/sites/TAInstrumentsTechnicalLibrary.
[2] Howard A., Barnes, Aberystwyth, 2000, p. 5.
[3] TA Instruments, 2017, https://www.tainstruments.com/pdf/brochure/BROCH -ARES-G2-2017-EN.pdf
[4] TA Instruments, 2025, https://www.tainstruments.com/pdf/brochure/ TA-Instruments-HR-Brochure-EN.pdf

CL2. SHAPE OF FLAVOR: TEA LEAF CHARACTERIZATION USING DYNAMIC IMAGE ANALYSIS

Miklós ATTILA
Anton Paar GmbH
pc-application@anton-paar.com | www.anton-paar.com

Particle sizing is a crucial analysis for tea leaves for determining both the sensory qualities of the final brew and the efficiency of industrial processing. First, particle size is highly important for the aroma of the tea. Larger particles release their flavor compounds more slowly, contributing to a milder and often more nuanced taste. In contrast, smaller particles offer faster extraction due to their greater surface area, but this can result in a bitter flavor and more rapid aroma loss. Second, for tea bag production, smaller and more uniform particles are advantageous, as they allow for consistent and efficient machine filling, improved dosing accuracy, and reduced steeping times.

Commercially available black tea leaves in bags were analyzed with the Litesizer DIA 500 instrument in Free Fall and Dry Jet mode. Litesizer DIA 500 is a single-camera, dual-objective instrument. The Free Fall mode disperses particles only via gravitational fall. The Dry Jet mode uses compressed air for sample dispersion. 500 mbar of air pressure were used in this experiment. The software offers a wide range of size and shape parameters to accurately characterize any particle and investigate the specific properties of interest. The most relevant size parameter in this report is the xA which is the equivalent diameter of a sphere (**Figure 1**).

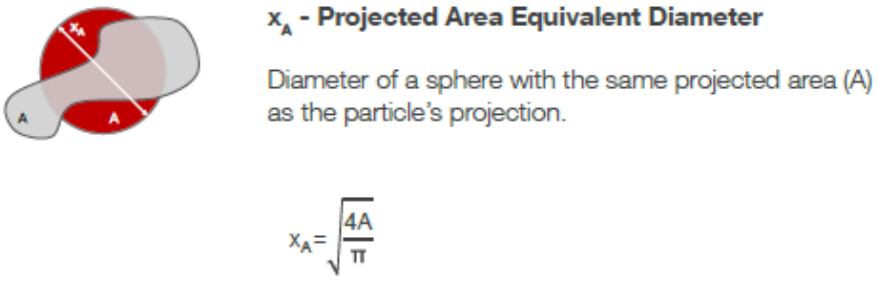

Figure 1. xA - projected area equivalent diameter.

The second important parameter used in this report is the aspect ratio, which is the ratio between the minimum and maximum Feret diameters (**Figure 2)**.

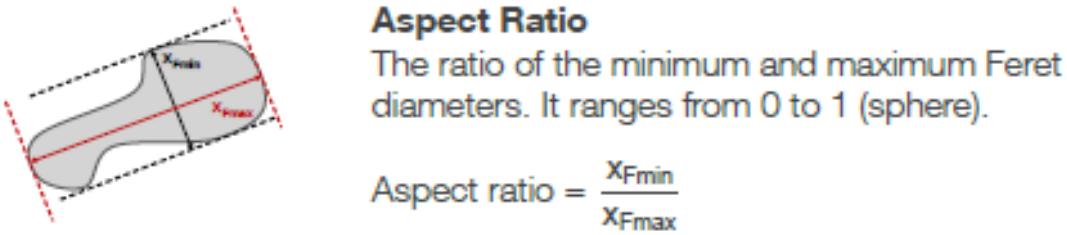

Figure 2. Aspect ratio shape parameter.

Free fall dispersion is a convenient measurement mode when the sample particles are large enough in terms of mass to disperse through gravitational fall. The two main parameters of interest are the xA (equivalent diameter) and the aspect ratio of the particles. They are displayed in the following table (**Table 1**).

Table 1. Volume-based size and shape distribution of black tea leaves in free fall mode.

Headings	xA [µm]	Aspect ratio
Q10	417	0.39
Q50	753	0.62
Q90	1161	0.79
Mean	**777**	**0.61**

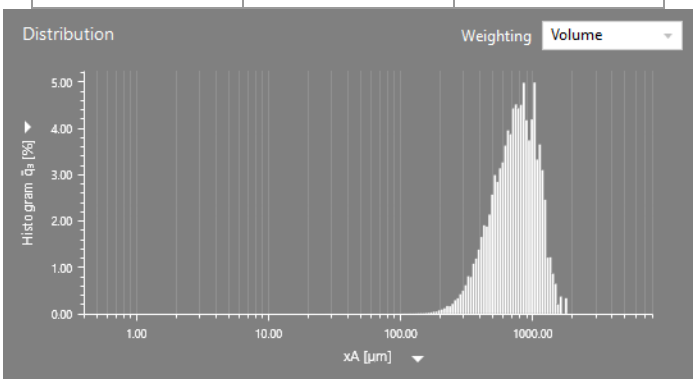

Figure 3. Volume-based particle size distribution of black tea leaves in free fall mode.

The particle size distribution displays a homogenous sample. However, if the individual pictures are observed, a large number of aggregates become visible.

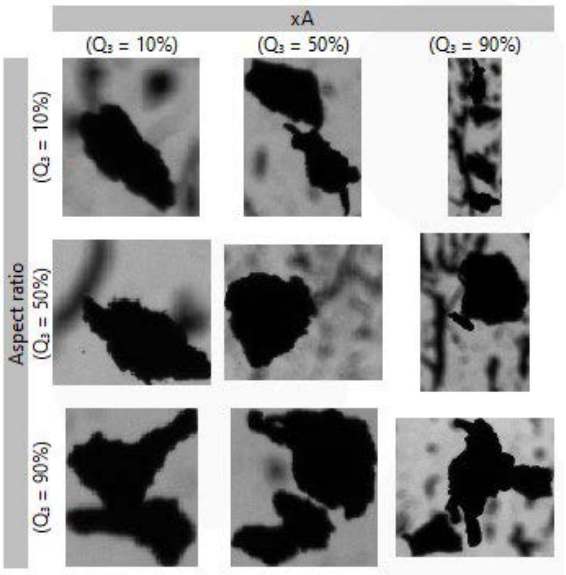

Figure 4. Grid of example pictures of the xA and the aspect ratio of black tea leaves measured in free fall mode.

The Litesizer DIA was able to accurately determine the particle size and shape of the tea sample. The majority of particles were found to be of irregular shape which can negatively impact the flowability of the product during the production and packaging processes.

References

[1]. D. Li, Y. Zhang, R. Tamura, T. Nakajima, Y. Caballero, *Food and Nutrition Sciences* 2023, 14(11), 1043-1056.
[2]. S. Sawamura, Y. Haraguchi, M. Yasuda, S. Matsusaka, *Nippon Shokuhin Kagaku Kogaku Kaishi* 2009, 56(2), 103-107

Oral Communications

OC1. NEW MULTI-STIMULI RESPONSIVE HYDROGELS

Adina Ferariu*, Irina Popescu, Sanda Bucatariu, Marieta Constantin, Gheorghe Fundueanu
Petru Poni Institute of Macromolecular Chemistry, Romanian Academy, Iasi, Romania
**ferariu.adina@icmpp.ro*

One of the major accomplishments of pharmaceutical corporations and researchers is the use of controlled release formulations for drug administration. These systems allow a precise dose of medication to be delivered gradually over an extended period of time, improving therapeutic outcomes while increasing patient comfort and compliance. However, this strategy isn't always appropriate as there are clinical circumstances in which the biologically active compound should only be given when normal physiological parameters are disrupted. This led to the proposal of sophisticated drug delivery systems, the majority of which are based on stimuli-sensitive or intelligent polymeric materials. These therapeutic systems can, for example, release drugs when normal physiological conditions are disturbed [1].

A lot of polymeric materials responsive to a single stimulus (such as temperature, pH, ionic strength or biomolecules) have been studied for drug-release applications. However, the need for materials with both broad utility and increased specificity to the application is ever-present. As a result, the current trend in stimuli-responsive drug delivery systems is the development of materials capable of responding to two or more stimuli in order to better mimic biological processes [2].

Therefore, this study presents the design and development of pH/temperature sensitive delivery systems able to release the biologically active compound only in the presence of certain biomolecules, acting as triggering agents. Poly(N-isopropylacrylamide) (poly(NIPAAm)) was chosen for this study because, in aqueous solution, it exhibits a sharp phase transition (having a lower critical solution temperature, LCST) at approximately 32 °C, close to the temperature of the human body [3]. The copolymerization of NIPAAm with pH-sensitive monomers leads to the formation of copolymers sensitive both to pH and temperature. It was observed that these types of copolymers lose their thermosensitivity when the functional groups are in an ionized state, but can regain their thermosensitivity after interaction with certain biomolecules [4]. Based on this, in this study, were obtained new intelligent hydrogels based on NIPAAm and a comonomer sensitive to pH which presents both amino and carboxylic groups, 4-imidazoleacrylic acid. The mechanism of response of these hydrogels was represented in **Figure 1**. The hydrogels obtained lose their thermosensitivity in simulated physiological conditions (at a pH of 7.4 and a temperature of 37 °C), when the carboxylic groups are in an ionized state, but collapse after “complexation” with triggering agents. As triggering agents were used model biomolecules with the opposite charge and hydrophobic character, specifically propranolol and ibuprofen.

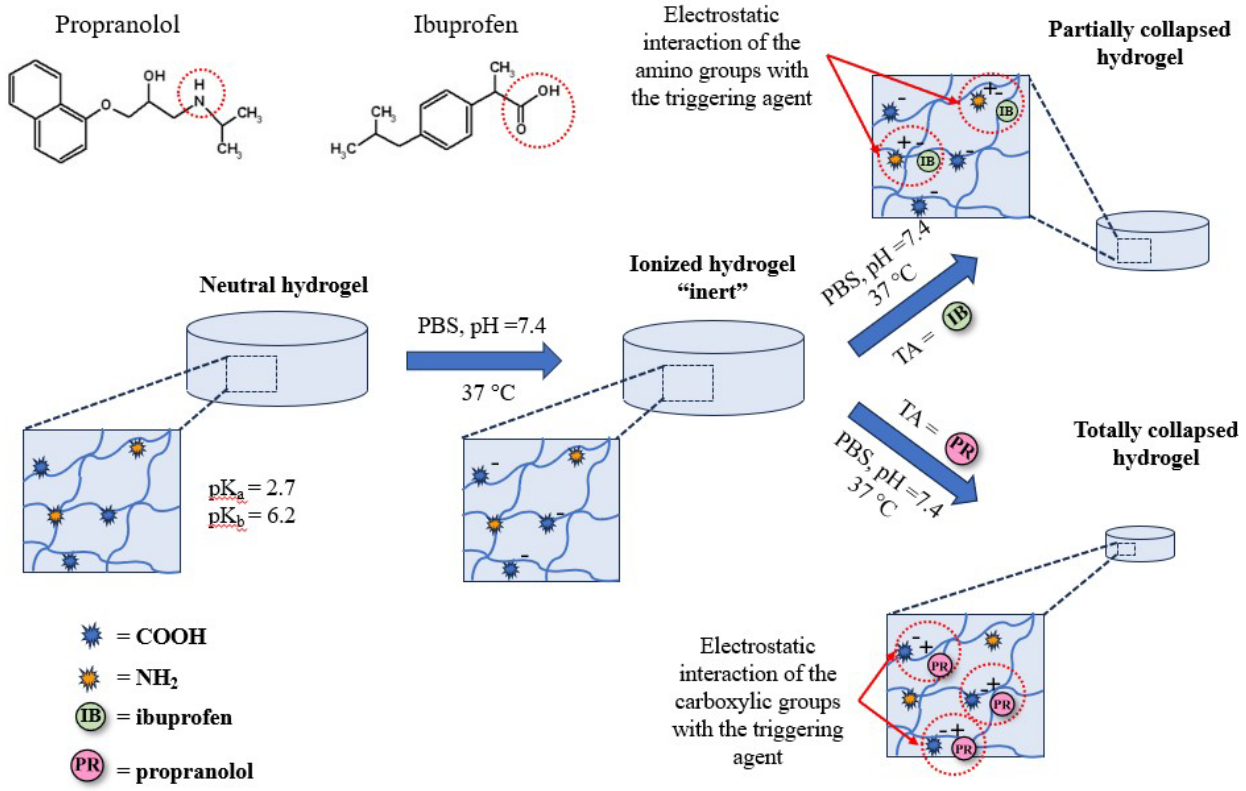

Figure 1. Schematic representation of the mechanism of response of the hydrogels, in simulated physiological conditions, after interaction with different triggering agents and the chemical structures of the model biomolecules used as triggering agents, propranolol and ibuprofen.

The obtained hydrogels were characterized from the morphological, structural and physico-chemical point of view. The LCST profiles of the studied copolymers were determined at different pH values simulating physiological fluids. Furthermore, the swelling and collapsing of the hydrogels with the variation of temperature was studied both in the presence and in the absence of triggering agent. The materials developed in this study are capable of recovering their sensibility to temperature after interaction with certain biomolecules, responding simultaneously to multiple stimuli (pH, temperature and biomolecules).

References

[1] M.A. Ward, T.K. Georgiou, *Polymers* 2011, 3, 1215-1242.
[2] B.M. Holzapfel, J.C. Reichert, J.T Schantz, U. Gbureck, L. Rackwitz, U. Nöth, F. Jakob, M. Rudert, J. Groll, D.W. Hutmacher, *Adv. Drug Deliv. Rev.* 2013, 65, 581–603.
[3] M. Heskins, J.E. Guillet, *J. Macromol. Sci. Chem.* 1968, 2, 1441-1455.
[4] M. Constantin, S. Bucatariu, V. Harabagiu, I. Popescu, P. Ascenzi, G. Fundueanu, *Eur. J. Pharm. Sci*. 2014, 62, 86-95.

OC2. RADIATION-MEDIATED SYNTHESIS OF SILVER NANOPARTICLES IN SILICA-BASED DRUG DELIVERY SYSTEMS WITH ANTIMICROBIAL PROPERTIES

Andreea-Simona Baltac [1,2*], Irina Atkinson[1], Daniela Culita[1], Simona Ionita[1], Andreea Elena Serban[2], Paul Mereuta[2], Daniel Negut[2], Mioara Alexandru[2], Raul Augustin Mitran[1]

[1] *"Ilie Murgulescu" Institute of Physical Chemistry, Romanian Academy, Bucharest, Romania*
[2] *"Horia Hulubei" National Institute of Physics and Nuclear Engineering, Romanian Academy, Magurele, Romania*
**andreea.manea@nipne.ro*

Antimicrobial resistance (AMR) has emerged as a profound global health threat, disrupting the efficacy of conventional therapeutic approaches and requiring the development of advanced treatments. These shortcomings have fueled the search for nanocarrier-based delivery platforms that can offer improved pharmacokinetics, targeted action, and sustained release profiles. Among the various nanostructured systems explored to address this challenge, mesoporous silica nanoparticles (MSNs) have garnered significant attention owing to their distinctive physiochemical characteristics, including high surface area, tunable pore structure, large pore volume, thermal stability, biocompatibility and inherently low cytotoxicity [1]. MSNs possess all attributes enabling highly efficient controlled and sustained release for bioactive agents. Silver-loaded silica materials have been previously reported in the literature [2], demonstrating broad-spectrum antimicrobial activity due to silver's ability to disrupt bacterial membranes, generate reactive oxygen species (ROS), and interfere with DNA replication [3]. Silver is usually introduced into silica matrices through chemical reduction, impregnation, or sol-gel techniques. These treatments require additional reducing agents or high-temperature treatments that could compromise drug stability and compromise the sterility of the samples [4].

This study employs gamma irradiation as an efficient and green reducing agent for Ag^+ ions. The silver cations are reduced *in situ* within the silica matrix, thus avoiding the use of chemical reductants and enabling better control over nanoparticle dispersion and oxidation state [5]. In this experiment, FDU-12 MSNs were synthesized through sol-gel method and subsequently impregnated with $AgNO_3$. Precursor-loaded matrices were exposed to gamma irradiation at 50 kGy using ^{60}Co sources, resulting the *in situ* formation of metallic silver nanoparticles (Ag^0) uniformly dispersed within the silica framework. The antimicrobial activity of antibiotic-loaded nanoparticles was evaluated using adapted agar-diffusion method (qualitative determination), time-kill test (quantitative evaluation) and broth microdilution method using resazurin in order to evaluate MIC (Minimum Inhibitory Concentration) and MBC (Minimum Bactericidal Concentration). The samples were tested for in vitro evaluation against *Staphylococcus aureus* ATCC 6538, *Escherichia coli* ATCC 8739 and *Pseudomonas aeruginosa* ATCC 9027.

Comprehensive physicochemical characterization confirmed the successful synthesis of the desired platforms. Wide-angle X-ray diffraction (XRD) was employed to investigate the crystallinity of FDU-12 samples. The diffraction pattern of pristine FDU-12 exhibits a broad signal centered around 22°, which is characteristic of amorphous silica. The specific diffraction peaks of metallic Ag can be noticed for all the Ag matrices. The silver diffraction peaks belong to the cubic

Fm3̄m space group (JCPDS No. 04-0783). The XRD patterns confirm the successful formation of crystalline Ag nanoparticles within the FDU-12 matrix. Scanning Electron Microscopy (SEM) analysis was performed to evaluate the morphological features of the samples.

Slight morphological changes are observed upon chloramphenicol or vancomycin loading. The spherical-to-polyhedral particle shape is conserved, while the surfaces appear slightly rougher, in comparison with the pristine sample. This change suggests that the drug molecules are present both on the SiO_2 particle surface and into the inner pore volume. The overall particle shapes are preserved, suggesting that drug loading does not significantly disrupt the silica framework. Energy dispersive X-ray spectroscopy (EDX) spectra provide further evidence for the successful incorporation of silver nanoparticles and the presence of other elemental constituents in the samples. All Ag-loaded samples exhibit clear Ag signals. Small, <30 nm Ag^0 nanoparticles are uniformly distributed in the samples. The textural properties of the matrices and drug-loaded samples were characterized by N_2 adsorption–desorption isotherms. All samples showed typical type IV isotherms with H1 hysteresis loops, confirming the mesoporous nature of the materials and indicating that the structural integrity of the silica framework was largely maintained after the various modifications. The average pore diameter is similar for all samples, which suggests that the drug molecules are present inside the mesopores, but they are strongly adsorbed onto the interior mesopore surface. Fourier transform infrared spectroscopy (FT-IR) verified characteristic vibrational bands associated with silica framework and antibiotic functional groups. All samples exhibit the characteristic bands of the silica-based FDU-12 structure, mainly the strong Si–O–Si stretching around 1050–1100 cm^{-1}, symmetric stretching near 800 cm^{-1}, and bending vibrations below 500 cm^{-1}. The drug loaded materials exhibit additional IR bands, such as the C=O stretching and the N–H bending vibrations, between 1500 - 1700 cm^{-1}. Samples containing chloramphenicol also contain a 1350 cm^{-1} fingerprint vibration, likely associated with C-H bonds. Inductively coupled plasma mass spectrometry (ICP-MS) analysis confirmed that the Ag-loaded FDU-12 material contains a significant amount of silver, around 3.22%, indicating that the gamma irradiation process effectively incorporated silver nanoparticles into the matrix. Bacterial viability assays highlighted the antimicrobial efficacy. The antimicrobial activity of the FDU-12 composites is strongly dependent on both the type of bacterial strain and the incorporated active agents. *S. aureus* was the most sensitive, while *P. aeruginosa* exhibited the lowest inhibition. The inclusion of silver consistently improved antibacterial outcomes compared to the same compositions without it. Systems containing both chloramphenicol and vancomycin-loaded were the most effective across all strains, achieving near-total bacterial eradication against *S. aureus*. Therefore, FDU-12 is an effective carrier for antimicrobial agents and the inclusion of silver nanoparticles significantly increases antibacterial performance. The composites containing both antibiotic drugs and silver nanoparticles have achieved superior antibacterial activity against all tested strains. These findings show the potential of Ag-FDU-12 antibiotic-loaded nanocomposites as robust and multifunctional antimicrobial delivery systems.

References

[1] M. Vallet-Regí., M. Colilla, I. Izquierdo-Barba, M. Manzano, *Molecules* 2018, 23(1), 47.
[2] Y. Li, Y. Yan, J. Wang, L. Li, F. Tang, *Colloids Surf. A: Physicochem. Eng. Asp.* 2022, 648, 129242.
[3] N. Durán, P.D. Marcato, R. de Conti, O.L. Alves, F.T.M. Costa, M. Brocchi, *J. Braz. Chem. Soc.* 2010, 21(6), 949-959.
[4] L. Xu, Y.Y. Wang, J. Huang, C.Y. Chen, Z.X. Wang, H. Xie, *Theranostics* 2020, 10(20), 8996-9031.
[5] A.S. Baltac, R.-A. Mitran, *Nanomaterials* 2025, 15(3), 218.

OC3. CINNAMON OIL AND CINNAMALDEHYDE: MIC TESTING FOR APPLICATIONS IN BOVINE ENDOMETRITIS

Paula Lorent (Cucu)[1,2]*, Mihai Mares[1], Iuliana Spiridon[2]
[1]*Faculty of Veterinary Medicine, "Ion Ionescu de la Brad" University of Life Sciences, Iasi, Romania*
[2]*Petru Poni Institute of Macromolecular Chemistry, Romanian Academy, Iasi, Romania*
**paula.cucu@iuls.ro*

Polymeric biomaterials are used to design biomaterials for biomedical applications due to their chemical and functional versatility, biocompatibility and biodegradability. They can be used as carriers for drug and gene delivery or as scaffolds in the tissue engineering and regenerative medicine. Natural polymers, such as chitosan, collagen, alginate or modified cellulose, are notable for their biocompatibility and antimicrobial activity, whereas polyesters such as polycaprolactone (PCL), polylactic acid (PLA), and poly (lactic-*co*-glycolic acid) (PLGA) offer mechanical properties improved, stability and controllable degradation rate [1]. Proper interaction with biological tissues ensures material integration and efficient regeneration, while degradation products must be non-toxic and easily metabolizable by the body [2]. The development of polymeric biomaterials in veterinary medicine represents a promising research area with significant potential to develop materials tailored for different animal species with reduced production costs and improved biological performance. Current trends include the creation of smart materials with antibacterial properties having ability to respond to biological stimuli, which can optimize healing and regeneration processes in modern veterinary practice [3]. In this study, new polymeric systems comprising alginate [4] and gelatin as matrix [5], designed as carriers for bioactive compounds are presented. Curcumin [5] and ginger (*Zingiber officinale*) [6] were selected as fillers due to their well-documented antimicrobial, anti-inflammatory, and antioxidant properties (relevant for infection management) and added into polymeric matrix (**Figure 1**). The new controlled-release and biocompatible systems could have potential applications in the treatment of bovines' endometritis by inhibiting pathogenic agents and reducing associated inflammatory processes.

Based on the results obtained from *in vitro* testing of cinnamaldehyde and cinnamon essential oil, we aim to exploit their antimicrobial potential. Thus, their minimum inhibitory concentration (MIC) against bacterial strains isolated from clinical samples was evaluated. Cinnamaldehyde exerts antibacterial effects through multiple complementary mechanisms. It targets the cell membrane, disrupting its structure and permeability, leading to the loss of membrane integrity and efflux of intracellular components. It also inhibits biofilm formation and reduces the expression of virulence-related genes, weakening the bacteria's ability to adhere and colonize. Cinnamaldehyde may interfere with cell communication systems (quorum sensing) and essential metabolic processes, affecting ATP synthesis and nutrient transport. Through these actions, the compound contributes to the inhibition of bacterial growth and multiplication, demonstrating significant potential as a natural antimicrobial agent (**Figure 2**). Bovine endometritis is a common reproductive disorder with a significant impact on animal health, caused by a variety of pathogenic and opportunistic bacteria. The most frequently isolated species include *Escherichia coli*,

Trueperella pyogenes, and *Streptococcus uberis*, which contribute to acute and chronic uterine inflammation and negatively affect reproductive function. Other species, such as coagulase-negative staphylococci (*Staphylococcus epidermidis*, *Staphylococcus haemolyticus*), *Aerococcus viridans*, *Moraxella ovis*, *Bacteroides ureolyticus*, and *Enterobacter asburiae*, although less studied, may promote uterine dysbiosis and complicate the clinical picture of disease.

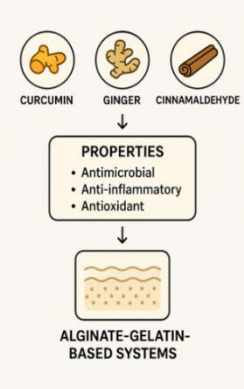

Figure 1. Properties of curcumin, ginger, and cinnamaldehyde.

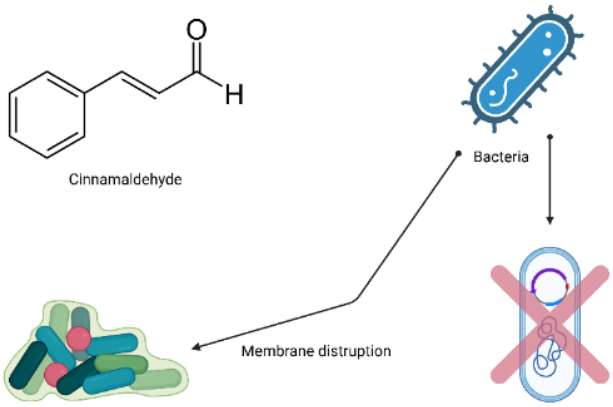

Figure 2. Antibacterial mechanisms of action of cinnamaldehyde.

MIC values of cinnamon essential oil and its main component, cinnamaldehyde, against bacteria isolated from bovine endometritis revealed a broad spectrum of antimicrobial activity. The most sensitive species were *Staphylococcus haemolyticus* and *Trueperella pyogenes*, for which the MIC was 0.01042% v/v for both substances, indicating strong inhibitory effects at very low concentrations. For *Streptococcus uberis* and *Bacteroides ureolyticus*, cinnamaldehyde showed lower MIC values compared to cinnamon oil, suggesting higher activity of the pure compound. For *Escherichia coli*, *Enterobacter asburiae*, *Moraxella ovis*, *Staphylococcus epidermidis*, and *Aerococcus viridans*, MIC values were similar for oil and cinnamaldehyde (0.02083–0.04167% v/v), indicating that cinnamon essential oil antimicrobial effect is largely attributable to the presence of cinnamaldehyde. Our findings suggest that both cinnamon oil and cinnamaldehyde have significant potential as natural adjuvant agents for the prevention and treatment of uterine infections in bovine, being effective against major and opportunistic pathogens involved in endometritis. These results, as well as literature data related to the anti-inflammatory properties of curcumin and ginger, support the efficacy of natural substances as adjuvants in the prevention and treatment of bovine endometritis. The present study is justified by the need to identify natural alternatives to antibiotics, considering the risk of bacterial resistance and the side effects of conventional treatments. The combined or individual use of these natural compounds can reduce uterine inflammation, inhibit bacterial growth, and improve reproductive performance and animal productivity, representing a sustainable and safe approach to managing bovine endometritis.

References

[1] Y.K Sung, S.W Kim, *Biomater. Res.* 2020, 24, 12.
[2] M. Chelu, A.M. Musuc, *Processes* 2023, 11(9), 2696.
[3] M. Broda, D.J Yelle, K. Serwańska-Leja, *Molecules* 2024, 29(4), 883.
[4] F. Abasalizadeh, M. Mohammadi, M.H. Farahani, *J. Biol. Eng.* 2020, 14, 227.
[5] R. Andreazza, A. Morales, S. Pieniz, J. Labidi, *Polymers* 2023, 15, 1026.
[6] C. Gago, A. Serralheiro, M.D.G Miguel, *Molecules* 2025, 30, 2450.

OC4. HEAT TRANSFER ANALYSIS INSIDE A SUPERCRITICAL WATER REACTOR FOR PROCESS OPTIMIZATION OF METAL OXIDE SYNTHESIS

Mihail-Calin Licu*, Florentina Maxim, Speranta Tanasescu
Institute of Physical Chemistry-Ilie Murgulescu, Romanian Academy, Bucharest, Romania
**mlicu@icf.ro*

Supercritical water (SCW) is a suitable reaction medium for the synthesis of functional nanomaterials with controlled structure, size and morphology [1]. It is now well-recognized that SCW cannot be regarded as a single homogeneous phase. Instead, the supercritical state can be divided into two distinct regions: a liquid-like and a gas-like state, separated by a transitional zone around the so-called Widom line. Crossing this boundary leads to sharp variations in density and a pronounced peak in heat capacity, reflecting the characteristic behavior associated with pseudo-boiling [2]. Heat transfer to supercritical fluids plays a pivotal role, as it directly affects both process performance and the design and optimization of the equipment. A major challenge in such conditions is heating transfer deterioration (HTD), which occurs due to the abrupt variations in thermophysical properties, particularly in the vicinity of the pseudo-boiling region. The understanding of this phenomenon can help optimizing the reactors operating conditions relevant to key chemical processes for supercritical hydrothermal synthesis of nanoparticles. Thus, the influence of working parameters including pressure, flow rate and onset heating power on the HTD was systematically investigated to identify the optimal conditions for zinc oxide (ZnO) nanoparticle synthesis under supercritical water conditions. ZnO nanostructures are promising candidates for lead-free piezoelectric materials, with their properties being strongly influenced by the synthesis method [3].

In the present work, two equipment working under SCW conditions were employed (**Figure 1**): NISA (Neutron Imaging Supercritical-water Analysis) for heat transfer analysis and SINAS ("*SINteză în Apă Supercritică*") for oxide synthesis.

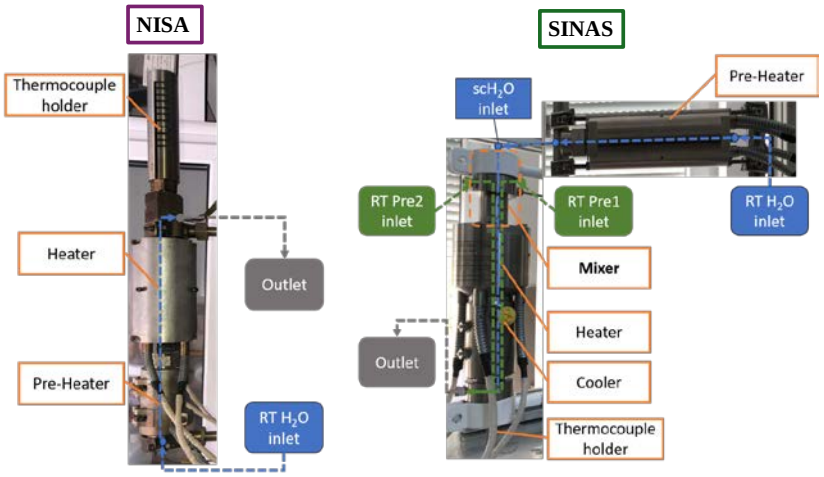

Figure 1. Experimental configurations employed for heat transfer analysis (NISA, left) and ZnO synthesis (SINAS, right).

Using NISA configuration, experimental data were collected and used to establish a correlation between the pseudo-boiling transition and HTD. The quantification of HTD was performed through a dimensionless parameter introduced by Longmire and Banuti [2], namely heat transfer deterioration magnitude, Δ^{HTD}, by developing an analytical methodology for local heat flux estimation at specific positions within a reactor, using experimental transient measurements during pseudo-boiling of water (**Figure 2**). This approach enables the assessment of localized thermal behavior and its deviation from conventional heat transfer correlations.

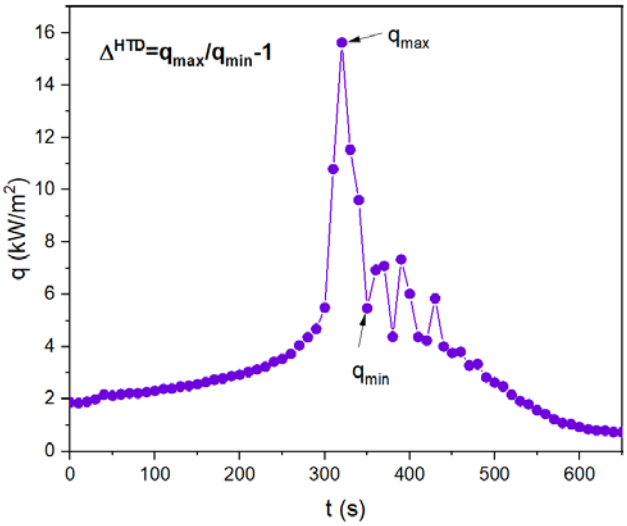

Figure 2. The heat transfer results in terms of wall heat flux with data obtained from pseudo-boiling analysis at 22.5 MPa, $T_{initial}$ = 573.15 K, $\dot{V}$ = 5 mL/min, P_{onset} = 20%P_{max}.

Using SINAS configuration, ZnO was successfully synthesized., Synthesis was performed under isobaric conditions at 250 bar using an aqueous solution of $Zn(NO_3)_2 \cdot 6H_2O$ as the zinc source and KOH as the mineralizer, both at 0.1 M concentrations. SCW was maintained at 450 °C and mixed rapidly with the precursor streams in a confined jet mixer. The total flow rate of water and precursors determined the residence time, while controlled heating ensured stable reaction temperatures. After rapid cooling, filtration, and depressurization via a back pressure regulator, ZnO was separated by centrifugation and dried. The resulting powders were characterized by XRD, Raman, and DLS, confirming pure hexagonal ZnO phase.

References

[1] T. Adschiri, S. Takami, M. Umetsu, S. Ohara, T. Naka, K. Minami, D. Hojo, T. Togashi, T. Arita, M. Taguchi, M. Itoh, *Bull. Chem. Soc. Jpn.* 2023, 96, 133-147.
[2] F. Maxim, K. Karalis, P. Boillat, D.T. Banuti, J.I. Marquez Damian, B. Niceno, C. Ludwig, *Adv. Sci.* 2021, 8, 2002312.
[3] N. Bhadwal, R. Ben Mrad, K. Behdinan, *Sensors* 2023, 23, 3859.
[4] N. Longmire, D.T. Banuti, *Int. J. Heat Mass Transf.* 2022, 193, 122957.

Acknowledgment: The topic of this study is included in the Yearly Research Plan approved by the Romanian Academy. The work with SCW at Institute of Physical Chemistry-Ilie Murgulescu is possible due to the Research Collaboration Agreement with Paul Scherrer Institute, Switzerland, group of Prof. C. Ludwig. The equipment used in this work, SINAS, was developed during the project APASUPER, by UEFISCDI grant number PN-III-P4-ID-PCE-2020-1241, within PNCDI III. The author thanks to Eng. C. Iacob, Computer Power SRL, for technical support.

OC5. UNVEILING THE ROLE OR UROCANIC ACID IN THE FORMATION OF SKIN CANCER

Petru Tirnovan[1]*, Dragos Lucian Isac[1], Mihaela Silion[1], Adina Coroaba[1], Aatto Laaksonen[1], Mariana Pinteala[1]
[1]Petru Poni Institute of Macromolecular Chemistry, Romanian Academy, Iasi, Romania
[2]Division of Physical Chemistry, Department of Materials and Environmental Chemistry, Arrhenius Laboratory, Stockholm University, Stockholm, Sweden
**tirnovan.petru@icmpp.ro*

Skin cancer is caused by the exposure of the skin to solar UV radiation, which, by affecting the cellular DNA is causing genetic mutations. It is one of the most dangerous form of cancer (e. g. melanoma) [1], characterized by the uncontrolled growth of the mutated cells in the epidermis. The exact mechanism through which it occurs is still unknown [2].

Urocanic acid, a compound that accumulates naturally in the outermost layer of the skin (stratum corneum), has been found to be a significant contributor to the occurrence of skin cancer. It is formed through the degradation of histidine rich keratinic proteins (filaggrin) and is present in the form of trans isomer, where it accumulates due to the absence of the urocanase [3]. By having similar absorption wavelength as the nucleotide bases and because of its outermost location in the skin, it protects DNA against direct UV irradiation, preventing T^T dimerization [4], [5], [6]. At the same time, once irradiated, it converts into the cis isomer (~70%) that has immunosuppressive effects [4], [7], inhibiting the natural genetic repair mechanisms and also manifests radical scavenging capabilities [8] [3], [9], which instead of decreasing their activity, contribute to the amplification of the reactive oxygen species (ROS) already existing in the intracellular medium [9], increasing the probability of mutations, by the formation of molecular fragments rich in oxygen with longer lifetime. Immunosuppression has a direct role in the proliferation of cancers, organisms that have not been immunosuppressed actually undergoing cancer regression [10].

The study of the intracellular medium is very difficult due to the complexity of the biological systems [11]. Through the combination of both experimental (in vitro degradation under UV radiation with H_2O_2 with analysis through HPLC-MS) and computational (QM, XTB) prediction methods we attempt to answer the key questions, to find which molecular species are responsible for the genetic mutations and further develop a strategy to inhibit their mechanism of action (MOA). From the experimental data we observed the formation of molecules/fragments with m/z values above and below the molecular mass of urocanic acid, stable for a period of hours with very good reproductivity over time. The use of the computational methods also gave good results (**Figure 1**) with the majority of the fragment masses (z=1) centered around the m/z values (±3 interval) already obtained from the experimental data.

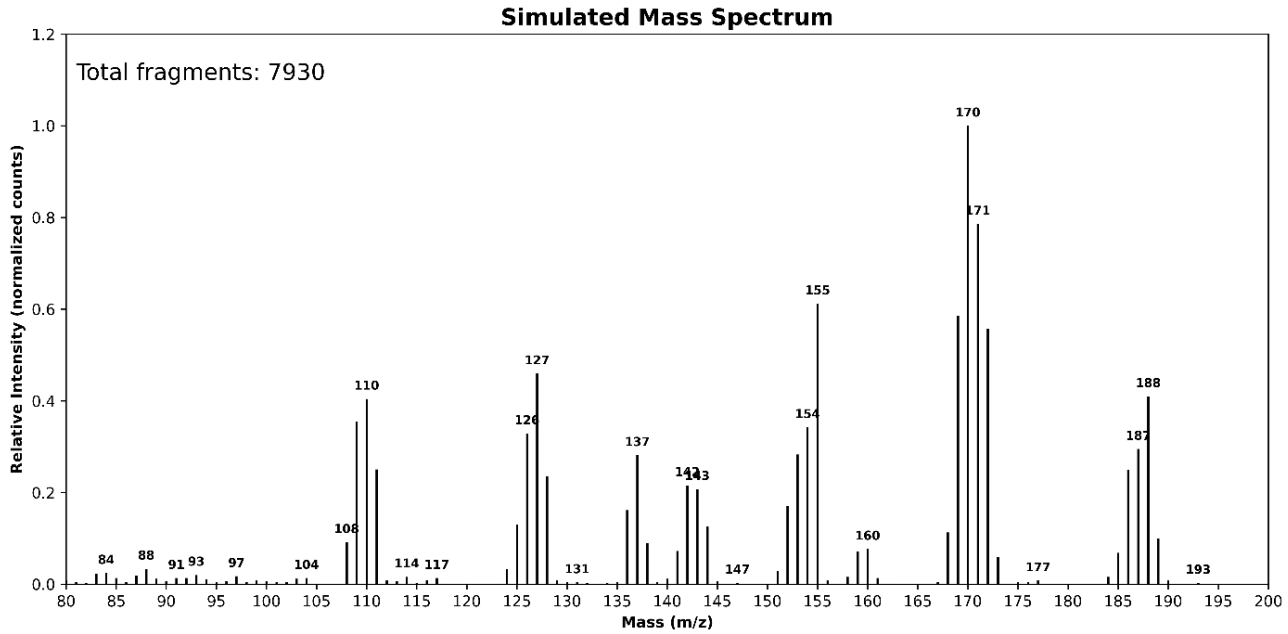

Figure 1. Plot of the simulated mass spectrum for the theoretically predicted fragments obtained from the reaction of urocanic acid with H_2O_2

References

[1] C. Caraviello, G. Nazzaro, G. Tavoletti, F. Boggio, N. Denaro, G. Murgia, E. Passoni, V. Benzecry Mancin, A.V. Marzano, *Cancers* 2025, 17(7), 2920.
[2] N. Hasan, A. Nadaf, M. Imran, U. Jiba, A. Sheikh, W.H. Almalki, S.S. Almujri, Y.H. Mohammed, P. Kesharwani, F.J. Ahmad, *Mol. Cancer* 2023, 22(1), 168.
[3] N. K. Gibbs, M. Norval, *J. Invest. Dermatol*. 2011, 131(1), 14–17.
[4] F.F. de Olivarius, H.C. Wulf, J. Crosby, M. Norval, *Photodermatol. Photoimmunol. Photomed*. 1996, 12(3), 95–99.
[5] C. Barresi, C. Stremnitzer, V. Mlitz, S. Kezic, A Kammeyer, M. Ghannadan, K. Posa-Markaryan, C. Selden, E. Tschachler, L. Eckhart. *J. Invest. Dermatol*. 2011, 131(1), 188–194.
[6] J. Cadet, T. Douki, *Photochem. Photobiol. Sci*. 2018, 17(12), 1816–1841.
[7] L. Roger McMullen, Innate Immune System of Skin and Oral Mucosa: Properties and Impact in Pharmaceutics, Cosmetics, and Personal Care Products, Wiley, 2011.
[8] A. Kammeyer, T.A. Eggelte, J.D. Bos, M.B.M. Teunissen, *Biochim. Biophys. Acta BBA - Gen. Subj*. 1999, 1428(1), 117–120.
[9] A. Kammeyer, T.A. Eggelte, H. Overmars, A. Bootsma, J.D. Bos, M.B.M. Teunissen, *Biochim. Biophys. Acta BBA - Gen. Subj*., 2001, 1526(3), 277–285.
[10] E.C. De Fabo, F.P. Noonan, *J. Exp. Med.* 1983, 158(1), 84–98.
[11] K. Luby-Phelps, *Mol. Biol. Cell* 2013, 24(17), 2593–2596.

Acknowledgment: This work is supported by European Union's Horizon Europe research and innovation programme under grant agreement No. 101086667, project BioMat4CAST (BioMat4CAST - "Petru Poni" Institute of Macromolecular Chemistry Multi-Scale In Silico Laboratory for Complex and Smart Biomaterials).

OC6. METABOLOMIC BIOMARKERS IN PHENYLKETONURIA (PKU)

Dan-Cristian Usurelu [1,2]*, Chiril Boiciuc[2], Daniela Blanita[2], Ecaterina Pavlovschi[1], Natalia Usurelu[2], Alina Nicolescu[3], Calin Deleanu[3]

[1]*IMSP Institute of Mother and Child, Chisinau, Republic of Moldova*
[2]*USMF "Nicolae Testemitanu", Chisinau, Republic of Moldova*
[3]*Petru Poni Institute of Macromolecular Chemistry, Romanian Academy, Iasi, Romania*
**dan.usurelu040599@gmail.com*

Introduction. Phenylketonuria (PKU) is an inherited metabolic disorder caused by mutations in the *PAH* gene, leading to deficient phenylalanine hydroxylase (PAH) enzyme activity. This enzymatic defect impairs the conversion of Phenylalanine (Phe) to Tyrosine (Tyr), resulting in the systemic accumulation of Phe and its toxic intermediate metabolites. The global incidence of PKU varies, with data from the Republic of Moldova indicating a frequency of approximately 1:7,000 newborns. Without early diagnosis through neonatal screening which detects elevated Phe in dried blood spots (DBS) this neurotoxic accumulation leads to severe, irreversible intellectual disability. The disease presents a wide clinical and biochemical spectrum, ranging from classic (severe) to mild forms. This variability is determined by the specific combination of over 3,370 described *PAH* mutations and their impact on residual enzyme activity. While management traditionally relies on strict dietary Phe restriction, and certain forms are responsive to tetrahydrobiopterin (BH4), this diet, although life-saving, is exceptionally burdensome and significantly decreases the patients' quality of life. Consequently, current research is focused on the long-term monitoring of PKU patients and developing alternative therapies to improve these outcomes [1].

Materials and Methods. This cross-sectional, observational study will investigate the relationship between molecular-genetic variants and specific metabolomic biomarkers in Phenylketonuria (PKU). PKU patients are enrolled from the national neonatal screening program following a positive fluorometric assay on dried blood spots (DBS). Enrollment is contingent upon a confirmed PKU diagnosis and subsequent genetic verification of *PAH* gene mutations. Exclusion criteria include the presence of other metabolic disorders, significant comorbidities, or the absence of informed consent. Positive screening results are confirmed using HPLC for blood amino acids, urinary organic acid analysis by 1H-NMR spectroscopy, and molecular genetic tests (PCR/Sanger). Following confirmation, patients are placed on a special low-Phe diet and are monitored for specific biomarkers in DBS, blood, and urine. Following informed consent, a multi-platform analytical approach will be used to assess the broad spectrum of metabolomic biomarkers at the diagnosis and long-term evaluation. In this order, 60 PKU patients are at genetic evidence at the Institute of Mother and Child from Chisinau, from which were collected DBS, blood and urine samples 1-4 times per month during 1 year that will be analyzed by the given methods. The final objectives are to establish clear associations between genotypes and metabolomic phenotypes, develop a dedicated PKU biobank (serum, plasma, urine, DNA), and complete the National Registry for Rare Diseases with this comprehensive data [2,3].

Results and Discussion. The foundation of this research is Moldova's well-organized national PKU screening program. This program's sustained neonatal coverage rate (exceeding 95% since 2010) ensures a comprehensive patient cohort, but this study emphasizes that early detection is only the first step. In Republic of Moldova the screening was initiated from 1989 and there were

tested nearly 1 million newborns, from which 134 PKU patients were confirmed (**Figure 1)**. To optimize management, detailed metabolomic and genetic analyses are essential. Analyzing the full amino acid spectrum via HPLC is crucial for individualizing diet therapy beyond simple Phe restriction, as high Phe levels can impair Large Neutral Amino Acid (LNAA) transport. The urinary spectrum of organic acids by 1H-NMR spectroscopy will provide the toxic metabolites of Phe (phenyllactic ac., phenylpyruvic ac., phenylacetic ac., etc.). Concurrently, molecular-genetic analysis is indispensable for definitive diagnostic confirmation, predicting disease severity, and guiding therapeutic choices (such as potential BH4 responsiveness). Therefore, this research integrates these advanced methods to elucidate the complex relationship between a patients's *PAH* genotype and their broader metabolomic profile. By correlating genetic data with specific metabolomic signatures, this study will contribute to understanding phenotype-genotype variability and PKU pathogenesis. We expect to identify novel biomarkers and generate clinical recommendations for adjusting diet therapy. Furthermore, by characterizing the mutations and metabolic profiles specific to the Moldovan population, this work will contribute valuable local data to international repositories (e.g., BIOPKU) and consolidate the National Registry for Rare Diseases. In conclusion, the relevance of this research lies in its potential to significantly improve the diagnosis, long-term management, and treatment of PKU, ultimately enhancing patient quality of life.

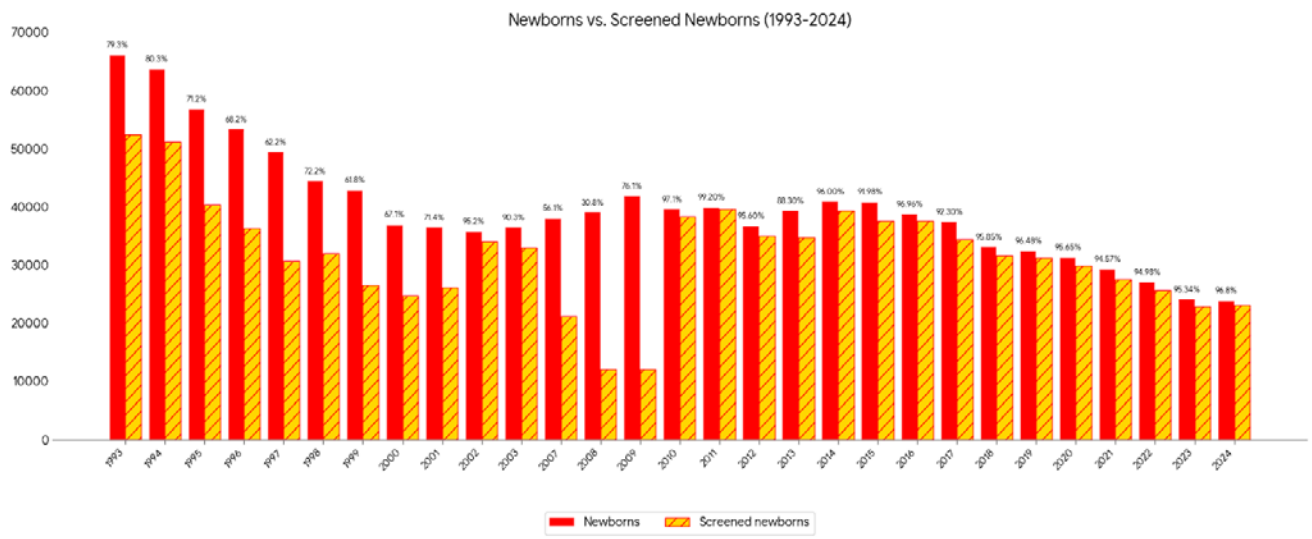

Figure 1. The dynamics of neonatal screening for PKU in Moldova.

References

[1] D. Perko, U. Groselj, V. Cuk, Z. Iztok Remec, M. Zerjav Tansek, A. Drole Torkar, B. Krhin, A. Bicek, A. Oblak, T. Battelino, B. Repic Lampret, *Int. J. Mol. Sci.* 2023, 24(3), 2487.
[2] Ö Öz, E.D. Akbulut, M.E. Karadağ, A. Gönel, İ Koyuncu. *Turkish J. Biochem.* 2021, 46, 0338.
[3] H. Rocha, A. Marcão, C. Sousa, H. Fonseca, L. Lopes, I. Carvalho, L. Vilarinho, *Rev. Esp Salud Publica*. 2021.

OC7. FUNCTIONALIZED STARCH FLOCCULANT FOR THE RECOVERY OF WATER PRODUCED BY PETROLEUM INDUSTRY

Melinda-Maria Bazarghideanu[1]*, Paulo Cristiano Silva da Rocha[2], Letícia Dias da Silva[2], Rita de Cassia Pessanha Nunes[2], Diana-Felicia Loghin[1], Marcela Mihai[1], Elizabete Fernandes Lucas[2,3]

[1]Petru Poni Institute of Macromolecular Chemistry, Romanian Academy, Iasi, Romania
[2]Universidade Federal do Rio de Janeiro, Instituto de Macromoléculas/LMCP, Rio de Janeiro, Brazil
[3]Universidade Federal do Rio de Janeiro, Programa de Engenharia Metalúrgica e de Materiais/COPPE/LADPOL, Rio de Janeiro, Brazil
**melinda.bazarghideanu@icmpp.ro*

Crude oil (petroleum, conventional crude oil, and conventional petroleum) is a nonrenewable resource that, despite the search for other energy sources, remains one of the most widely used energy sources around the world. Due to the chemical complexity and diversity of oil reserves, their extraction and transformation into useful products present significant challenges. During petroleum production, stable water/oil emulsions are formed and can be classified in water-in-oil emulsion (w/o) (water droplets dispersed in an oil phase) and oil-in-water emulsion (o/w) (oil droplets dispersed in a water phase). The water polluted with oil products can be treated by physical, biological and chemical processes (including chemical precipitation or flocculation) [1,2].

At present, polymers are widely used as flocculants by the petroleum industry to remove oil from water. Most of the polymeric flocculant's performance is related to their chemical structure and concentration, but the characteristics of the o/w emulsion are also an important factor for their efficiency. Recently, the use of natural polymers such as starch has attracted considerable attention due to their abundant content in nature, low cost, high biocompatibility, biodegradability, and bioactivity. Starch containing numerous free hydroxyl group that facilitate the chemical modification with synthetic polymers for the development of suitable materials for water cleaning.

In the last years, depending on the kinds of produced waters from petroleum and oil products, native and modified starches have been used as row materials in the preparation of novel sorbents [3]. In this context, the overall objective of this study was to create different copolymer based on starch and synthetic polymers, and their evaluation as flocculants for the produced water treatment process, using synthetic oily water prepared with two kinds of crude oils. The copolymers were obtained in two stages, by functionalization of three types of starch (potato (PS), wheat (WS) and rice (RS)): (1) grafting acrylonitrile on starch (Starch-g-PAN) and (2) the transformation of nitrile groups by the amidoximation reaction of the grafted copolymers in the presence of hydroxylamine (**Figure 1**). For their evaluation as flocculants synthetic oily water prepared with two kinds of crude oils (heavy and light oil) was used. The oily water at ~ 100 and 1000 ppm of oil was obtained using ~2500 and 25000 ppm of heavy oil in brine and ~200 and 2000 ppm of light oil in brine, respectively. Jar tests were performed in order to evaluate the flocculants efficiency and were carried out, without and with 100 and 300 ppm of flocculant in brine.

The efficiencies were reported in terms of percentage reduction of total oil and grease (TOG) compared to TOG before the Jar test procedure. The TOG was determined by fluorimetry, because it is the fastest and simplest method. The measurements were performed using a benchtop fluorimeter.

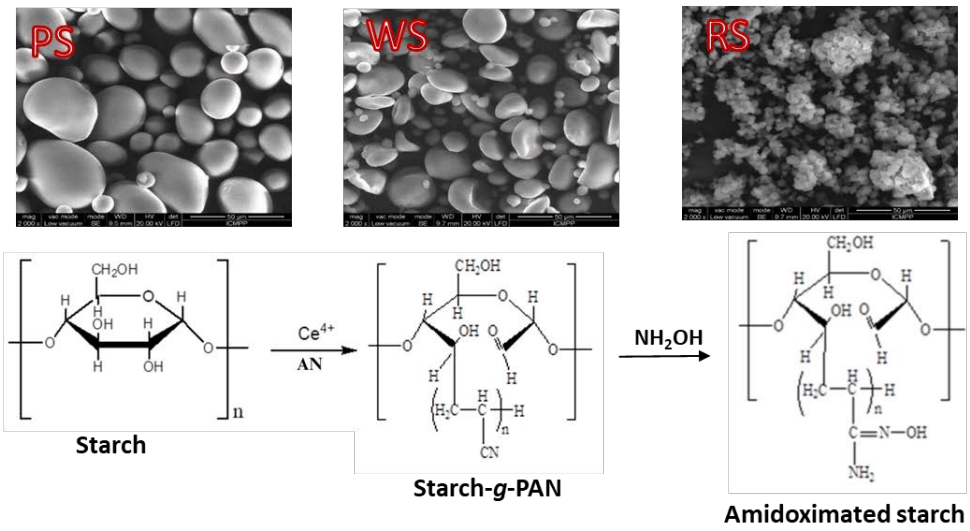

Figure 1. SEM micrographs (scale bar 50 µm) of initial starches and the synthesis reaction of modified starches.

The results show that in the case of samples prepared with heavy oil (API = 13.25), the starch-based flocculants exhibited some efficiency. The values were very similar for the two concentrations of oil in the water (100 and 1000 ppm), but the efficiency was lower when compared to the commercial flocculant. On the other hand, a high potential for starch-based polymers as flocculating agents was observed in the case of synthetic water prepared with light oil (API= 26.4), at a concentration of 100 ppm of oil. The efficiency was even higher than the commercial flocculant already commonly used. When the oil concentration was increased to 1000 ppm, the flocculants efficiencies were reduced, but was still higher than the efficiency of the commercial flocculant.

In conclusion, the results highlight how important is the availability of different products to be applied under different conditions. Starch-based additives have the additional advantage of being naturally based.

References

[1] J.G. Speight, *Heavy Oil Recovery and Upgrading*, Ed. Gulf Professional Publishing, 2019, 3-47.
[2] E. E. Sirotkina & L. YU. Novoselova, *Chem. Sust. Develop.* 2005, 13, 359–375.
[3] F. Zhanga, X. Peia, K. Zhaia, C.Wanga, Y. Bai, B.Zhanga, Y. Wanga, Y. Tanc, K. Xua, P. Wang, *Int. J. Biol. Macromol.* 2020, 162, 1118–1126.

Acknowledgements: The authors would like to thank Equinor, ANP, FAPERJ (E-26/200.974/2021), CNPq (305.565/2022-2) and CAPES. This work was financially supported by the project POLYSACCHARIDE BASED (BIO)HYBRID NANOSTRUCTURES (HYBSAC), project number PNRR-III-C9-2022-I8-201, within the National Recovery and Resilience Plan.

OC8. NEW SCHIFF BASE LIGANDS FOR 3*d*, 3*d*-4*f*, 4*f*, AND 4*f*-4*f* ' COMPLEXES

Diana-Ioana Eftemie[1,2]*, Teodora Mocanu[3], Sergiu Shova[4], Diana Dragancea[2], Mihai Raduca[1,2], Marius Andruh[1,2]

[1]*Faculty of Chemistry, Department of Inorganic Chemistry, Organic Chemistry, Biochemistry and Catalysis, University of Bucharest, Bucharest, Romania*

[2]*"C. D. Nenitzescu" Institute of Organic and Supramolecular Chemistry, Romanian Academy, Bucharest, Romania*

[3]*Petru Poni Institute of Macromolecular Chemistry, Romanian Academy, Iasi, Romania*

**diana.eftemie@s.unibuc.ro*

The synthesis of 3*d*, 3*d*-4*f*, 4*f* or even 4*f*-4*f* ' polynuclear complexes represents a domain of high interest, due to the intriguing magnetic and luminescent properties they can exhibit [1-3]. The design of ligands used for their preparation must fulfill an important condition, namely to ensure a precise control over the nuclearity and spin topology of the resulting polynuclear complexes. Schiff bases are a class of ligands which are appropriate to reach this goal, as the selection of the suitable precursors allows for the control of the number and type of donor atoms, as well as the number of chelate rings [4,5]. Moreover, multicompartmental ligands of varying sizes can be generated, which are capable of accommodating different metal ions, in a selective way.

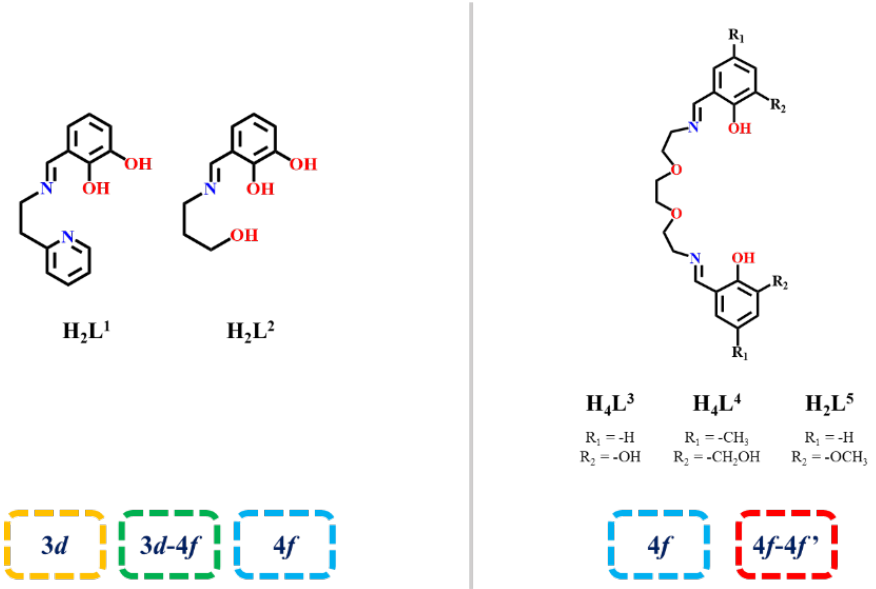

Figure 1. Structure of Schiff base ligands.

Two different types of Schiff base ligands have been used in order to synthesize homo- and heteropolynuclear complexes (**Figure 1**). The first type is obtained by the condensation reaction between 2,3-dihydroxybenzaldehyde and an amine partner such as 2-(aminoethyl)pyridine ($H_2\mathbf{L^1}$) or 3-amino-1-propanol ($H_3\mathbf{L^2}$) in a 1:1 molar ratio. These ligands are tetradentate and feature two asymmetric compartments. The ligand $H_2\mathbf{L^1}$ has been previously utilized in the literature for the synthesis of a tetranuclear Cu(II) complex [6]. We used this ligand for the preparation of Zn(II) complexes (**Figure 2 – a, b**). Additionally, these Schiff bases ($H_2\mathbf{L^1}$and $H_3\mathbf{L^2}$) give rise to both homopolynuclear 4*f* (Figure 2d) and heteropolynuclear 3*d*–4*f* complexes (**Figure 2c**).

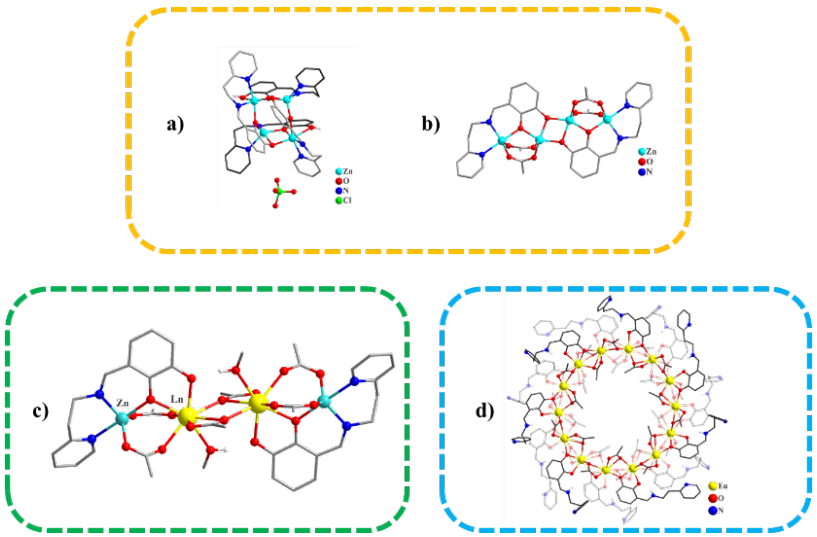

Figure 2. Molecular structure of a,b) Zn(II); c) 3*d*-4*f* and d) 4*f* complexes derived from H_2L^1.

The second type of Schiff bases is represented by a wide range of side-off bicompartmental type ligands. These are formed by the 1:1 condensation of various aldehydes, such as 2,3-dihydroxybenzaldehyde (H_4L^3), 2-hydroxy-3-hydroxymethyl-5-methylbenzaldehyde (H_4L^4) or *o*-vanillin (H_2L^5), with 1,8-diamino-3,6-dioxaoctane. Depending on the choice of reaction partners, these ligands have different denticities, some of them presenting two compartments of similar size or compartments of differing sizes. They have been used for the synthesis of 4*f* and 4*f*–4*f* ' polynuclear complexes.

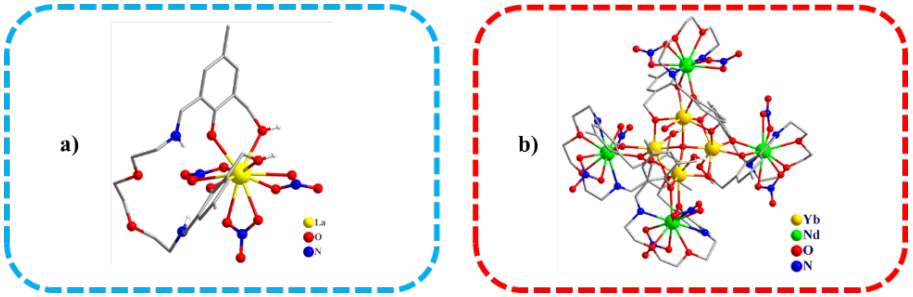

Figure 3. Molecular structure of a) 4*f* and b) 4*f*–4*f* ' complexes derived from $H_4\mathbf{L}^4$.

All compounds have been characterized by single crystal and powder X-ray diffraction, UV-VIS and IR spectroscopies. Also, photoluminescence analysis of some complexes has been performed.

References

[1] C. Alexandre, Z. Guo, P.B. Glover, S. Faulkner, Z. Pikramenou, *Chem. Rev.* 2025, 125, 2269-2370.
[2] R. Janowski, M. Wyczesany, S. Chorazy, *Chem.Commun.* 2023, 59, 5961-5986.
[3] R. Marin, G. Brunet, M. Murugesu, *Angew.Chem.Int.Ed.* 2021, 60, 1728-1746.
[4] M. Andruh, *Chem.Commun.* 2011, 47, 3025-3042.
[5] M. Andruh, *Dalton Trans.* 2015, 44, 16633-16653.
[6] E. Gojon, S.J. Greaves, J.-M. Latour, D.C. Powey, G.W. Smith, *Inorg. Chem.* 1987, 26, 1457-1459.

Acknowledgment: The financial support from European Union through NextGenerationEU, programme-PNRR-III-C9-2023-I8 (contract no.760230) is gratefully acknowledged. Also, Eftemie Diana extend her thanks to Dr. Cristina Tăbleț, Dr. Ingrid Freuze, Dr. Mihaela Florea, Dr. Niculina Hădade, Dr. Daniel Avram and Dr. Carmen Tiseanu for their help.

OC9. TARGETED REMOVAL OF PHENOLIC POLLUTANTS FROM WATER USING METAL-ORGANIC FRAMEWORKS IMPREGNATED WITH IONIC LIQUIDS

Marcela Iosivoni[1]*, Nicoleta Plesu[1], Bianca Maranescu[2], Lavinia Lupa[3], Aurelia Visa[1]
[1]*"Coriolan Dragulescu" Institute of Chemistry, Romanian Academy, Timisoara, Romania*
[2]*Faculty of Chemistry, Biology, Geography, West University of Timisoara, Timisoara, Romania*
[3]*Faculty of Industrial Chemistry and Environmental Engineering, Politehnica University, Timisoara, Romania*
**miosivoni@gmail.com*

Phenol (PH) and phenol derivatives are problematic organic pollutants in industrial wastewater resulting from petrochemical processes. These compounds present a significant risk to the environment and human health due to their high toxicity and persistence. Conventional water treatment methods face substantial challenges in effectively removing these pollutants because of their high-water solubility and the extremely high cost of these techniques. Therefore, there is an urgent need to develop sustainable, cost-effective, and highly efficient adsorbent materials to ensure the safety of water resources.

Guided by the 12 principles of green chemistry, we synthesized metal-organic frameworks (MOFs) through alternative synthesis methods, namely hydrothermal synthesis [1,2], sonochemical and microwave assisted synthesis, using water as solvent. The MOFs have been synthesized from etidronic acid (HEDP) with different metal salts, such as bivalent metal ions Co^{2+}, Ni^{2+}, as well as trivalent metal ion Ce^{3+}. Figure 1 presents the alternative synthesis methods and their advantages.

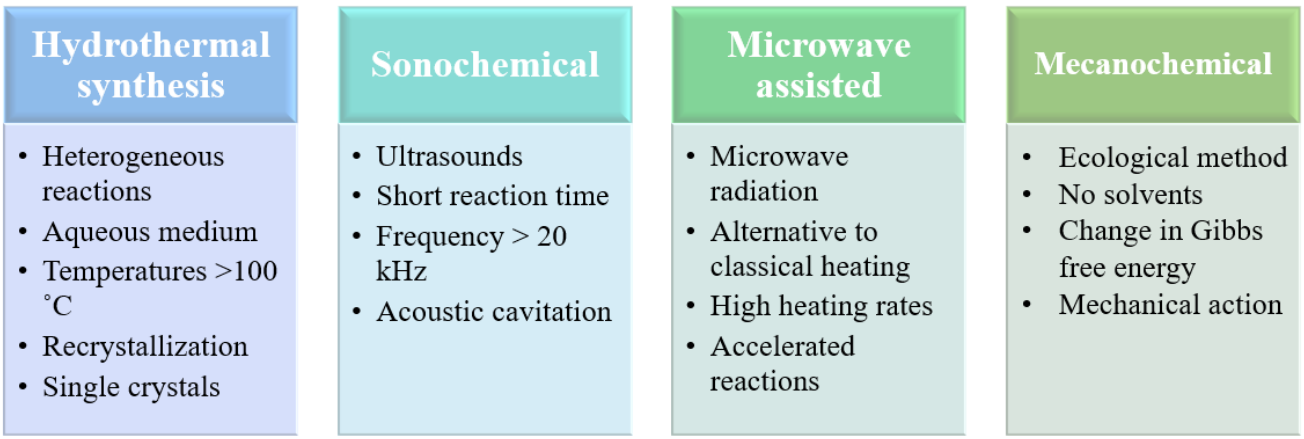

Figure 1. Alternative synthesis methods and their advantages.

In order to improve their adsorption performance, the synthesized MOFs (CoHEDP, NiHEDP, CeHEDP) were functionalized with imidazolium-based ionic liquid, namely 1-ethyl-3-methylimidazolium chloride and 1-hexyl-3-methylimidazolium chloride, resulting IL@MOF. All materials (CoHEDP, CeHEDP, NiHEDP, IL@MOF) have been characterized using Fourier Transform Infrared Spectroscopy (FTIR), X-ray diffraction (XRD), thermogravimetric analysis (TGA) and Scanning Electron Microscopy (SEM).

The adsorption capacity of the synthesized metal-organic frameworks unimpregnated and impregnated with ionic liquids to phenol and phenol derivatives was tested. The highest performance was observed for the cerium-based framework, while the lowest performance was obtained for the nickel-based MOF.

The materials functionalized with 1-hexyl-3-methylimidazolium chloride exhibited the highest adsorption capacity. The best result was achieved by CeHEDP impregnated with the ionic liquid (IL), showing a twofold increase in the maximum adsorption capacity for 2,6-dimethylphenol compared to the pristine MOF. The adsorption process followed the Langmuir isotherm model. This strong fit suggests that the adsorption of phenol derivatives onto the studied materials occurs primarily through physical sorption [3].

The electrochemical oxidation (EO) process of phenol (PH) released from the exhausted adsorbent was investigated using platinum (Pt) and graphite electrodes, in different media (saline, basic, and acidic) and at various temperatures, in order to achieve electrochemical regeneration of the spent adsorbent. In the presence of phenol, the current densities decreased with the increasing number of scan cycles, suggesting a decline in the electrochemical activity of the anode. The decrease in anodic activity is attributed to the formation of EO products resulting from the incomplete oxidation of phenol. Preliminary results indicate that the main species formed during the degradation process are hydroquinone, resorcinol, and p-benzoquinone, as confirmed by UV-Vis spectroscopic data.

This research study successfully confirms the synthesis of a new class of cost-effective materials with proven effectiveness in purifying water contaminated with phenol and phenol derivatives. The adsorption mechanism analysis, supported by strong fit with the Langmuir, indicates that the removal of pollutants occurs predominantly via physical sorption. Following the adsorption process, the regeneration of the spent adsorbent was preliminarily investigated through electrochemical methods.

References

[1] P. Anastas, J. Warner, *Green Chemistry: Theory and Practice*, Oxford University Press, New York, 1998.
[2] Y. Zhao, Z. Wang, Z. Bao, H. Xing, Z. Zhang, B. Su, Q. Yang, Y. Yang, Q. Ren, *Separ. Purif. Technol.* 2018, 195, 238-243.
[3] L. Lupa, N. S. Tolea, M. Iosivoni, B. Maranescu, N. Plesu, A. Visa, *RSC Advances* 2024, 14, 4759-4777.

Acknowledgment: This work is partially supported by Program no 2, from the „Coriolan Drăgulescu" Institute of Chemistry Timisoara, Romania and by a grant of the Ministry of Research, Innovation and Digitization, CNCS-UEFISCDI, project number PN-III-P4-PCE-2021-0089, within PNCDI III.

OC10. GUAR/GELATIN MATRIX AS PLATFORM FOR *VACCINIUM VITTIS- IDAEA* EXTRACT RELEASE

Irina Apostol*, Narcis Anghel, Iuliana Spiridon
Petru Poni Institute of Macromolecular Chemistry, Romanian Academy, Iasi, Romania
**apostol.irina@icmpp.ro*

Biodegradability, biocompatibility and low toxicity are the main advantages of natural polymers-based materials, making them suitable for cosmetic use [1]. This study aimed to develop materials for potential topical drug delivery applications. Thus, guar (Gu) and gelatine (Ge) were used as the matrix components while lignin (Li), lignin aspartate (LiAs), lignin succinate (LiSc) and *Vaccinium vittis-idaea* (Vv) extract as fillers. The formulations (Gu/Ge, Gu/Ge/Vv, Gu/Ge/Li, Gu/Ge/Li/Vv, Gu/Ge/LiAs, Gu/Ge/LiAs/Vv, Gu/Ge/LiSc, Gu/Ge/LiSc/Vv) were prepared *via* the casting method.

The Vv extract has a total phenolic content (TPC) of 37.02 mg gallic acid (GAE)/g extract and a total flavonoid content (TFC) of 84.0 mg quercetin (QE)/g extract.

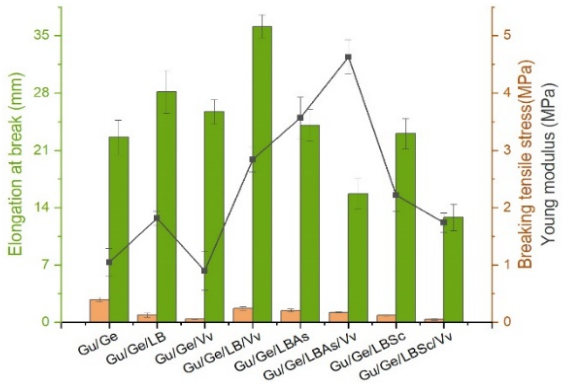

Figure 1. Mechanical properties of the obtained materials.

Tensile properties of the obtained materials were evaluated (**Figure 1**). The decrease in mechanical strength after fillers' adding is mainly due to replacing of some linkages established between matrix components that led to weakening of overall film structure [2]. The incorporation of Vv extract made the films more rigid and less flexible, while Li and its derivatives addition resulted in the increased flexibility (elongation at break) and reduced tensile strength. This behaviour may be correlated to the hydrophobic nature of Li, which creates a more heterogeneous microstructure.

The opacity of the materials increased with the filler's addition.

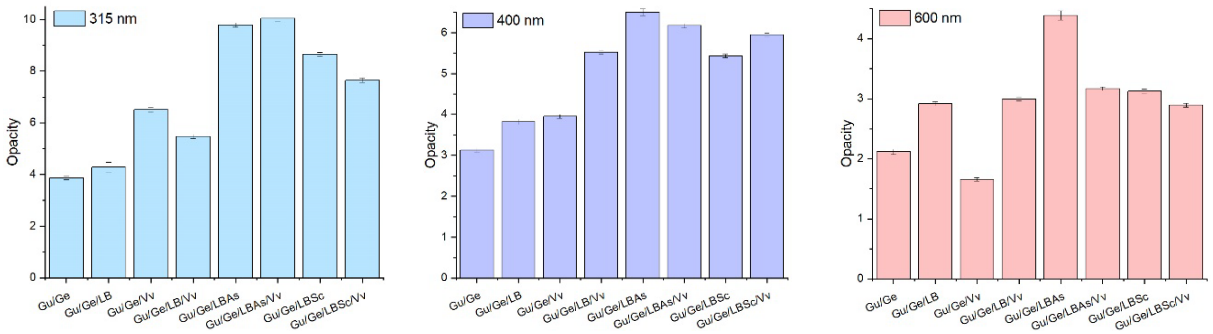

Figure 2. Materials opacity.

The color and complex structure of lignin and the presence of polyphenols in Vv extract enhanced light scattering within matrix (**Figure 2**).

The antioxidant activity of the obtained materials (Table 1) was evaluated by DPPH free radical scavenging activity method. It was found that the presence of Vv extract greatly enhanced radical scavenging ability. This could be due to the presence of hydrophobic amino acids and aromatic amino acids from the extract [3].

Table 1. Antioxidant activity of the obtained materials.

Material	DPPH inhibition (%)
Gu/Ge	1.89±1.26
Gu/Ge/Vv	19.62±1.89
Gu/Ge/Li	29.95±0.96
Gu/Ge/Li/Vv	29.74±1.26
Gu/Ge/LiAs	16.45±1.26
Gu/Ge/LiAs/Vv	9.70±1.59
Gu/Ge/LiSc	11.81±1.93
Gu/Ge/LiSc/Vv	20.46±1.46

Release kinetics of Vv natural extract revealed that Weibull model is proper for fitting the experimental data (R^2 values between 0.976–0.996) (**Figure 3**).

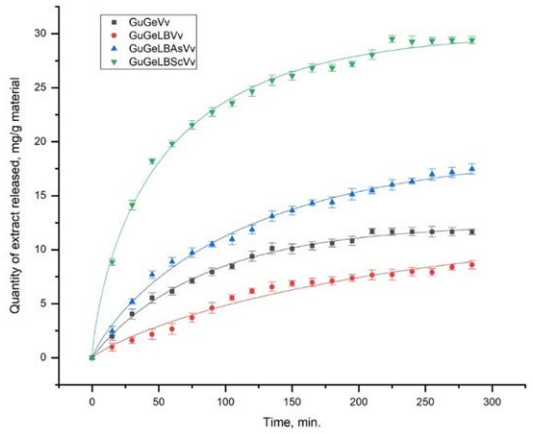

Figure 3. Release kinetic of Vv extract from tested materials according to Weibull model

The shape parameter, d, which was < 1 for all samples, indicating a Fickian diffusion-controlled release consistent with the expected behavior of these systems.

According to the obtained results, the Gu/Ge/LBSc/Vv material is best suited for applications requiring rapid and efficient extract release (~98%), while Gu/Ge/LB/Vv shows potential for sustained delivery. These findings support the design of customizable delivery systems for targeted therapeutic applications.

Overall, the obtained results demonstrate a strong correlation between the structure of the materials and biological properties. The combination of natural polysaccharides and protein with functionalized lignins/phenolic-rich plant extracts led to the sustainable materials exhibiting antioxidant effect.

References

[1] P. J. Manna, T. Mitra, N. Pramanik, V. Kavitha, A. Gnanamani et al., *Int. J. Biol. Macromol.*2015, 75, 437.
[2] R. Jafari, M. Zandi and A. Ganjloo, *J. Polym. Environ.* 2023, 31, 1568.
[3] Y. Feng, D. Yuan, C. Cao, B. Kong, F. Sun et al., *Food Hydrocoll.* 2022, 131, 107756.

OC11. POLYMER/SAND COMPOSITES WITH FAST SORPTION TOWARD SOLUBLE ORGANIC POLLUTANTS

Timeea-Anastasia Ciobanu*, Florin Bucatariu, Larisa-Maria Petrila, Marius-Mihai Zaharia, Marcela Mihai

Petru Poni Institute of Macromolecular Chemistry, Romanian Academy, Iasi, Romania
**timeea.ciobanu@icmpp.ro*

Water pollution has become one of the most critical issues our society is facing. Numerous studies documenting the concentration of various pollutants in water flows and their effect on human health have been published in recent years [1]. Pollutants can obstruct sunlight from penetrating water bodies, thereby hindering photosynthesis in aquatic plants, or they can accumulate in the tissues of marine organisms. As a result, an entire ecosystem can be destabilized and bioaccumulation of pollutants can have a negative impact on higher trophic levels, even on humans [2]. The search for water cleaning solutions has been a priority, and researchers have designed several treatment methods, such as ultra- and nanofiltration, advanced oxidation processes, sorption, etc. One of the simplest and most cost-effective approaches is the use of composite sorbents, which can effectively remove various classes of pollutants. The approach proposed in the current study consists of obtaining core-shell composite particles based on natural quartz sand and weak polyelectrolytes (PE), namely poly(ethyleneimine) (PEI) and poly(sodium methacrylate) (PMANa), designed for pollutant sorption and solid phase extraction applications [3] (**Scheme 1**).

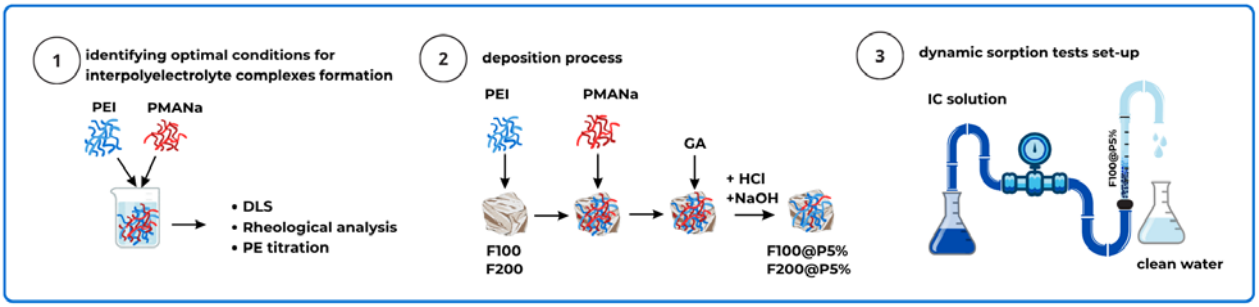

Scheme 1. Polymers/sand composite fabrication for pollutants removal: interpolyelectrolyte complexes characterization (1), PE deposition process (2) sorption experimental set-up (3).

The core-shell composite particles were obtained through the direct deposition of PEI and PMANa onto quartz sand particles. For this, the initial sand sample was sieved using a Retsch vibratory sieve shaker (Retsch LLC, Haan, Germany), separating it into two samples with different particle sizes, labeled as F100 and F200, with average particle sizes of 180 µm and 250 µm, respectively. Dynamic Light Scattering (DLS) analysis, using the Litesizer DLS 500 equipment (Anton Paar, Graz, Austria), and PE titration using a Particle Charge Detector Mutek PCD-03 (GmbH, Herrsching, Germany), were employed to determine the appropriate molar ratio between the structural units of the two PEs at different pH values by observing complex formation and stability. Rheological measurements, conducted with the MCR 92 Rheometer (Anton Paar, Austria), helped establish the PE concentrations necessary for precipitating the interpolyelectrolyte complexes by examining the behavior of 1 M and 0.01 M concentrated PEI/PMANa complexes as a function of shear rate at 25 °C. The sand/PE composites were prepared as follows: 1 M PEI aqueous solution

was first deposited onto sand particles, followed by the addition of 1 M PMANa aqueous solution under stirring, in a 5% (w/w) PE/sand ratio. To stabilize the PE shell, glutaraldehyde was used as a chemical cross-linker. The composites then underwent a flexibilization treatment with NaOH and HCl solutions, which caused the desorption of weakly bound PE chains from the polymeric shell, resulting in two composites labeled F100@P5% and F200@P5%. The elemental composition of the samples was semi-quantitatively assessed using an EDAX Octane Super SDD detector integrated into a Scanning Electron Microscope (SEM) (Verios G4 UC, Thermo Scientific, Brno-Černovice, Czech Republic). The resulting composites were loaded into an OMNIFIT chromatographic glass column to evaluate their sorption/desorption capacity using an anionic dye, Indigo Carmine (IC), as a model pollutant. Several tests involved passing IC solutions of varying concentrations through a glass column with a Shenchen peristaltic pump, which controlled the flow rate. The dynamic sorption of IC was studied in a multi-parameter setup to analyze how influent concentration, flow rate, pressure drop, and particle size influence the sorption process. Additionally, the material's capacity to concentrate IC molecules was assessed through solid-phase extraction by eluting the sorbed IC in NaOH. UV-Vis measurements were used to quantify both the sorption and concentration capacities of the composites, performed with a SPEKOL 1300 spectrophotometer (Analytik Jena, Germany) at $\lambda = 610$ nm.

DLS measurements and PE titration results indicated that the optimal conditions for PEI/PMANa interaction are $6 < pH < 7.5$ and the molar ratio PEI: PMANa = 10:8. The rheological measurements demonstrated that, at 1M concentration, the complex exhibited a 1 kPa·s shear viscosity in bulk, characteristic of highly condensed organic matter, indicating high affinity between the complementary polymeric chains. SEM/EDAX analysis confirmed the deposition of the PE shell onto the surface of the inorganic core. The dynamic sorption experiments demonstrate that, under non-competitive conditions, the sorption efficiency of these composites is influenced by particle size rather than flow rate, suggesting that F100@P5% is the more suitable option. After 10 sorption/desorption cycles, the F100@P5% composites showed good reusability, losing only 10% of their sorption capacity by the end of the 10th cycle. Lastly, UV-Vis spectroscopy confirmed that 95% of the diluted IC solution (0.2 mg/L) passing through the column was sorbed and subsequently eluted in 3 mL of 0.1 M NaOH, resulting in a calculated concentration factor of 2000x.

The results from the sorption/desorption tests demonstrate that the proposed material can be effectively used in multiple cycles for removing anionic dyes and for solid phase extraction.

References

[1] Y. Vasseghian, S. Hosseinzadeh, A. Khataee, E. Dragoi, *Sci. Total Environ.* 2021, 796, 149000;
[2] G. Bhendekar, P. Bele, V. Wankhade, *Internat. J. Life Sci.* 2024, 12(2),219-221;
[3] F. Bucatariu, L.M. Petrila, T.A. Ciobanu, M.M. Zaharia, M. Mihai, *Appl. Sci.* 2025, 15, 10725;

Acknowledgements: This work was supported by a grant of the Ministry of Research, Innovation and Digitization, CNCS-UEFISCDI, project number PN-IV-P1-PCE-2023-1545, within PNCDI IV.

OC12. HOST–GUEST INTERACTIONS BETWEEN FUNCTIONALIZED NITROXIDE RADICALS WITH β- AND γ-CYCLODEXTRINS STUDIED BY EPR SPECTROSCOPY

Muhammed Alkali[1]*, Alexandru Gabriel Bucur[1], Jean-Patrick Joly[2], Gabriela Ionita[1]
[1]*Institute of Physical Chemistry – Ilie Murgulescu, Romanian Academy, Bucharest, Romania.*
[2]*Aix Marseille University, ICR (UMR 7273), Marseille, France.*
**muhammed.alkali@s.unibuc.ro*

Introduction. Nitroxide radicals are molecular probes that are useful for studying local environments via electron paramagnetic resonance (EPR) spectroscopy. The signals associated with these compounds are often sensitive to changes in motion, polarity, and molecular interactions [1]. Cyclodextrins (CDs) are ring-shaped molecules with a hydrophobic inner cavity and a hydrophilic outer surface. They can trap small molecules inside their cavities, forming host–guest complexes in water. Among them, β-CD has a medium-sized cavity consisting of 7 glucose units, while γ-cyclodextrin is larger, having 8 glucose units. Consequently, when a nitroxide enters a cyclodextrin cavity, its EPR spectrum changes, usually by showing line broadening and changes in hyperfine splitting. These effects indicate how strongly and deeply the radical is included within the host [2]. In this ongoing study, we investigated how derivatives of 3-carboxy-PROXYL (1a, 1b, 1c & 1d) and an isomeric pair of a phosphorylated nitroxide (2a & 2b), as shown in **Scheme 1**, interact with β- and γ-CDs in water using EPR measurements taken at different cyclodextrin concentrations.

Methodology. The radicals from 3-carboxy PROXYL derivatives (1a-d) were prepared by slightly modifying methodologies employed elsewhere [3]. The reaction involved firstly protecting the hydroxydic acid as an allyl ester before carrying out a Steglich esterification with 3-carboxy PROXYL, whose -OH group from the carboxylic acid had also been protected as an O-acylisourea group. The phosphorylated compounds were reproduced based on the protocols detailed in the work referenced in [4]. These compounds were alternatively characterized structurally by NMR and/or mass spectrometry studies. The EPR spectra of radicals were recorded in various solutions of CDs.

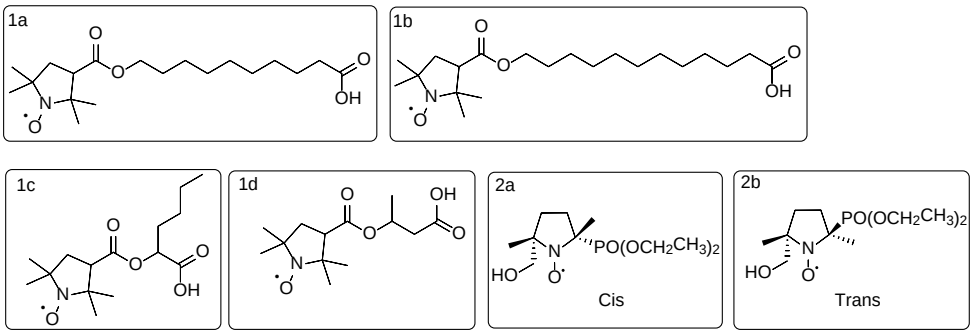

Scheme 1: Structures for the synthesized radicals.

Results and discussions. The analysis of the EPR spectra (**Figure 1**) of all the spin probes indicates that upon complexation with CDs, the nitrogen hyperfine splitting parameter (aN) decreases relative to the free radicals in water and this decrease is more pronounced for γ-CD than for β-CD which indicates a deeper inclusion of the radical into the γ-CD cavity.

For the radicals 2a & b in water, the phosphorus hyperfine splitting (aP) is smaller for the cis isomer than for the trans isomer (**Table 1**). Upon complexation with β-CD (using the highest conc. of 10^{-2} M as an example), the cis isomer shows essentially no change in aP, whereas the trans isomer exhibits an increase of approx. 1 G. In contrast, γ-CD (using the highest studied conc. of 10^{-1}M) produces larger increases approximately 3 G for the cis isomer and 5 G for the trans isomer, indicating a deeper inclusion in γ-CD.

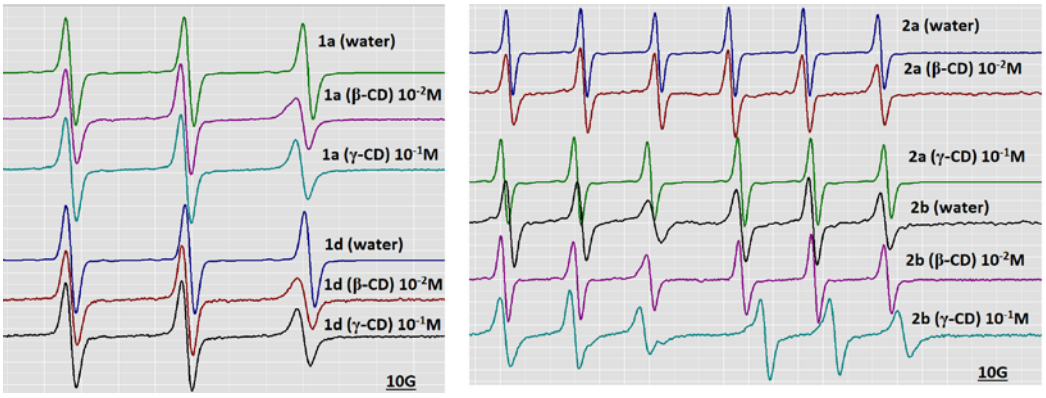

Figure 1: Selected EPR spectra obtained from the study.

To probe rotational dynamics, simulations were used to determine the rotational correlation time (τ), which was found to increase for all the studied complexes by approximately one order of magnitude compared to the free radicals, indicating that CD binding restricts radical mobility. Slightly larger τ values are observed for γ-CD complexes than for the β-CD complexes, which is attributable to the larger size of γ-CD relative to β-CD.

Table 1: Values for the hyperfine splitting constants for selected EPR spectra (β- and γ-CD concentrations are 10^{-2}M and 10^{-1}M, respectively).

	water		β-CD		γ-CD	
Samples	**aN**	**aP**	**aN**	**aP**	**aN**	**aP**
1a	16.08424	--	15.63091	--	15.37391	--
1b	16.06996	--	15.61663	--	15.36677	--
1c	16.1285	--	15.63805	--	15.39175	--
1d	16.13921	--	15.64876	--	15.41317	--
2a	15.03	44.89	14.83	44.89	14.46	46.41
2b	14.77	47.74	14.15	48.78	13.95	52.33

References

[1] H. Karoui, F.L. Moigne, O. Ouari, P. Tordo, *Stable Radicals*; Hicks, R. G., Ed.; Wiley, 2010, 173–229.
[2] G. Ionita, S. Mocanu, I. Matei, *Phys. Chem. Chem. Phys.* 2020, 22(21), 12154–12165.
[3] A. Jordan, K.D. Whymark, J. Sydenham, H.F. Sneddon, *Green Chem.* 2021, 23(17), 6405–6413.
[4] G. Audran, L. Bosco, P. Brémond, T. Butscher, J.-M. Franconi, K. Kabitaev, S.R.A. Marque, P. Mellet, E. Parzy, M. Santelli, E. Thiaudière, S. Viel, *RSC Adv.* 2016, 6(7), 5653–5670.

Acknowledgment: The authors wish to thank the Ministry of Research, Innovation and Digitization through the Romanian National Recovery and Resilience Plan, for funding. Project PNRR-III-C9-2023 – I8 "Host-guest chemical molecular systems for healthcare applications (OMRI for identifying inflammatory pathologies)"; project code: CF97/31/072023; contract no. 760283 - 03/27/2024.

OC13. TUNABLE SUBSTITUTED IMIDAZOLIUM AND BENZIMIDAZOLIUM PRECURSORS FOR IONIC LIQUID DESIGN

Rares-Georgian Mocanu*, Alina Nicolescu, Sergiu Shova, Irina Rosca, Narcisa Marangoci, Mariana Pinteala, Dana Bejan
Petru Poni Institute of Macromolecular Chemistry, Romanian Academy, Iasi, Romania
**mocanu.rares@icmpp.ro*

The development of ionic liquids (ILs) reflects the ongoing pursuit of solvents that are both sustainable and adaptable, offering an environmentally friendly substitute for conventional volatile organic compounds. Ionic liquids are a distinct class of organic salts characterized by melting points below 100 °C [1]. Owing to their unique attributes, such as negligible vapor pressure, wide electrochemical window, high thermal stability, and structural tunability, these compounds have attracted considerable attention for their potential in a broad range of chemical and industrial applications [2].

This study presents the synthesis and characterization of a novel series of precursors designed for the development of ionic liquids derived from substituted imidazolium and benzimidazolium cations. Multiple organic salts were obtained via quaternization reactions of iodophenyl-substituted imidazole and benzimidazole precursors. By systematically varying the alkylating agent, the physicochemical properties of the resulting compounds, including melting point, viscosity, electronic characteristics, and hydrophobicity, can be effectively tuned.

The synthesis for the selected compounds follows a multi-step process (**Figure 1**):

(I) The synthesis of the precursor, through an Ullmann coupling reaction between p-diiodobenzene and either benzimidazole or imidazole, catalyzed by Cu_2O [3];

(II) The quaternization reaction of the imidazole or benzimidazole precursor, using halogenoderivatives, with the formation of halide salts;

(III) The substitution of the halide anion through metathesis reactions.

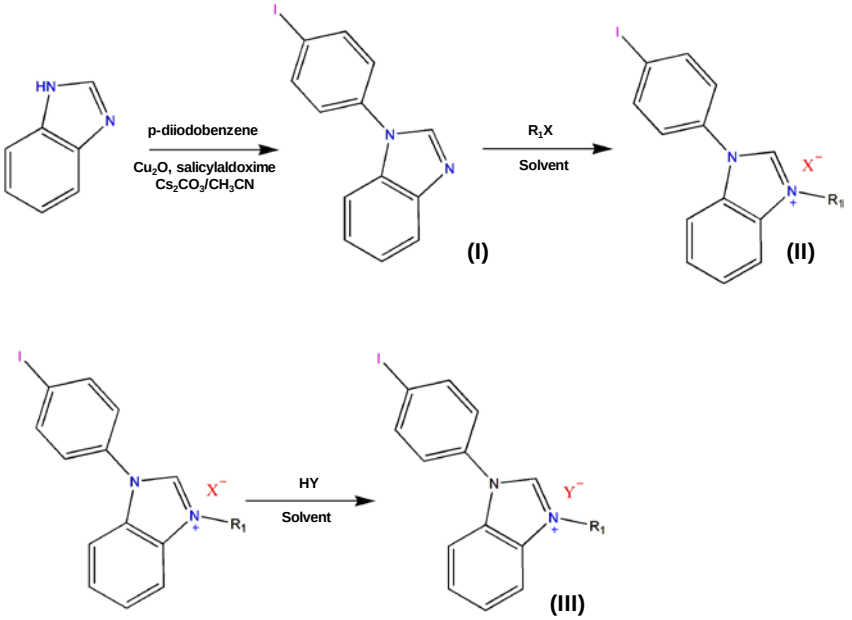

Figure 1. Reaction steps for the synthesis of the studied organic salts.

The synthesized compounds were comprehensively characterized using a combination of spectroscopic and analytical techniques to confirm their physicochemical properties. NMR spectroscopy provided detailed information on the molecular structure and purity of the synthesized compounds, while mass spectrometry confirmed the molecular weights and the presence of the desired cationic species. FT-IR spectroscopy was employed to identify characteristic functional groups. Thermogravimetric Analysis (TGA) and Differential Scanning Calorimetry (DSC) were carried out to evaluate the thermal stability and phase transition behavior of the compounds. Additionally, single-crystal X-ray diffraction was performed on selected samples to determine their molecular and crystal structures, as shown in **Figure 2.**

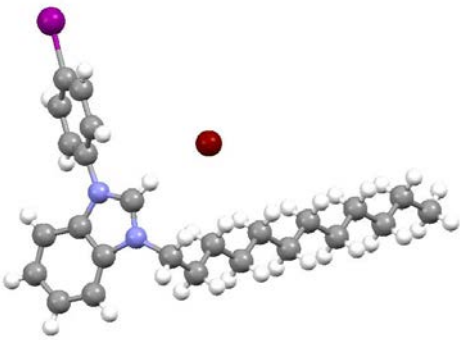

Figure 2. Crystal structure for 1-dodecyl-3-(4-iodophenyl)-benzimidazole bromide.

To further assess their potential for practical applications, selected compounds were screened for antimicrobial activity against representative bacterial strains, providing preliminary insights into their possible bioactive properties.

Furthermore, the structural diversity of the cations allows for the exploration of correlations between molecular architecture and physicochemical behavior. The insights gained from this study provide valuable guidance for the rational design of task-specific ionic liquids. The inherent versatility of these systems highlights their potential as next-generation materials across a wide range of technological applications.

References

[1] P. Wasserscheid and T. Welton, *Ionic Liquids in Synthesis*: Second Edition, vol. 1. 2008.
[2] K. Matuszek, S. L. Piper, A. Brzęczek-Szafran, B. Roy, S. Saher, J. M. Pringle, D. R. MacFarlane, *Adv. Mater.* 2024, 36.
[3] D. Bejan, L. G. Bahrin, S. Shova, M. Sardaru, L. Clima, A. Nicolescu, N. Marangoci, V. Lozan, C. Janiak, *Inorg. Chim. Acta* 2018, 482, 275.

Acknowledgment: This work was financially supported by a grant from the National Research Authority, project no. PNRR-III-C9-2023-I8-161, MultiPodGaN, contract no. 760285/27.03.2024, within the National Recovery and Resilience Plan.

OC14. ELECTROCHEMICAL METHODS FOR STUDYING THE HOST-GUEST INTERACTION OF CYCLODEXTRINS WITH NITRONYL-NITROXIDE RADICALS DERIVATIVES

Andreea Iuliana Ftodiev[1,2]*, Mihai Marian Radu[1], Loredana Preda[1], Alexandru Vincentiu Florian Neculae[1], Alexandru Gabriel Bucur[1,2], Gabriela Ionita[1]
[1]*Institute of Physical Chemistry – Ilie Murgulescu, Romanian Academy, Bucharest, Romania*
[2] *Department of Analytical Chemistry and Physical Chemistry, Faculty of Chemistry, University of Bucharest, Romania*
**andreea.ftodiev@s.unibuc.ro*

Introduction. Nitronyl nitroxides (NNs), containing two nitrogen atoms in a symmetric nitroxide environment, and imino nitroxides (INs), defined by a nitroxide group linked to an imino nitrogen, are compounds of interest due to their magnetic and chemical properties, their stable nature and distinct EPR signatures that are used as contrast agent in magnetic resonance imaging and drug delivery. Although nitroxides radicals have a high reduction rate in living systems, they can be trapped in a cyclodextrin cavity to form stable host-guest systems. Cyclodextrins (CDs), which act as ”host” molecules, are cyclic oligomers of glucose that possess hydrophobic cavities capable of forming inclusion complexes with diverse organic and inorganic molecules. Including the nitroxides in this host-guest system prolong their stability in vivo and make them more reliable for applications in biomedical field [1-4]. The inclusion complexes between nitroxides and CDs are studied with different techniques such as UV-VIS, EPR and electrochemical methods. We decided to use electrochemical methods due to their simplicity, fast response time, low cost and minimal sample preparation [5]. We used cyclic voltammetry to understand the electrochemical behavior of some nitroxide based radicals (NNB, NNP and INB) presented in **Figure 1** and to study the ”host-guest” interaction. For these investigations, two different cyclodextrins (β-cyclodextrin and γ-cyclodextrin) were employed.

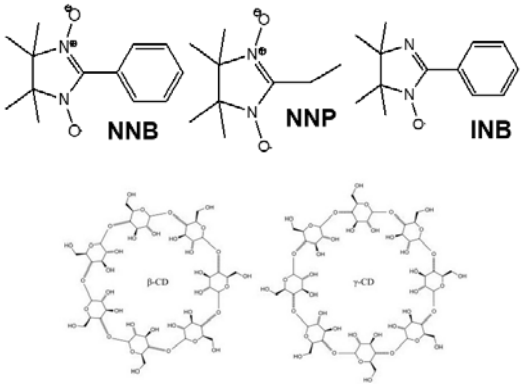

Figure 1. Chemical structure of studied radicals (NNB, NNP and INB) and of cyclodextrins used as host (β-cyclodextrin and γ-cyclodextrin) [6].

The experiments were performed in a three-electrode system in a KCl aqueous solution at room temperature. The electrochemical cell consisted of a platinum electrode as the counter electrode, a silver chloride electrode as the reference and a glassy carbon or a platinum one as the working electrode. Cyclic voltammograms were recorded both in the absence and the presence of CDs at

scan rates between 5 mV/s and 1000 mV/s. For the experiments in the presence of CDs, the host was added successively at different molar ratios host: guest from 1:4 to 13:1. The voltammograms in the absence of CDs are presented in **Figure 2**. For NNB a reversible voltammogram can be seen, oxidation being a quasi-reversible electrochemical process. A similar trend was observed for NNP. In the case of INB, the voltammogram shape indicated an irreversible voltammogram which shows an irreversible electrochemical oxidation process.

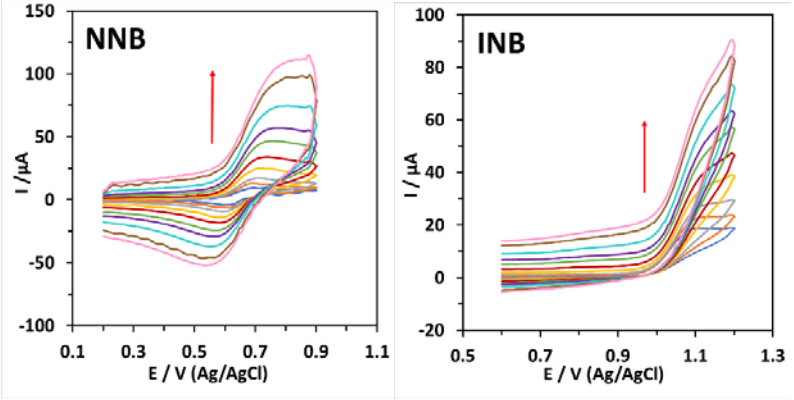

Figure 2. Voltammograms of the compounds NNB and INB in the absence of CD.

In the presence of CDs, the electrochemical mechanism remained the same, regardless the type of CDs. With the addition of CDs, the current associated with the oxidation peak decreased and the potential slightly shifted to higher positive values. Based on the literature [7] and our results, we consider that the nitroxides derivatives were included in the CDs' cavity. Accordingly, we determined the inclusion constant, K_i, for all the complexes [7]. The inclusion constant had values higher than 190 $mol^{-1} \cdot dm^3$ for all the inclusion complexes. From these investigations valuable information was obtained about the electrochemical behavior of these nitronyl-nitroxides radicals. The results obtained showed how the electrochemical behavior of these nitroxide-based radicals is directly linked to their structure. The inclusion of the radicals in the cavity of CDs is observed, no matter the type of CD.

References

[1] R.K. Strizhakov, E.V. Tretyakov, A.S. Medvedeva, V.V. Novokshonov, V.G. Vasiliev, V. I. Ovcharenko, O.A. Krumkacheva, M.V. Fedin, E.G. Bagryanskaya, *Appl. Magn. Reson.* 2014, 45, 1087–1098.
[2] Yu. G. Budnikova; T. V. Gryaznova; M. K. Kadirov; E. V. Tret'yakov; K. V. Kholin; V. I. Ovcharenko; R. Z. Sagdeev; O. G. Sinyashin, *Russ. J. Phys. Chem. A.* 2009, 83, 1976–1980.
[3] O.A. Krumkacheva, M.V. Fedin, D.N. Polovyanenko, L. Jicsinszky, S.R. Marque, E.G. Bagryanskaya, *J. Phys. Chem. B.* 2013, 117, 8223.
[4] G. Ionita, A. Caragheorgheopol, H. Caldararu, J. Leonie, V. Chechik, *Org. Biomol. Chem.* 2009, 7, 598-602.
[5] C. Wang, J. Liu, J. Kong, X. Zhang, *Analytica Chimica Acta* 2020, 1136, 19-24.
[6] R.V. Moiseev, P.W.J. Morrison, F. Steele, V.V Khutoryanskiy, *Pharmaceutics* 2019, 11, 321.
[7] M. Vilar, M. Navarro, *Electrochim. Acta* 2010, 56, 305-313.

Acknowledgment: "Chemical host-guest molecule systems for health applications" OMRI for identification of inflammatory pathologies), PNRR-III-C9-2023-I8-CF97, contract no. 760283/ 27.03.2024, project code CF97/ 31072023.

OC15. SENSITIVE COATINGS BASED ON *ORTHO*-PHENANTHROLINE POLYMER FOR DETECTION OF 2-METHYL-1-BUTANOL VAPOURS

Maria-Daniela Secman*, Loredana Vacareanu, Mariana-Dana Damaceanu
Petru Poni Institute of Macromolecular Chemistry, Romanian Academy, Iasi, Romania
**secman.daniela@icmpp.ro*

10-Phenanthroline is a rigid bidentate ligand with particular value in coordination chemistry due to its ability to form stable complexes with a wide variety of metal ions, including both main group metals and transition metals. In addition to its high chemical stability, phenanthroline also has remarkable physicochemical properties, which enable its applicability in various fields of research and technology, such as homogeneous catalysis, coordination architectures with luminescent properties, supramolecular chemistry, or advanced sensor technology. A key aspect in defining the versatility of this molecule is the presence of eight distinct positions that can be functionalized [1]. This feature gives phenanthroline exceptional structural flexibility, remarkable for a compact ligand, making it a valuable molecular platform for the design of multifunctional systems. In this context, its derivatives have been integrated into numerous functional assemblies, with applications ranging from sensitizers in dye-sensitized solar cells to biofunctionalized luminescent probes with antibodies for advanced biomedical uses.

Volatile organic compounds (VOCs) are known as indoor air pollutants that affect the environment and human health. VOCs can be released either by synthetic sources like paints, solvents, cleaning solutions, cosmetics, or aerosol sprays, or simply can come from natural sources such as microorganisms. 2-Methyl-1-butanol is a microbial VOC used as fuel substitute in biofuels, as well as solvent for chemical reactions and liquid extractions. Also, this VOC is produced by microorganisms from indoor atmosphere, and exposure to it for long time may reduce lung function, cause nocturnal breathlessness, eyes irritation, etc. Moreover, 2-methyl-1-butanol and its isomers may exert various levels of toxicity to living organisms [2]. Therefore, it is very important to explore new materials and sensor devices able to detect this specific VOC.

Along these lines, in this study we present the synthesis of a conjugated polymer based on *ortho*-phenanthroline and its evaluation as polymer coatings in what regard the capacity to detect 2-methyl-1-butanol. The chemical structures of the monomers and the resulted polymer were confirmed by spectroscopic methods such as NMR and FT-IR. The surface morphology of the polymer coatings (**Figure 1a**) was evaluated using SEM technique, which highlighted a compact morphology, with uniformly distributed granular aggregates over the entire film surface (**Figure 1b**). These granules can be attributed to the close packing arrangement through π-π interactions of the rigid polymeric chains containing bulky phenanthroline units.

The polymer coatings were further investigated for the sensing ability towards 2-methyl-1-butanol in form of vapours. The detection tests were performed by using different spectroscopic techniques (UV-Vis absorption, fluorescence, FT-IR spectroscopies) and QCM (quartz crystal microbalance). For this purpose, thin films were prepared by drop-casting a polymer solution in THF of known concentration onto a quartz or glass substrates, at room temperature.

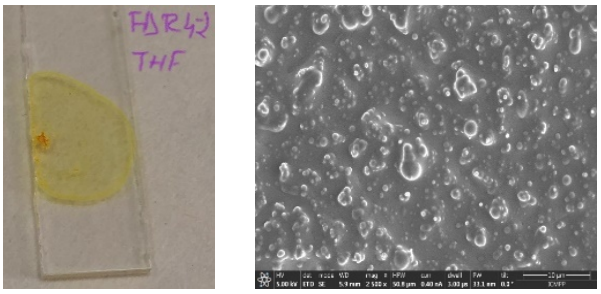

Figure 1. a) Image of the polymer-coated glass and b) the corresponding SEM micrograph.

To evaluate the sensing capacity of the synthesized polymer, first UV-Vis absorption and fluorescence spectra were recorded by sequentially exposing the polymer film to 2-methyl-1-butanol vapours for 5, 10, 20, 40, 60, 90, and 120 seconds. After only 5 seconds of exposure to this VOC, significant spectral changes occurred in both absorbance and transmittance spectra, with transmittance decreasing by 5%. This behaviour indicates a fast and effective interaction between the polymer and the VOC vapours. Mostly, this polar polymer has the capacity to attract the alcohol molecules through dipolar interactions and to swell when interacting, leading to changes in the polymer volume. The fluorescence spectra revealed a progressive decrease of the main fluorescence band up to 20s, after which no changes were observed, while FT-IR spectroscopy showed clear modifications (basically drops) of the specific band's intensities with the exposure time increase.

Finally, QCM technique was involved for the quantitative evaluation of the adsorbed/absorbed 2-methyl-1-butanol vapours. In this regard, a thin polymer film was obtained by drop-casting a diluted polymer solution onto 10 MHz AuQ crystal substrate at room temperature. After drying, the AuQ crystal loaded with the polymer was placed in a homemade QCM measurement setup. The polymer's ability to adsorb 2-methyl-1-butanol vapours was confirmed by the decrease of the resonance frequency upon exposure to this analyte, which corresponded to the crystal/polymer mass increase due to vapor adsorption/absorption.

In conclusion, a new conjugated polymer based on *ortho*-phenanthroline was successfully synthesized and structurally confirmed. It was processed into thin coatings with a homogeneous granular morphology which display high sensitivity and rapid response to 2-methyl-1-butanol vapors. This was demonstrated by various spectroscopic methods and QCM techniques, suggesting its potential for use as coatings in sensing devices like Mach-Zehnder Interferometer (MZI) sensors.

References

[1] C. Queffélec, P.B. Pati, Y. Pellegrin, *Chem. Rev.* 2024, 124(11), 6700-6902.
[2] D.-K. Nguyen,T.P. Nguyen, Y.-R. Li, M. Ohme-Takagi, Z.-H. Liu, T.-T. Ly, V.-A. Nguyen, N.-N. Trinh, H.-J. Huang, *Ecotox. Environ. Safe.* 2024, 272, 116055.

Acknowledgment: This work was financially supported by Horizon Europe (HEU 2021-2027) under grant agreement no. 101135796 (COMPAS).

OC16. SYNTHESIS OF 1,2,3-TRIAZOLE-1,4-DISUBSTITUTED DERIVATIVES *via* Cu(I)-CATALYZED HUISGEN AZIDE-ALKYNE CYCLOADDITION

Camelia-Georgiana Marandis[1,2,*], Dorina Amariucai-Mantu[1], Vasilichia Antoci[1], Catalina-Ionica Ciobanu[3], Ionel I. Mangalagiu[1], Marcela Mihai[2]
[1]*Faculty of Chemistry, "Alexandru Ioan Cuza" University of Iasi, Iasi, Romania*
[2]*Petru Poni Institute of Macromolecular Chemistry, Romanian Academy, Iasi, Romania*
[3]*ICI-CERNESIM, "Alexandru Ioan Cuza" University of Iasi, Iasi, Romania*
**marandiscamelia01@gmail.com*

The cycloaddition reactions represent powerful tools in organic synthesis for the construction of heterocyclic compounds. Among them, 1,3-dipolar cycloadditions continue to receive considerable attention from the scientific community, even though the concept was introduced by Rolf Huisgen decades ago. In particular, the Cu(I)-catalyzed Huisgen 1,3-dipolar cycloaddition of azide and alkynes (CuAAC) provides an efficient route to 1,2,3-triazoles-1,4-disubstituted. This type of cycloaddition is considered a classic example of click chemistry, a concept devised by K.B. Sharpless, H. C. Kolb and M.G. Finn to denote stereospecific reactions, simple to perform and water insensitive that lead into high-yield products with a great structural diversity [1,2].

One of the goals of pharmaceutical science is represented by the constant search of new molecules and constructs that exhibit specific biological activity. Even though the molecular design could easily conceive, the real problem results from synthesis and purification steps [3]. In this context, click chemistry become more accepted and studied for its simplicity and efficiency in generation of new hybrid or chimeric compounds with azaheterocycle skeleton which are biocompatible and pharmaceutically relevant. The resulting compounds of click reactions with 1,2,3-triazole structure can serve as linkers between different pharmacophore groups within the hybrid or hybrid-chimeric compounds, leading to their exploitation in the field of drug discovery [4].

In this respect, to contribute to the progress of this research topic, this study reports the synthesis and characterization of new hybrid-chimeric compounds with triazole structure using a terminal alkyne derivative and a series of alkyl/acyl azides *via* 1,3-dipolar cycloaddition approach, in line with click chemistry strategies (**Figure 1**). The process optimization was focused on parameters such as: molar ratios, heating time, Cu(I) source and solvent system with the aim of maximizing yield and ensuring the reproductibility of the process. During the experimental work, it was observed that the Cu(I) source and solvent system influence the most how the reaction proceeds, thus affects the yield of the final product. On the other hand, the yields of compounds obtained using acyl azides depends on the substituent of the phenacyl moiety. The key precursors were obtained through a straightforward strategy which involves two steps: quaternization of quinoline nitrogen atom in order to obtain the quaternary salt, followed by [3+2] dipolar cycloaddition reaction of quinolinium *N*-ylide generated *in situ* from quaternary salt and a variety of activated symmetrical and non-symmetrical substituted acetylenic dipolarophiles.

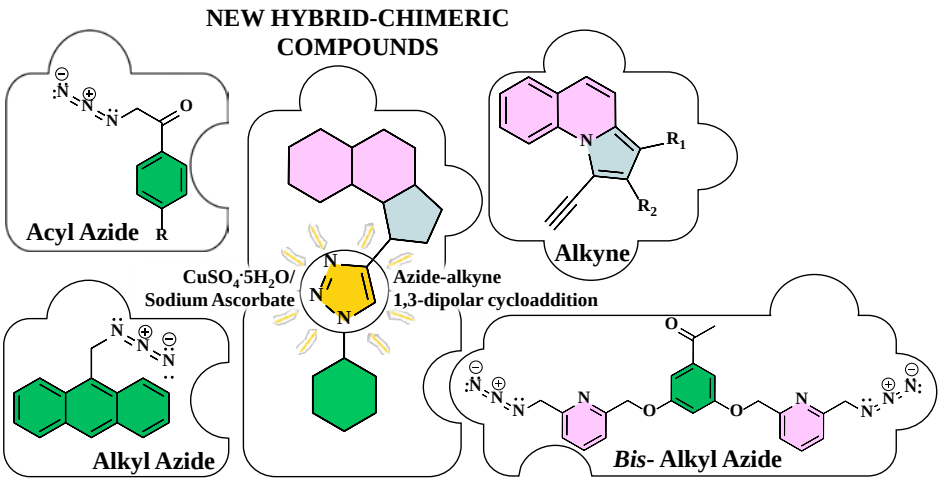

Figure 1. Design in the class of new hybrid-chimeric compounds.

The structure of new compounds was proven by performing NMR experiments: ^{1}H-NMR, ^{13}C-NMR and two-dimensional experiments - homonuclear correlations (^{1}H-^{1}H) COSY and heteronuclear correlations (^{1}H-^{13}C)-HMQC and (^{1}H-^{13}C)-HMBC. The NMR spectra were recorded on a Bruker Avance III 500 MHz spectrometer operating at 500 MHz for ^{1}H and 125 MHz for ^{13}C. Also, IR spectra were recorded to identify the functional groups of the synthesized compounds using the FT-IR Agilent Cary 630 spectrometer in attenuated total reflectance (ATR) mode. NMR analysis indicates the obtaining of 1,2,3-triazole-1,4-disubstituted derivatives through the signals of proton of triazole cycle (position 5) and those specific for azide and alkyne components. Additional evidence which confirms the proposed structure is constituted by the absence of the specific alkyne proton presented in the intermediate cycloadduct spectrum. This observation indicates that the triple bond participates in the formation of the triazole ring. Characteristic absorbtion bands observed in the IR spectra confirmed the presence of the expected functional groups such as stretching vibrations of ester -C-O- and >C=O groups from the alkyne component, ketonic >C=O group from the azide component and other specific bands depending on the azide structure.

Overall, the results of the study reveal an efficient approach in line with click chemistry strategies applied in order to synthesize the designed triazole derivatives whose structure was validated through spectral analysis.

References:

[1] M. Breugst, H. Reissig, *Angew. Chem., Int. Ed*. 2020, 59, 12293–12307.
[2] P. Kalra, R. Kaur, G. Singh, H. Singh, G. Singh, N. Pawan, G. Kaur, J. Singh, *J. Organomet. Chem.*2021, 944, 121846.
[3] J. Kaur, M. Saxena, N. Rishi, *Bioconjung. Chem.* 2021, 32, 1455-1471.
[4] A. Manoharan, J. Jayan, T. M. Rangarajan, K. Bose, F. Benny, R. S. Ipe, S. Kumar, N. Kukreti, M. A. Abdelgawad, M. M. Ghoneim, H. Kim, B. Matew, ACS Omega 2023, 8, 44437-44457.

Acknowledgements: Acknowledgment is given to infrastructure support from the Operational Program Competitiveness 2014–2020, Axis 1, under POC/448/1/1 Research infrastructure projects for public R&D institutions/Sections F 2018, through the Research Center with Integrated Techniques for Atmospheric Aerosol Investigation in Romania (RECENT AIR) project, under grant agreement MySMIS no. 127324. Authors are also gratefully to CERNESIM center, for NMR experiments.

Posters

PP1. PHENANTHRIDINIUM MONOQUATERNARY SALTS: SYNTHESIS, STRUCTURAL INSIGHTS, AND ANTIMICROBIAL ACTIVITY

Ashraf Al-Matarneh[1,2]*, Florentina Gabriela Lazar[2], Irina Rosca[2], Alina Nicolescu[2], Cristina Maria Al-Matarneh[2], Ionel I. Mangalagiu[1]
[1]Faculty of Chemistry, Alexandru Ioan Cuza University of Iasi, Iasi, Romania
[2]Petru Poni Institute of Macromolecular Chemistry, Romanian Academy, Iasi, Romania
**dr.ashraf.matarneh@gmail.com*

Monoquaternary salts of heterocycles are emerging as promising compounds in biomedical research due to their structural versatility and broad biological activities. Among these, nitrogen-containing heterocycles have gained particular attention in medicinal chemistry, serving as essential frameworks in modern drug discovery. Over 75% of FDA-approved drugs incorporate nitrogen heterocycles [1], underscoring their importance in enhancing pharmacological profiles through modulation of solubility, lipophilicity, and hydrogen-bonding capacity. These structural features contribute to wide-ranging therapeutic applications, including antibacterial, antifungal, antimalarial, anti-inflammatory, and anticancer effects [2].

Within this class, phenanthridine derivatives stand out as particularly versatile bioactive molecules. Besides their known cytotoxic and DNA-binding properties exemplified by phenanthriplatin, a platinum-based phenanthridine complex with potent antitumor activity [3], these derivatives also display broad-spectrum antimicrobial efficacy. Several phenanthridine-based compounds have shown activity against drug-resistant bacterial strains such as *Streptococcus spp*. [4], and parasitic species including Leishmania [5]. Their mechanisms of action are diverse, involving disruption of microbial cell wall permeability and inhibition of host proteins essential for pathogen replication, as reported in anti-leishmanial and anti-PEDV (porcine epidemic diarrhea virus) studies [6].

Building upon our previous research [7], the present study focuses on the design, synthesis, and antimicrobial evaluation of ten new phenanthridinium salts. Additionally, their incorporation into cyclodextrin complexes was examined to improve solubility and bioavailability. The findings contribute to a deeper understanding of structure–activity relationships in phenanthridine-based monoquaternary salts and highlight their potential as promising antimicrobial agents for future therapeutic development.

Monoquaternary salts **3a–j** were synthesized via direct N-alkylation of phenanthridine (1) using substituted 2-bromo/iodo compounds (**2a–j**) in acetone under reflux (**Scheme 1**). The resulting monoquaternary salts precipitated from the reaction mixture and were isolated by filtration. To explore the influence of substituents on reactivity and physicochemical properties, a diverse series of benzyl halides (**2a–j**) bearing sterically and electronically varied functional groups was employed. Two main factors guided substituent selection: steric variation and electronic effects.

The structures of all synthesized compounds were confirmed by ^{1}H and ^{13}C NMR spectroscopy, supported by homo- and heteronuclear 2D correlation experiments (^{1}H–^{1}H COSY, ^{1}H–^{13}C HSQC, and ^{1}H–^{13}C HMBC), as well as IR and mass spectrometry.

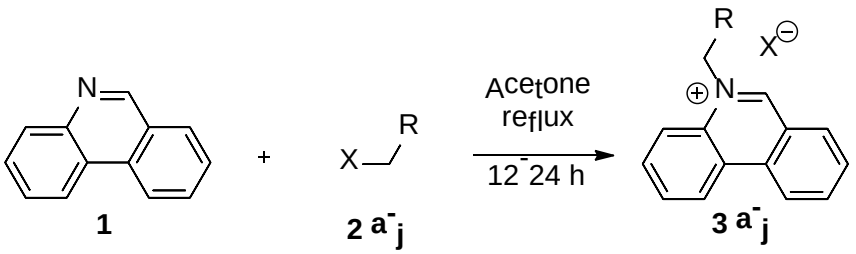

a) R = CH_2, X = Br;
b) R = C≡CH, X = Br;
c) R = $OCOCH_3$, X = Br;
d) R = $CONH_2$, X = I;
e) R = CN, X = Br;
f) R = *p*-$OMePh$, X = Br;
g) R = $COPh$, X = Br;
h) R = *p*-FPh, X = Br;
i) R = $CONH$-*p*-SO_2NH_2Ph, X = Br;
j) R = *p*-$CNPh$, X = Br;

Scheme 1. Reaction pathway for obtaining phenanthridinium monoquaternary salts (**3a–j**).

The antimicrobial activities of the synthesized compounds were assessed using disk diffusion assays. Among the tested samples, compounds **3e** and **3f** exhibited broad-spectrum activity against all tested strains. Minimum inhibitory concentration (MIC) and minimum bactericidal concentration (MBC) tests supported these results. The lowest MIC (0.15 mg/mL) was recorded for compound **3e** against *C. albicans*. MIC values of 0.31 mg/mL were obtained for **3f** (*S. aureus*, *C. glabrata*), **3b** (*K. pneumoniae*), and **3a** (*C. glabrata*). Corresponding MBC values (0.62 mg/mL) were observed for the same compound–strain pairs. For most other compounds, MBC values could not be determined within the tested concentration range (up to 20 mg/mL), and MIC was considered the highest concentration tested.

This study reports the synthesis and structural characterization of ten new phenanthridinium-based monoquaternary salts. The results reveal clear structure–activity relationships influenced by steric and electronic factors of the substituents. Several compounds, particularly **3e**, **3b**, **3f**, and **3a**, exhibited potent and selective antimicrobial activity against bacterial and fungal pathogens. These findings support continued exploration of phenanthridine-derived monoquaternary salts as promising scaffolds for the development of novel antimicrobial agents.

References

[1] M.-C. Sardaru, C.-M. Al Matarneh, N. Simionescu, I.I. Mangalagiu, M. Pinteala, R. Danac, *Rev. Roum. Chim.* 2024, 69, 63–74.
[2] J. Jampilek, *Molecules*. 2019, 24, 3839.
[3] I. Kock, D. Heber, M. Weide, U. Wolschendorf, B. Clement, *J Med. Chem*. 2005, 48, 2772–2777.
[4] P. Lasák, K. Motyka, V. Kryštof, J. Stýskala, *Molecules* 2018, 23, 2155.
[5] A.E. Czapar, Y.-R. Zheng, I.A. Riddell, S. Shukla, S.G. Awuah, S.J. Lippard, N.F. Steinmetz, *ACS Nano*. 2016, 10, 4119–4126.
[6] S. Zhang, S. Zhang, Y. Wang, Y. Zhang, S. Liang, S. Fan, D. Chen, G. Liu, *Arch. Microbiol*. 2023, 205, 371.
[7] A. Al-Matarneh, N. Simionescu, A. Nicolescu, N. Cibotariu, R. Danac, M. Al-Matarneh, I.I. Mangalagiu, *J Biochem. Mol. Toxicol*. 2025, 39, 70443-70460.

Acknowledgment: This work was supported by a grant of the Romanian National Authority for Scientific Research, CNCS – UEFISCDI, project PN-IV-P7-7.1-PED-2024-1008. (76PED/05.05.2025).

PP2. FLUOROSULFONYL-FUNCTIONALIZED NITROGEN HETEROCYCLES: SYNTHESIS AND CHARACTERIZATION

Florentina-Gabriela Lazar*, Cristina Al-Matarneh, Mariana Pinteala
Petru Poni Institute of Macromolecular Chemistry, Romanian Academy, Iasi, Romania
lazar.florentina@icmpp.ro

Considering their distinct reactivity and wide range of pharmacological applications, sulfonyl fluoride derivatives have become a significant class of chemicals in contemporary chemical biology and pharmaceutical research. This functional group is distinguished by its chemical stability in physiological conditions while maintaining its ability to engage in specific covalent interactions inside the active sites of enzymes, especially with nucleophilic amino acid residues includes serine, threonine, lysine, and tyrosine [1].

The presence of the sulfonyl fluoride fragment may influence important physicochemical characteristics, such as polarity, lipophilicity, and hydrogen-bond acceptor capacity, according to medicinal chemistry theory. Moreover, the sulfur center in the -SO_2F group is a privileged instrument in the production of covalent enzyme inhibitors and chemical probes because of its electrophilic property, enabling for exquisite control over reversible or irreversible target engagement [2]. Furthermore, the sulfonyl fluoride group's essential stability and electrophilic nature make it easier to use in the creation of covalent inhibitors, activity-based probes, and molecular modulators of key metabolic processes. These characteristics give modern medicinal chemistry a strong and flexible base, facilitating the creation of next-generation medication candidates with precise biological action and long-lasting effectiveness [3].

Nitrogen-containing heterocycles are also important scaffolds in the search for new therapeutic drugs because of their chemical plasticity, which enables the quick creation of structural analogues with optimal pharmacokinetic and pharmacodynamic profiles. Since the sulfonyl fluoride group (-SO_2F) can interact specifically with nucleophilic residues in enzyme active sites or receptor domains through covalent bonds, its incorporation into various heterocyclic frameworks provides further opportunities to fine-tune molecular recognition and reactivity. By improving target specificity and reducing off-target effects, this covalent but manageable reactivity raises the therapeutic index as a whole [2].

In this study, the main objective was the development of a new series of monoquaternary salts derived from nitrogen heterocycles functionalized with sulfonyl fluoride group. The heterocycles selected for the reaction included both monocyclic and polycyclic systems, such as pyridine, quinoline, isoquinoline, phenanthridine, benzo[*f*]quinoline, 1,7- and 1,10-phenanthroline, phthalazine, benzimidazole, imidazole, and pyridazine (**Figure 1**). This structural diversity was chosen to explore the influence of the heteroaromatic scaffold on the chemical reactivity and biological potential of the obtained compounds [4].

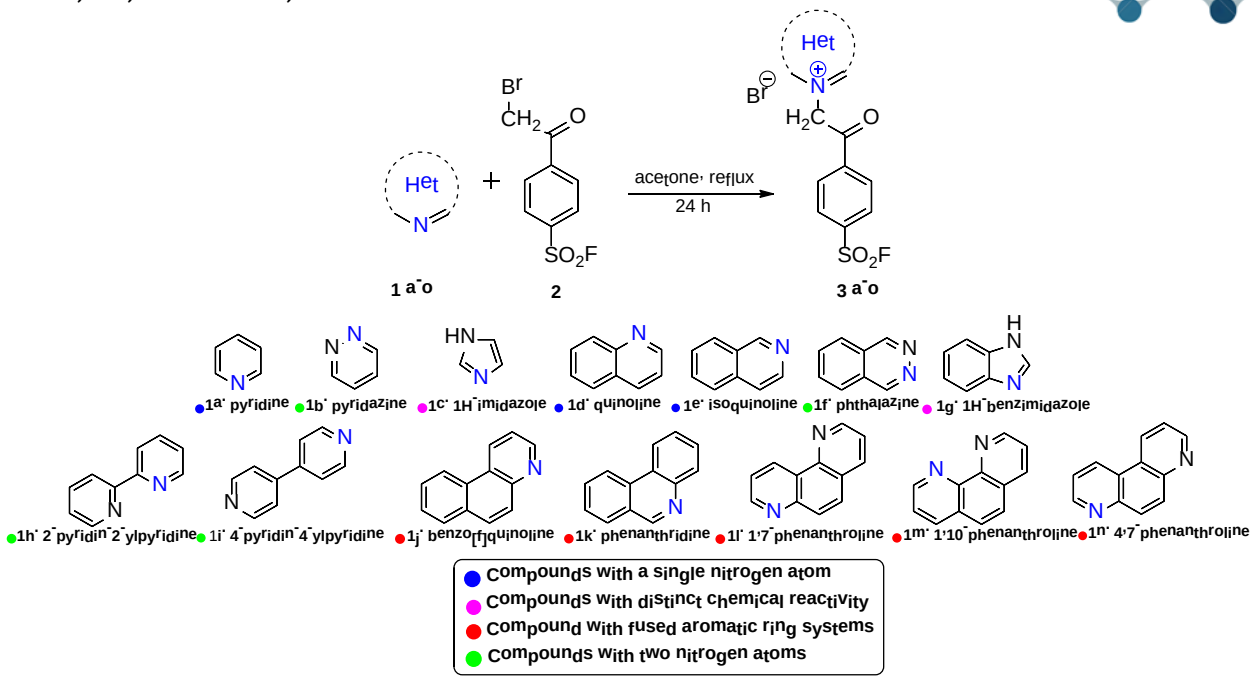

Figure 1. Scheme for the synthesis of monoquaternary salts.

The synthesized compounds were characterized using spectroscopic methods, including nuclear magnetic resonance (^{1}H and ^{13}C NMR), infrared spectroscopy (FTIR), and mass spectrometry (MS). The analyses confirmed the formation of the desired salts, as well as the structural features specific to each compound. Additionally, the pharmacokinetic properties of the synthesized compounds were evaluated, revealing favorable parameters for their development as new therapeutic agents. Most of the compounds exhibited good gastrointestinal absorption and were able to cross the blood–brain barrier, suggesting adequate bioavailability and potential applicability in treatments targeting the central nervous system. These results indicate that the series of synthesized monoquaternary salts is promising for medicinal chemistry, providing viable candidates for the development of new drugs.

Based on the properties observed in the series of monoquaternary salts, we have recently initiated the exploration of cycloaddition reactions via [*3+2*]-dipolar mechanisms. This stage is still at its early phase, and our aim is to obtain products with increased structural rigidity, while retaining the flourosulfonamide groups and nitrogen-containing cores to facilitate interactions with biomolecular targets.

References

[1] S.N. Carneiro, S.R .Khasnavis, J. Lee, T.W. Butler, J.D. Majmudar, *Org. Biomol. Chem*. 2023, 15, 1356-1372.
[2] Y.C. Dong, L-J. Wang,*Adv. Synth. Catal.* 2025, 367, e202401475.
[3] S.W. Lucas, R.Z. Qin, K.P. Rakesh, K.S. Sharath Kumar, H.-L. Qin, *Bioorg. Chem.*, 2023, 130, 106227-106248.
[4] C. Al-Matarneh, M Sardaru, N. Simionescu, I. Mangalagiu, M.Pinteala, R.Danac, *Rev. Roum. Chim.*, 2024, 69, 63-74.
[5] C. T. Supuran, *Nat. Rev. Drug Discov.* 2008, 7, 168–181.

Acknowledgment: This work was supported by a grant of the Romanian National Authority for Scientific Research, CNCS – UEFISCDI, project PN-IV-PCB-RO-MD-2024-0018. (43PCBROMD/2025).

PP3. DEEP LEARNING-BASED COMPUTER VISION SYSTEM FOR INTELLIGENT PLASTIC WASTE SORTING IN THE CIRCULAR ECONOMY

Madalina-Maria Enache*, Carmen Teodosiu
"Cristofor Simionescu" Faculty of Chemical Engineering and Environmental Protection, "Gheorghe Asachi" Technical University of Iasi, Iasi, Romania
**madalina-maria.enache-cozma@student.tuiasi.ro*

The transition toward a Circular Economy model has become a strategic imperative at the global level, particularly in light of challenges posed by the sustainable management of plastic waste. Despite the consolidation of legislative frameworks, such as Directive EU 2019/904, plastic recycling rates remain below established targets [1]. The primary obstacle lies in the inability to obtain secondary material flows that are both monopolymeric and uncontaminated. Conventional collection and sorting systems face significant operational constraints, especially at the initial stage of waste generation, where rapid and accurate identification of polymer types is essential to ensure the quality of recycled material. Traditional visual methods are inherently subjective, while spectroscopic approaches, such as Near-Infrared (NIR) technology, entail high implementation costs that hinder scalability within urban infrastructure [2].

In response to these limitations, the proposed research is grounded in the development of an innovative software framework based on Artificial Intelligence (AI). The central objective is to design and methodologically validate a computer vision system capable of real-time multi-polymer classification at the point of collection. By integrating technologies aligned with Industry 4.0, the aim is to significantly enhance the purity of collected fractions, thereby transforming plastic waste from an ecological burden into a high-value economic resource [2].

The theoretical foundation of the project is based on deep learning, a branch of artificial intelligence recognized for its effectiveness in visual pattern recognition. For the task of polymer classification, a convolutional neural network (CNN) architecture has been selected, optimized for object detection. This approach enables the processing of raw waste images and the automatic extraction of complex features such as texture, shape, opacity, and labeling, facilitating the differentiation between various types of plastic. To identify the most effective model, a comparative analysis will be conducted between state-of-the-art architectures documented in the literature, including computer vision model architecture YOLOv8, known for its inference speed, and Region Based Convolutional Neural Networks Mask R-CNN, noted for its precise segmentation of contaminated polymers. The final model will be selected based on an optimal balance between classification accuracy and processing latency, both of which are critical for real-time applications [3].

The implementation of the system will follow a structured three-phase approach. The initial phase involves the construction of a robust dataset comprising several thousand manually annotated images, covering multiple polymer classes as well as background categories. These images will be carefully curated to include variations in lighting and material wear, ensuring model generalizability.

In the subsequent phase, the selected CNN model will be trained on highperformance computing platforms, employing techniques such as transfer learning and data augmentation to enhance performance and mitigate overfitting. The system will output classification labels accompanied by confidence scores, enabling clear and rapid interpretation of the identified plastic type. The final phase will focus on the development of an intuitive software interface, integrable into a mobile application, a smart Internet of Things (IoT) container prototype, or even a waste sorting station. Functional validation will be conducted through pilot testing in both controlled and real-world environments [4].

The scientific contribution of this project lies in demonstrating the feasibility of multi-polymer classification using exclusively visual data, thereby overcoming the limitations associated with spectroscopic sensor-based infrastructures. The results will be leveraged to create a visual dataset accessible to the scientific community, contributing to the standardization of benchmarks in waste classification. From an industrial sustainability perspective, the integration of the proposed solution into plastic waste management systems is expected to yield substantial impact. Enhancing the purity of collected fractions will enable the recycled material to meet quality standards for high-end or food-grade applications, thereby increasing its economic value. Furthermore, the scalable nature and low implementation costs, attributable to the use of standard cameras, render the solution particularly suitable for urban environments and collection service providers. By reducing sorting errors, material losses will be minimized and energy consumption associated with reprocessing will be optimized.

In conclusion, this project presents an integrated approach, leveraging advanced technologies to address a pressing ecological challenge. It offers a practical model for the application of Waste Management 4.0 principles, essential for the sustainable and circular transformation of contemporary communities.

References

[1] Directive (EU) 2019/904 of the European Parliament and of the Council of 5 June 2019 on the reduction of the impact of certain plastic products on the environment, Official Journal of the European Union, L 155, 12.06.2019, pp. 1–19. Available at: https://eur-lex.europa.eu/legal-content/EN/TXT/PDF/?uri=CELEX:32019L0904&from=EN

[2] F.R. Sayem, M.S.B. Islam, M. Naznine, M. Nashbat, M. Hasan-Zia, A.K.A. Kunju, A. Khandakar, A. Ashraf, M.E. Majid, S.B.A. Kashem, M.E.H. Chowdhury, *Neural Comput. Appl.* 2025, 37, 4567–4583.

[3] J. Choi, B. Lim, Y. Yoo, Advancing Plastic Waste Classification and Recycling Efficiency: Integrating Image Sensors and Deep Learning Algorithms, *Appl. Sci.* 2023, 13, 10224.

[4] S. Wen, Y. Yuan, J. Chen, A Vision Detection Scheme Based on Deep Learning in a Waste Plastics Sorting System, *Appl. Sci.* 2023, 13, 4634

PP4. CHARACTERIZATION OF WATER RETENTION PVA/CASEIN/LIGNIN NANOPARTILESC HYDROGELS FOR SUSTAINABLE AGRICULTURE

Cosmina-Maria Bogza*, Maria-Cristina Popescu, Carmen-Mihaela Popescu
Petru Poni Institute of Macromolecular Chemistry, Romanian Academy, Iasi, Romania
**bogza.cosmina@icmpp.ro*

Introduction. In agricultural and horticultural contexts, superabsorbent hydrogels have been used to improve the physical properties of soil and reduce the need for frequent irrigation due to these properties [1]. According to research, lignin nanoparticles can pass through the tegument of seeds and enter the tissues of seedlings. This allows biocides and insecticides to be applied to plants at low concentrations, which boosts crop yields [2]. PVA is typically used in agriculture since it is non-toxic, easily degrades in the environment, and is soluble in water [3]. At the same time, it has been demonstrated that the application of casein could considerably enhance morpho-physiological characteristics like plant height, the fresh and dry weights of leaves and stems [4].

Experimental. Preparation of hydrogels. Poly(vinyl alcohol) and casein solutions in different mass ratios were used to prepare the hydrogels, to which lignin was added in different concentrations (2%, 5%, 10%). The obtained solutions were poured into Petri dishes and placed in the freezer at -20 ^{o}C for 20 h - the freeze cycle. The frozen gel was removed at room temperature (25 ^{o}C) for 4 hours - the thaw cycle. The process was repeated 5 times.

Chemical structure of hydrogels

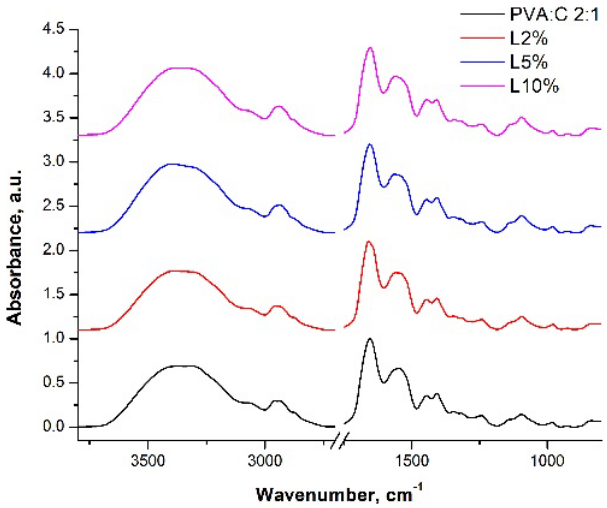

Figure 1. FT-IR spectra of hydrogels.

PVA:C (2:1) hydrogels with varying lignin nanoparticle concentrations (2%, 5%, and 10%) exhibit distinctive absorption bands in their FT-IR spectra that correspond to O–H stretching (~3300 cm^{-1}), C–H stretching (~2900 cm^{-1}), and C=O/C=C vibrations (~1700–1500 cm^{-1}).

Increasing the concentration enhances the intensity of these bands, indicating stronger interactions and successful incorporation of the lignin into the PVA:C matrix.

The swelling characteristics and kinetics

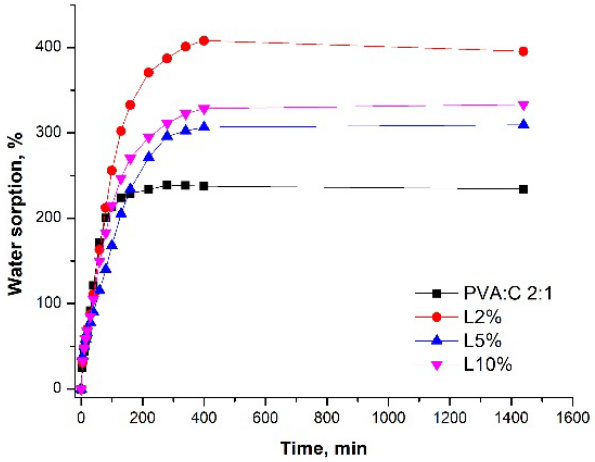

Figure 2. Water sorption of hydrogels.

For hydrogels containing twice the amount of PVA relative to casein and different concentrations of lignin nanoparticles, it can be seen that the introduction of any amount of (L) leads to an increase in the absorption rate.

Table 1. Kinetic constants for the swelling process of hydrogels.

Sample Cod	Temperature		
	20°C	37°C	45°C
	Diffusion exponential (n)		
PVA:C 2:1	0.68	0.71	0.86
L2%	0.57	0.59	0.59
L5%	0.51	0.67	0.8
L10%	0.52	0.74	0.8

For PVA:C 2:1 hydrogels, it can be seen that their diffusion exponential increases with increasing temperature. The observed results can be attributed to the lowered relaxation rate of network chains caused by the amount of PVA chains. This unmistakably shows a change in the water transport mechanism from the Fickian to the anomalous type. For those containing 2% L swelling exponent remains approximately the same.

Conclusion. Taken together, the results suggest that incorporating lignin, a renewable and underutilized biopolymer, leads to materials with favorable performance characteristics for ecological agriculture. These hydrogels offer a sustainable approach to water management in soil, with the potential to support improved crop resilience and resource efficiency.

Reference:

[1] L. Xie, M. Liu, B. Ni, Y. Wang, *Ind. Eng. Chem. Res.* 2012, 51, 3855–3862.
[2] F. Sara, I. Clemente, A. Papini, C.Tani, S. Schiff, M.C. Salvatici, *ACS Sustain. Chem. Eng.* 2019, 7, 4429–4440.
[3] F. H. Khoerunnisa, Y. Sonjaya, N. Chotimah, *J. Environ. Chem. Eng.* 2016, 4, 4863–4869.
[4] A. Jorkesh, M.H. Aminifard, *Adv. Hort. Sci.* 2019, 33, 227–233.

PP5. HETEROSTRUCTURES OF METAL NANOPARTICLES AND LAYERED DOUBLE HYDROXIDES AS ACTIVE SOLAR RESPONSIVE CATALYSTS FOR POLLUTANTS REMOVAL

Oleg Tihon*, Sofronia Bouariu, Gabriela Carja
"Cristofor Simionescu" Faculty of Chemical Engineering and Environmental Protection; Gheorghe Asachi Technical University of Iasi, Iasi, Romania
**oleg.tihon@student.tuiasi.ro*

In response to the EU's strengthened environmental regulations to combat pollution, there has been growing interest in developing advanced nanocomposite systems designed as highly efficient photocatalysts for degrading hazardous pollutants. In nanostructured catalysts, photon-dependent transport phenomena at the nanoscale enable unique photoresponsive functions that are unattainable with bulk materials [1]. However, precisely tuning these photocatalytic properties through controlled catalyst nanoarchitectonics and harnessing the collective behavior of joined nanounits remains a key challenge in the field. Layered double hydroxides (LDH) are a class of anionic clays widely recognized for their remarkable catalytic properties. Owing to their unique self-reconstruction, or "memory effect," LDHs can restore their layered structure after partial disruption. By exploiting this feature, we recently developed a straightforward synthesis route for metal nanoparticle/LDH heterostructures (MeNP/LDH), joining the nanounits structural versatility with enhanced catalytic functionality [2].

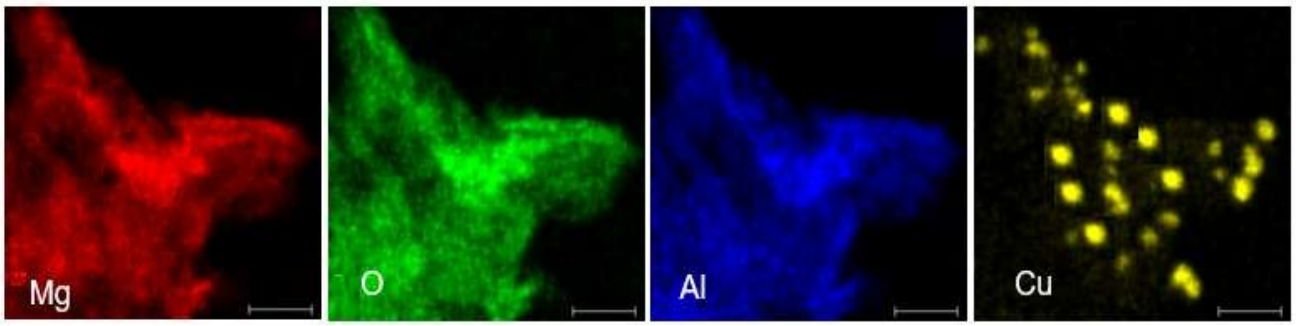

Figure 1. HAADF-STEEM elemental mapping image of CuNP/MgAlLDH (scale bar is 30 nm).

This work focuses on the fabrication of CuNP/MgAlLDH and CuNP/ZnAlLDH heterostructures and their evaluation for phenol degradation in aqueous solution. Phenol, a carcinogenic and persistent pollutant, poses serious environmental and health risks, making its efficient removal from water an urgent challenge.

By exploiting the structural "memory effect" of LDHs in copper acetate aqueous solution, the LDH, matrix reconstructs its layered structure through the intercalation of acetate anions while simultaneously Cu^{2+} ions are organized as small nanoparticles on the LDH platelets. By tuning the LDH composition, well-crystallized MgAlLDH and ZnAlLDH matrices with a Me^{2+}/Me^{3+} molar ratio of 3:1 were successfully designed.

CuNP/MgAlLDH and CuNP/ZnAlLDH catalysts were thoroughly characterized using XRD, TG/DTG, XPS, and UV-Vis spectroscopy to determine their crystalline structure, chemical composition, and photoresponsive properties. HAADF-STEM elemental mapping images was performed to study the morphological features and composition of the samples [3].

The photocatalytic tests to study the degradation of p-nitrophenol (p-NPh) were carried out in a glass- reactor with a cooling system; the reactor was placed in an appropriate position for a full illumination by a solar light simulator (UNNASOL US800, 250 W) used as an irradiation source. The results revealed that the CuNP/MgAlLDH and CuNP/ZnAlLDH heterostructures consist of copper nanoparticles with an average diameter of 10 nm, that are directly formed and deposited on the larger (~120 nm) LDH nanoparticles. The size of the CuNP increased in the catalysts derived by calcination at 550°C. UV-VIS analysis and the calculated optical direct band gap (Eg) values confirmed the high absorbance capabilities of the samples under both UV and solar light, as well as the formation of Cu- LDH heterojunctions. Furthermore, XRD analysis clearly points that the structural features of the LDH are fully recovered only after 4 hours of the structural reconstruction. Over eight hours of testing, CuNP/ZnAlLDH showed the highest phenol degradation efficiency, achieving nearly 97% degradation under solar irradiation. In contrast, the derived mixed oxides of CuO/ZnO/$ZnAl_2O_4$ achieved only 57% of phenol degradation.

These findings suggests that the size of CuNP own a critical role to establish increased photocatalytic performances. Among the photocatalytic systems examined in this study, the highest efficiency for phenol degradation was observed with CuNP/ZnAlLDH. The resulting degradation slurry contained no detectable traces of p-benzoquinone, with the mineralization products being CO_2 and water. Furthermore, the presence of highly hydroxylated brucite-type sheets in the LDH structure provided an additional advantage for the photodegradation.

This study presents key advances in the design of efficient and reusable solar-driven CuNP/LDH heterostructures, providing a robust platform for the photochemical degradation and removal of hazardous and persistent organic pollutants. The results highlight the strong potential of these heterostructures as sustainable materials for environmental remediation and circular catalytic applications.

References

[1] M.E. King, M.V.F. Guzman, M.B. Ross, *Nanoscale* 2022, 14, 602-611.
[2] G. Mikami, F. Grosu, S. Kawamura, Y. Yoshida, G. Carja, Y. Izumi, *Appl. Catal. B* 2016, 199, 260-271.
[3] D. Gilea, E.M. Seftel, T. Van Everbroeck, G. Ababei, P. Cool, G. Carja, *Catalysis Today* 2024, 425, 114342.

Acknowledgment: Oleg Tihon acknowledge a Ph.D. Grant from the Ph.D. School of Technical University “Gheorghe Asachi” of Iasi.

PP6. POLYMERIC MICROPARTICLES FOR CONTROLLED RELEASE OF NORFLOXACIN: PREPARATION AND EVALUATION

Alexandru-Mihail Serban*, Alexandra Vieru, Irina Rosca, Alina-Gabriela Rusu, Loredana Elena Nita
Petru Poni Institute of Macromolecular Chemistry, Romanian Academy, Iasi, Romania
**serban.alexandru@icmpp.ro*

Introduction

Antimicrobial resistance represents one of the main threats to global public health, with millions of deaths associated with or directly caused by it annually. The most effective alternative for improving the results of current therapies used in the treatment of such infections is the encapsulation of antibiotics in a drug delivery system. Microparticulate drug delivery systems gain extensive attention due to their intrinsic advantages, like small dimension, high surface-to-volume ratio, adequate circulation time, and enhanced encapsulation efficiency [1]. Since biocompatibility and biodegradability are essential requirements that must be met by the materials involved in the preparation of such systems, polyester-based microparticles are frequently encountered in drug delivery studies. In this context, our group reported the synthesis and characterization of poly(ethylene brassylate-co-squaric acid), PEBSA, [2–4], a polyester material obtained by copolymerization of ethylene brassylate with squaric acid, two monomers obtained from renewable sources. By bringing together a 17-membered macrolactone and an acid with polar functional groups, a biocompatible and biodegradable copolymer with amphiphilic character, thermo-responsive behaviour, and improved thermal stability is obtained. To facilitate the preparation of microparticles, a variant of the copolymer synthesized by the emulsion polymerization technique, PEBSA_Brij, was chosen due to its good dispersibility in water and ability to form small-sized structures. The aim of the study was the preparation and characterization of an oral controlled drug delivery system by encapsulating norfloxacin, a broad-spectrum antibiotic prescribed against both Gram-negative and Gram-positive bacteria, within PEBSA_Brij microparticles.

Materials and methods

The microparticles were obtained through the precipitation technique, NRF being incorporated *in situ* into the copolymer matrices [4]. The preparation method involved the dropwise addition of NRF solution in DMSO into PEBSA_Brij solution at two different polymer-to-drug volumetric ratios, 1:1 and 2:1, under vigorous magnetic stirring. The obtained complex was stirred for 24 hours and subsequently precipitated in a Tween 80 solution. The purification process involved several cycles of centrifugation, washing, and redispersion in distilled water. Polymeric microparticles dimensions, zeta potential, chemical structure, encapsulation efficiency, release behaviour, and antimicrobial properties against *E. Coli*, *S. aureus*, and *E. faecalis* were studied.

Result and Conclusions

The schematic representation of the PEBSA_Brij/NRF microparticulate drug delivery system, obtained through the precipiation technique, is illustrated in **Figure 1a**. DLS investigation revealed that all microparticles exhibited a monomodal size distribution, with their hydrodynamic diameter (D_H) decreasing as the amount of loaded NRF increases (see **Figure 1b**).

These changes underline the successful encapsulation of the drug and suggest a reduction of initial microparticles D_H and the formation of more compact structures as NRF content increases due to the establishment of physical intermolecular bonds. Zeta potential values indicated the good colloidal stability of the microparticles and the encapsulation of NRF inside PEBSA_Brij matrices. The FTIR spectra (**Figure 1c**) confirmed the chemical structure of the microparticles and the formation of hydrogen bonds. As shown in **Figure 1d**, the microparticles exhibited a biphasic release profile, with an initial burst phase lasting up to 120 minutes, followed by a sustained release over 24h. The results of the antimicrobial assays were consistent with the NRF content present in the microparticles, thus illustrating good activity against Gram-negative strains and moderate effectiveness against Gram-positive strains. The obtained results highlight the significant potential of PEBSA_Brij/NRF microparticles for use as oral drug delivery systems. Furthermore, extensive *in vitro* and *in vivo* studies are needed to further validate these findings.

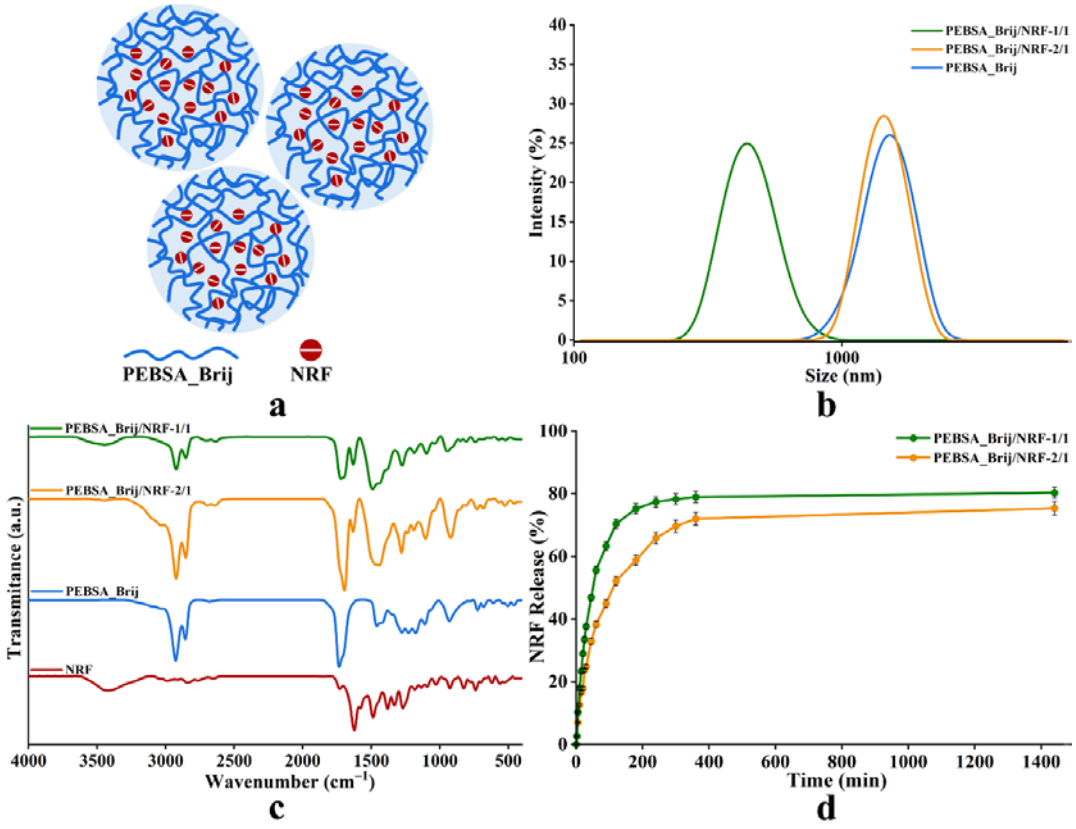

Figure 1. a) Schematic representation of PEBSA_Brij/NRF microparticles; b) Size distribution of microparticles; c) FTIR spectra of microparticles, PEBSA_Brij, and NRF; d) *In vitro* drug release.

References

[1] S.G. Carvalho, A.M. dos Santos, A.L. Polli Silvestre, A.G. Tavares, M. Chorilli, M.P. Daflon Gremião, *Expert Opin. Drug Deliv*. 2023, 20, 1231–1249.
[2] A.P. Chiriac, E. Stoleru, I. Rosca, A. Serban, L.E. Nita, A.G. Rusu, A. Ghilan, A.-M. Macsim, L. Mititelu-Tartau, *Biomed. Pharmacother*. 2022, 149, 112919.
[3] A.P. Chiriac, M. Asandulesa, I. Stoica, N. Tudorachi, A.G. Rusu, L.E. Nita, V.M. Chiriac, D. Timpu, *Polym. Test.* 2022, 109, 107555.
[4] A.-M. Șerban, I. Nacu, I. Rosca, A. Ghilan, A.G. Rusu, L.E. Niță, R.N. Darie-Niță, A.P. Chiriac, *Pharmaceutics* 2024, 16, 550.

PP7. SYNTHESIS OF NITRONYL-NITROXIDE HALOGENATED DERIVATIVES AND COMPLEXATION WITH CYCLODEXTRINS

Mihaela-Lavinia Ciutu*, Alexandru Vincentiu Florian Neculae, Carla-Cezarina Paduretu, Alexandru Gabriel Bucur, Georgiana-Alexandra Sanda, Elena-Gabriela Ionita
Institute of Physical Chemistry - Ilie Murgulescu, Romanian Academy, Bucharest, Romania
**laviniamihaela.ciutu@yahoo.com*

Introduction. Nitronyl nitroxides are characterized by an unpaired electron delocalized over an N-O···N-O fragment, which contributes to their stability and distinct magnetic properties.The spin density of nitronyl nitroxide (NN) radicals can be influenced by substituents, as studied through electron spin resonance (ESR) analysis of benzimidazole-NN radicals. Host-guest interactions using EPR spectroscopy are also reported in the literature, particularly for nitroxide radicals and cyclodextrins. Several articles involving NN interaction with cyclodextrins are also reported [1-3].

Materials and methods. Herein we report the synthesis of a series of nitronyl nitroxides obtained by reaction of 2,3-bis(hydroxylamino)-2,3-dimethylbutane with the following halogenated benzaldehydes: 2-chlorobenzaldehyde, 2,3-dichlorobenzaldehyde, 4-chlorobenzaldehyde, 3-bromobenzaldehyde, 4-bromobenzaldehyde, 2-fluorobenzaldehyde (**Figure 1**).

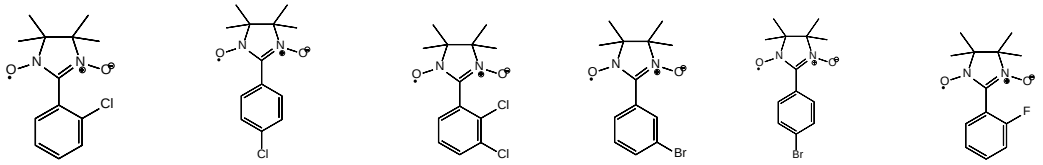

Figure 3. Chemical structure of studied halogenated derivatives of nitronyl-nitroxide radical.

These nitronil nitroxide were characterised by EPR spectroscopy and high resolution ESI mass spectroscopy. All these nitroxides have the same EPR features defined by hyperfine splitting constants $a_{N1} = a_{N2} = 7.69$ G and consist in 5 line- spectrum with the ratio between them 1:2:3:2:1. (**Figure 2**).[4-5].

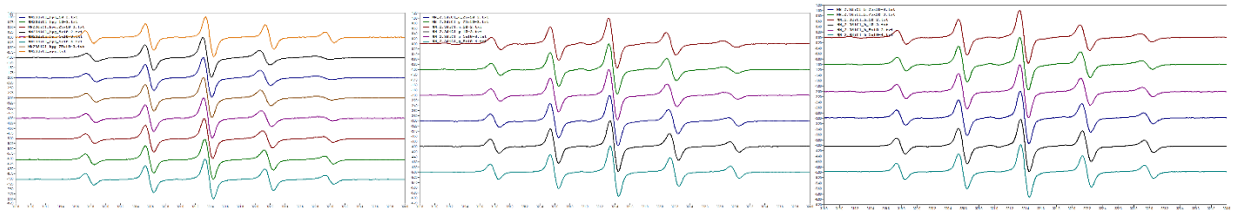

Figure 2. EPR spectra of NN-2,3 dichlorobenzaldehyde in solutions of cyclodextrins.

Further, we investigated their capacity to form inclusion complexes with β -CD, γ-CD and HP-γ-CD aiming to evidence the influence of geometric features of cyclodextrins on the host-guest complexation. In **Figure 3** are presented the EPR spectra of NN 2.3-dichlorobenzaldehyde in solutions of cyclodextrins at concentration of cyclodextrins in the range $0\text{-}10^{-2}$ M for β-CD and 0-5 $\times 10^{-2}$ M for γ-CD and HP-γ-CD.

Results and discussions.

The experimental spectra of each NN in the absence and in the presence of cyclodextrins were simulated in order to obtain the parameters of free and complexed NN (table 1). As can be noticed in (**Figure 2**) at higher concentration of CD the changes in a_N and rotational correlation time are obvious. The values are presented in **Table 1** and were used to estimate the binding constants.

Table 1. Spectral parameters for the nitronyl-nitroxide spin probe 2,3-dichlorobenzaldehyde complexed with cyclodextrins.

	Specia 1					Specia 2				
[b-CD] (M)	**aN (G)**	**aN (G)**	**lg(tcorr)**	**tau**	**%**	**aN (G)**	**aN (G)**	**lg(tcorr)**	**tau**	**%**
0	8.04	8.03	-9.6842	$2.06x10^{-10}$	100	-	-	-	-	-
$5x10^{-4}$	8.07	8.08	-9.6726	$2.12x10^{-10}$	86.07	7.84	7.83	-8.4079	$3.9x10^{-9}$	19.93
10^{-3}	8.13	8.09	-9.6919	$2.03x10^{-10}$	73.55	7.88	7.85	-8.3140	$4.85x10^{-9}$	33.52
$2.5x10^{-3}$	7.86	7.85	-9.6790	$2.09x10^{-10}$	59.88	8.13	8.16	-8.3193	$4.79x10^{-9}$	43.50
$5x10^{-3}$	8.07	7.72	-9.6033	$2.49x10^{-10}$	40.48	7.73	7.71	-8.1425	$7.2x10^{-9}$	55.64
$7.5x10^{-3}$	8.84	7.57	-9.5989	$2.51x10^{-10}$	12.68	7.93	7.92	-8.1672	$6.80x10^{-9}$	89.55
10^{-2}	7.59	8.51	-9.7099	$1.95x10^{-10}$	16.59	7.91	7.90	-8.3204	$4.78x10^{-9}$	99.88

	Specia 1					Specia 2				
[g-CD] (M)	**aN (G)**	**aN (G)**	**lg(tcorr)**	**tau**	**%**	**aN (G)**	**aN (G)**	**lg(tcorr)**	**tau**	**%**
0	8.04	8.03	-9.6842	$2.06x10^{-10}$	100	-	-	-	-	-
$5x10^{-4}$	8.06	8.07	-9.845	$1.42x10^{-10}$	70	7.69	7.70	-8.0615	$2.42\ x10^{-9}$	30
10^{-3}	8.06	8.10	-9.6892	$2.04x10^{-10}$	63.38	7.71	7.71	-8.1861	$6.51x10^{-9}$	40
$2.5x10^{-3}$	8.04	8.04	-9.6811	$2.08x10^{-10}$	61.05	7.61	7.59	-8.2455	$5.68x10^{-9}$	40.97
$5x10^{-3}$	8.02	8.01	-9.6735	$2.12x10^{-10}$	47.91	7.57	7.59	-8.1833	$6.55\ x10^{-9}$	53.52
$7.5x10^{-3}$	8.04	8.06	-9.6246	$2.37x10^{-10}$	31.85	7.64	7.63	-8.4256	$3.75\ x10^{-9}$	75.95
10^{-2}	8.05	8.01	-9.6913	$2.03x10^{-10}$	28.89	7.63	7.60	-8.0676	$8.55\ x10^{-9}$	72.87

	Specia 1					Specia 2				
[HP-g-CD] (M)	**aN (G)**	**aN (G)**	**lg(tcorr)**	**tau**	**%**	**aN (G)**	**aN (G)**	**lg(tcorr)**	**tau**	**%**
0	8.04	8.03	-9.6842	$2.06x10^{-10}$	100	-	-	-	-	-
$5x10^{-4}$	8.05	8.05	-9.7137	$1.93x10^{-10}$	70	7.56	7.63	-8.0050	$9.88x10^{-9}$	30
10^{-3}	8.07	8.03	-9.7433	$1.8x10^{-10}$	64.64	7.73	7.58	-8.1510	$7.06x10^{-9}$	40
$2.5x10^{-3}$	8.03	8.04	-9.7533	$1.76x10^{-10}$	60.15	7.50	7.58	-8.1754	$6.67x10^{-9}$	44.88
$5x10^{-3}$	8.04	8.04	-9.6535	$2.22x10^{-10}$	34.92	7.54	7.54	-8.1060	$7.83x10^{-9}$	56.03
$7.5x10^{-3}$	8.12	8.13	-9.7001	$1.99x10^{-10}$	24.19	7.78	7.76	-8.2540	$5.57x10^{-9}$	87.09
10^{-2}	-	-	-	-	-	7.76	7.76	-8.2553	$5.55x10^{-9}$	-
$5x10^{-2}$	-	-	-	-	-	7.72	7.72	-8.2409	$5.74x10^{-9}$	-

References

[1] B. Esat, I. Fidan, S. Bahceci, Y. Yerli, L. Sari, *Magn. Reson. Chem.* 2009, 47, 641–650
[2] O.A. Krumkacheva, M.V. Fedin, D.N. Polovyanenko, L. Jicsinszky, S.R.A Marque, E.G. Bagryanszky, *J. Phys. Chem. B* 2013, 117, 27, 8223–8231
[3] G. Ionita, A. Caragheorgheopol, H. Caldararu, L. Jones, V. Chechik, ***Org. Biomol. Chem.*** 2009, **7**, 598-602.
[4] M. Fettouhi, Benzo-15-Crown-5, *Molecular Crystals and Liquid Crystals Science and Technology*.,2001,356(1),365-369
[5] C. Hirel, J. Pécaut, S. Choua, P. Turek, D.B. Amabilino, J. Veciana, P. Rey, *Eur. J. Org. Chem.* 2005, 348-359.

Acknowledgment: Chemical host-guest molecule systems for health applications (OMRI for identification of inflammatory pathologies), PNRR-III-C9-2023-I8-CF97, contract no. 760283/ 27.03.2024, project code CF97/ 31072023.

PP8. SYNTHETIC ROUTE TO HETERICYCLIC SCHIFF BASES AS PRECURSORS FOR BIOACTIVE CU(II) COMPLEXES

Alexandra Birzu*, Mihaela Dascalu, Gheorghe Roman, Vladimir Arion, Maria Cazacu
Petru Poni Institute of Macromolecular Chemistry, Romanian Academy, Iaşi, Romania,
**birzu.alexandra@icmpp.ro*

Introduction

Schiff bases, a class of compounds discovered over 150 years ago, have emerged as key compounds in medicinal chemistry due to their remarkable biological activities and structural versatility. Defined by the presence of an imine group (−CH=N− or >C=N−), Schiff bases are synthesized through the condensation of primary amines with aldehydes or ketones. Their ability to form stable complexes with metal ions through coordination involving electron-donor atoms such as nitrogen or oxygen greatly enhances their pharmacological potential. Notably, heterocyclic Schiff bases, especially those incorporating nitrogen-containing scaffolds such as benzimidazole or indole, have demonstrated a wide spectrum of biological properties including anticancer, antimicrobial, antitumor, antioxidant or anti-inflammatory, while complex formation with metal ions further improves this activity [1-4].

As a part of a multi-step synthetic strategy starting from 4-methoxy-1*H*-indole-2-carboxylic acid, the preliminary steps for the preparation of the Schiff base of 3-methoxy-8-oxo-5,6,8,9-tetrahydro-7*H*-benzo[5,6]azocino[3,4-*b*]indole-indole with 2-pyridinecarboxaldehyde, intended for subsequent coordination to Cu(II) to obtain complexes with potential anticancer activity are presented herein.

Experimental

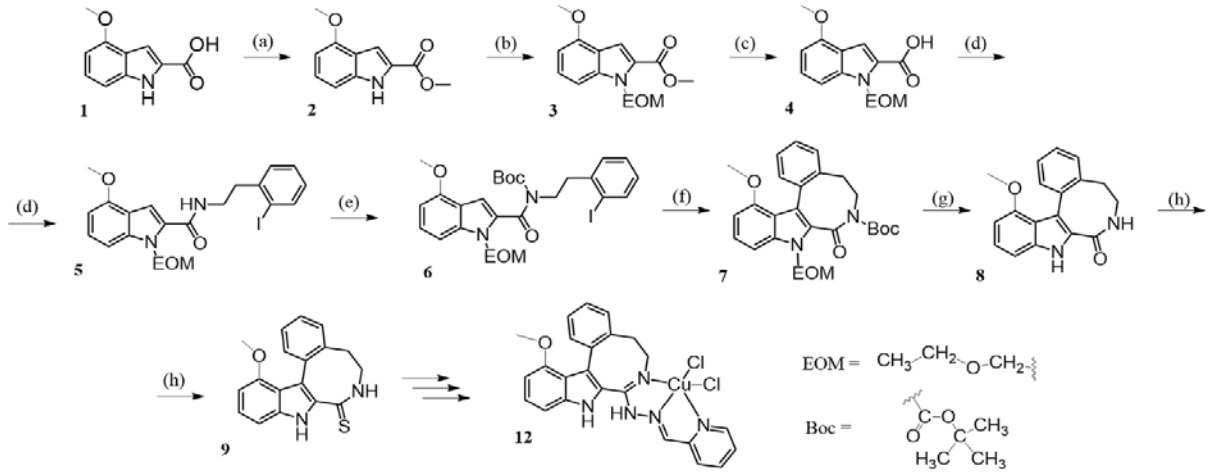

Scheme 1. Synthetic pathway toward a new methoxy-substituted indolobenzazocine-based ligand. Reaction conditions: (a) concentrated H_2SO_4, methanol, reflux, overnight; (b) chloromethyl ethyl ether, NaH, DMF, room temperature, overnight; (c) $LiOH \cdot H_2O$, ethanol/water, reflux, 2 h; (d) 2-(2-iodophenyl)ethanamine, EDCI·HCl, DMAP, DCM, 0 °C→ room temperature, 18 h; (e) Boc_2O, DMAP, dry MeCN, room temperature, 18 h; (f) $Pd(CH_3COO)_2$, PPh_3, Ag_2CO_3, dry DMF, inert atmosphere, 110 °C, 2 h; (g) aqueous HCl, dioxane, 80 °C, 2 h; (h) P_2S_5/Al_2O_3, dry toluene, 110 °C, 1 h.

Results and discussion

Preliminary modeling studies suggested that introducing methoxy substituents on either the indole moiety or the benzene ring could enhance the biological activity of second-generation indolobenzazocine-based complexes [3]. The synthesis of this novel ligand in a manner similar to analogous compounds [4] is outlined in **Scheme 1**. The synthetic sequence starts with esterification of a commercially available indolecarboxylic acid **1** with methanol, in the presence of sulfuric acid as catalyst, under reflux, to give the methyl ester **2**. This product was then *N*-alkylated with chloromethyl ethyl ether to introduce an ethoxymethyl (EOM) protecting group. Hydrolysis of the ester under basic conditions with lithium hydroxide in an ethanol–water mixture yielded the corresponding acid **4**, which was then coupled with 2-(2-iodophenyl)ethanamine using 1-ethyl-3-(3-dimethyllaminopropyl)carbodiimide hydrochloride (EDCI·HCl) and 4-dimethylaminopyridine (DMAP) in dichloromethane at 0 °C to afford the secondary amide **5**. Protection of the amide nitrogen with a *tert*-butoxycarbonyl (Boc) group afforded compound **6**, the key precursor for ring closure step. The tetracyclic indolobenzazocine core in compound **7** was assembled via a Pd(II)-catalyzed intramolecular Heck-type cyclization using $Pd(OAc)_2$, Ag_2CO_3, and PPh_3 in dry DMF, under an argon atmosphere at 110 °C. Removal of both Boc and EOM groups was then performed with dilute hydrochloric acid in dioxane under heating to obtain compound **8**. The thionation step to obtain the thiolactam intermediate **9** was carried out under an argon atmosphere in anhydrous toluene, using a composite of phosphorus pentasulfide and aluminum oxide (P_2S_5/Al_2O_3) as the thionating agent. Further functionalization steps, required to complete the synthesis of the target ligand, are currently under investigation. All intermediates that have been synthesized so far have been purified either by column chromatography or by recrystallization, and their structures were fully confirmed by NMR spectroscopy and, in several cases, by X-ray single-crystal diffractometry as well.

Conclusions

In summary, a synthetic route toward a methoxy-substituted indolobenzazocine-based ligand has been successfully developed up to the formation of the tetracyclic core structure, and further functionalization of this scaffold has also been examined. The synthetic approach incorporates strategic functional group transformations, protective group manipulations, and a key Pd-catalyzed intramolecular Heck cyclization to construct the required indolobenzazocine scaffold. Although further steps designed to complete for the completion of the synthesis of the Schiff base are ongoing, the intermediates obtained to date have been purified and characterized.

References

[1] N. Behera, T. Behera, J. Rout, S. Moharana, *IntechOpen.* 2024.
[2] A.A. Shanty, J.E. Philip, E.J. Sneha, M.R. Prathapachandra Kurup, S. Balachandran, P.V. Mohanan, *Bioorg. Chem.* 2017, 70, 67–73.
[3] C. Wittmann, O. Dömötör, I. Kuznetcova, G. Spengler, J. Reynisson, L. Holder, G. J. Miller, E. A. Enyedy, R. Bai, E. Hamel, V. B. Arion, *Dalton Trans.* 2023, **52**, 9964-9982.
[4] I. Kuznetcova, M. Ostojić, N. Gligorijević, S. Aranđelović, V.B. Arion, *Inorg. Chem.* 2022, 61, 20445-20460.

Acknowledgements

This work was financially supported by a grant from the Romanian National Authority for Research, project no. PNRR-III-C9-2023-I8-99 within the National Recovery and Resilience Plan.

PP9. FUNCTIONALIZED INDOLIZINES AS POTENTIAL ANTICANCER AGENTS

Roxana Ciorteanu[1,2], Catalina Ciobanu[3], Ionel I. Mangalagiu[2], Ramona Danac[2]*
[1] *ICI - RECENT AIR Center, "Alexandru Ioan Cuza" University of Iasi, Iasi, Romania*
[2]*Faculty of Chemistry, "Alexandru Ioan Cuza" University of Iasi, Iasi, Romania*
[3]*Institute of Interdisciplinary Research - CERNESIM Centre, "Alexandru Ioan Cuza" University of Iasi, Iasi, Romania*
**rdanac@uaic.ro*

Heterocyclic compounds, particularly azaheterocycles, occupy a central role in the field of medicinal chemistry, due to their prevalence in bioactive molecules, including pharmaceuticals, natural products, and agrochemicals [1-2]. The heterocyclic scaffolds can mimic biological molecules and interact effectively with diverse biological targets, including enzymes, receptors, and nucleic acids.

Indolizines, as fused bicyclic nitrogen systems, have gained attention due to their planar structure, extended conjugation, and capacity to form π-stacking and hydrogen bonding interactions with key biological targets. Indolizine-based compounds have demonstrated a range of biological activities, with notable efficacy in anticancer applications, including the inhibition of tubulin polymerization, EGFR signaling disruption and induction of apoptosis in various cancer cell lines [3].

The introduction of substituents has been widely utilized in medicinal chemistry to adjust the physicochemical and biological properties of drug candidates. Function of the size, polarizability, and ability to engage in various intermolecular bonding, a substituent can enhance binding affinity and target selectivity [4]. Thus, bromine incorporation enhances drug's physicochemical properties, binding affinity, while an ester substitution, by introducing a key hydrogen-bond acceptor also can improve binding properties and selectivity.

Although different substitution patterns on the pyridine ring of indolizine have been investigated for the anticancer activity (figure 1), reports on halogenated indolizines are very limited. The substitution with an ester group was investigated especially at the C-1 position of the indolizine and has emerged as particularly advantageous. Thus, C1-ester-containing indolizines have consistently demonstrated enhanced cytotoxic potential compared to their acid or amide analogues [5].

In this context, aiming to explore their anticancer potential, a series of new indolizine derivatives bearing bromine or carboxyethyl substituents on the pyridine ring of the indolizine (figure 1) was generated using a [3+2] cycloaddition approach as key step. The structures of the new compounds were confirmed using spectral methods (NMR, IR).

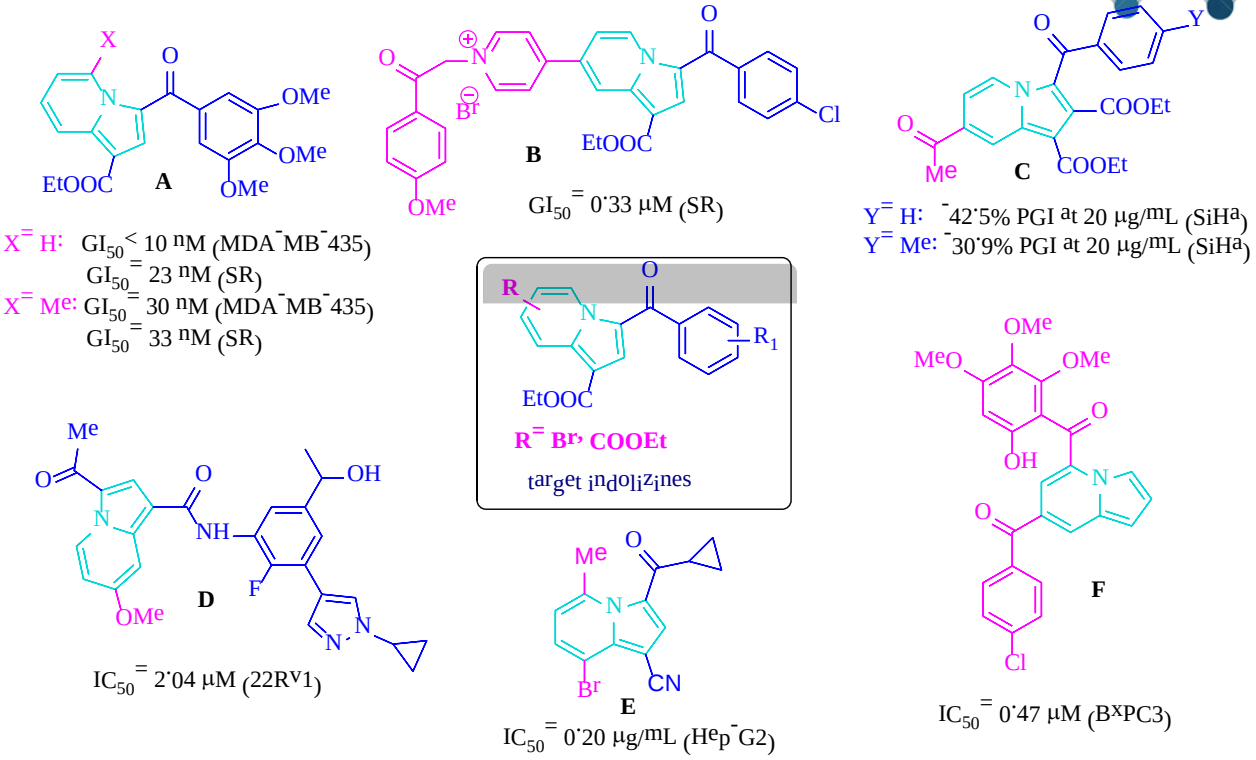

Figure 1. Reported anticancer indolizines.

The new series of compounds have already been tested for their anticancer activity at the National Cancer Institute (NCI, US) against a panel of 60 human tumor cell lines and the results are discussed herein.

References

[1] P. Arora, V. Arora, H.S. Lamba, D. Wadhwa, *Int. J. Pharma Sci. Res.* 2012, 3(9), 2947–2954.
[2] C.M. Marshall, J.G. Federice, C.N. Bell, P.B. Cox, J.T. Njardarson, *J. Med. Chem.* 2024, 67(14), 11622-11655.
[3] N. Ramalakshmi, S. Amuthalakshmi, R. Yamuna, S.A. Anton, S. Arunkumar, *DPC.* 2021, 13(2), 60-69.
[4] G. Cavallo, P. Metrangolo, R. Milani, T. Pilati, A. Priimagi, G. Resnati, G. Terraneo, *Chem. Rev.* 2016, 116(4), 2478–2601.
[5] A. Ghinet, C.M. Abuhaie, P. Gautret, B. Rigo, J. Dubois, A. Farce, D. Belei, E. Bicu, *Eur. J. Med. Chem.* 2019, 89, 115-127.

Acknowledgment: We acknowledge CERNESIM Research Centre at "Al. I. Cuza" University of Iasi for NMR experiments and the US National Cancer Institute (NCI) for anticancer testing of the compounds.

PP10. SORPTION OF NATURAL POLYSACCHARIDES ON ION EXCHANGE RESINS

Alina-Petronela Moraru*, Marius-Mihai Zaharia, Florin Bucatariu, Marcela Mihai
Petru Poni Institute of Macromolecular Chemistry, Romanian Academy, Iasi, Romania
**moraru.alina@icmpp.ro*

Due to their porous, multi-channeled morphology and the presence of both electrostatic and steric interactions, ion-exchange resins display a broad spectrum of sorption characteristics. The desirable properties of ion exchange resins as sorbents are the high sorption capacity, high selectivity, reusability, fast kinetics—rapid equilibration with toxic-containing solutions—and a high mechanical strength of the exchanger particles. The ion-exchange capacity of the resins, as well as their chemical, thermal, and mechanical stability, depends on the chemical and morphological structure of the three-dimensional (3D) cross-linked matrix and on the type and number of ionic functional groups present [1]. Polysaccharides are abundant biomacromolecules from various sources (plants, animals, and microorganisms) [2]. In recent years, polysaccharides have aroused the wide attention of researchers for their excellent biological activities (e.g., antioxidants), biocompatibility, nontoxicity, and biodegradability [3]. Some polysaccharides commonly exist as salts; the counterions (e.g., Na, Cl, and others) needed to be removed before being complexed with the corresponding metal ions by using ion exchange resins before the desired complex could be formed.

The aim of this work is to synthesize and characterize ion-exchange resins and to study their interaction with different polysaccharides aiming in a further study to obtain complexes/hybrid nanostructured materials composed of natural ionizable macromolecules and metal ions and/or metal nanoparticles. Ion-exchange resins (IExRs) were synthesized by copolymerizing divinylbenzene, ethyl acrylate, and acrylonitrile with a 3% degree of cross-linking (DEA_3), following a previously reported procedure illustrated in **Figure 1a** [1].

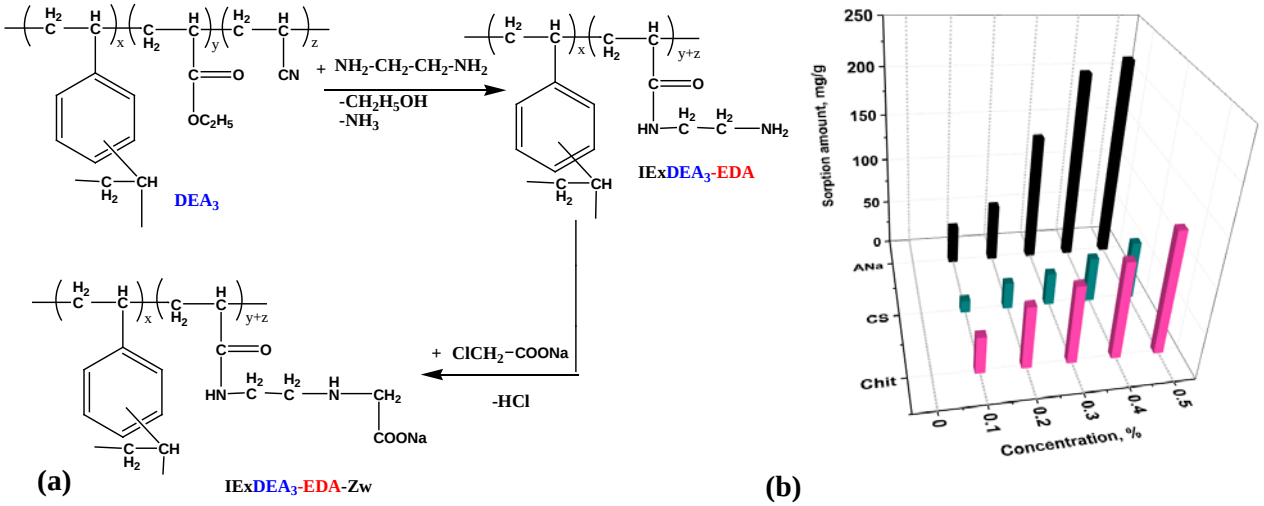

Figure 4. (a) Synthesis scheme of the ion exchangers. (b) Sorbed amount (mg/g) of chitosan (Chit), chondroitin sulfate (CS), and sodium alginate (ANa) on ion-exchange resins as a function of polysaccharide concentration.

Weak cationic and anionic resins were obtained by introducing amino functional groups using ethylenediamine (EDA) or triethylenetetramine (TETA). Subsequently, these resins were reacted with sodium chloroacetate to produce zwitterionic resins (Zw). Sorption experiments were carried out by mixing 1 mL of zwitterionic resin with 5 mL of polysaccharide solutions (chitosan (Chit), sodium alginate (ANa), and chondroitin sulfate (CS)) at concentrations of 0.1%, 0.2%, 0.3%, 0.4%, and 0.5% (w/v). The mixtures were placed on a mechanical shaker and agitated at room temperature for 24 hours to reach equilibrium.

Figure 1b illustrates the variation of the sorbed amount (mg/g) of different polysaccharides chitosan, chondroitin sulfate, and sodium alginate on ion-exchange resins as a function of their initial concentration. Both types of polyelectrolytes (either polyanions or polycations) could be sorbed onto zwitterionic beads. Sorption is favored mostly by attractive electrostatic interactions; polyanions (ANa, CS) are sorbed onto positive sites (-NH-CH_2-CH_2-NH_3^+) and polycations (Chit) onto negative sites (-COO^-). The amount sorbed onto gel beads depends on the equilibrium concentration of each polyelectrolyte; this amount increased with the increasing concentration in all cases. The lowest sorbed amount, reported for CS, could be attributed to the polymer chain conformation. The CS is a strong anionic polyelectrolyte; thus, the polymer chains are fully stretched. Thus the sorption of polymeric chains will show the lowest value. The ANa and Chit presented a more coil conformation, compared with CS, in aqueous solution due to the weak character of the functional group. In this case more macromolecular chains could be anchored onto the beads surface. Because the zwitterionic beads presented more basic groups (two secondary amines onto structural unit) compared with acidic groups (one carboxylic), the ANa will be sorbed in a higher amount than Chit.

The overall, synthesized zwitterionic ion-exchange resins based on acrylic copolymers has sorption capacity for both polycations and polyanions. Due to the higher number of basic groups on the zwitterionic resins, the sorption of polyanions (sodium alginate) was more pronounced than that of polycations (chitosan) while the lowest sorption was observed for chondroitin sulfate, due to its highly stretched chain conformation, which limits its interaction with the resin surface.

References

[1] M.M. Zaharia, A.L. Vasiliu, M.A. Trofin, D. Pamfil, F. Bucatariu, S. Racovita, M. Mihai, *React. Funct. Polym.* 2021, 166, 104997.
[2] E.J. Murphy, G.W. Fehrenbach, I.Z. Abidin, C. Buckley, T. Montgomery, R. Pogue, P. Murray, I. Major, E. Rezoagli, *Polymers* 2023, 15, 2373.
[3] X. Li, F. Jiang, M. Liu, Y. Qu, Z. Lan, X. Dai, C. Huang, X. Yue, S. Zhao, X. Pan, C. Zhang, *J. Agric. Food Chem.* 2022, 70(23), 6922–6942.

Acknowledgment:

This work was financially supported by a grant of the Ministry of Research, Innovation and Digitization, CNCS-UEFISCDI, project number PN-IV-P1-PCE-2023-0738, within PNCDI IV.

PP11. HOST-GUEST INTERACTIONS IN CYCLODEXTRIN-GRAFTED POLYACRYLATES

Georgiana-Alexandra Sanda[1,2]*, Ludmila Aricov[1], Mihaela-Lavinia Ciutu[1], Gabriela Ionita[1]
[1]*Institute of Physical Chemistry – Ilie Murgulescu, Romanian Academy, Bucharest, Romania*
[2]*Faculty of Chemistry, University of Bucharest, Bucharest, Romania*
**georgiana-alexandra.sanda@s.unibuc.ro*

Biocompatibility, durability and sensitivity make xanthene dyes popular in biological applications in the textile and paper sector [1]. Among xanthenes, one fluorescent cationic dye stands out, respectively rhodamine B (RhB). This water-soluble compound is used in biological dyeing, printing, veterinary medicine and other areas [2]. Sodium polyacrylate (NaPA) is a polymer that, in aqueous environments, can modulate interactions. Its polyelectrolytic nature, molecular structure, effectiveness as a dye adsorbent and other properties influence significantly fluorophore states [3,4]. Attaching hydrophobic side groups can further enhance NaPA's properties [5-8]. In this study, we aimed to create new polymers featuring a fluorescence control mechanism and improved absorption and for adsorbed dyes. Our approach exploited NaPA's polyelectrolytic nature by grafting alkyl chains of varying hydrophobicity and tosylated β-cyclodextrins. The host-guest complexation was proved by EPR measurements. Synthesis of PAA using β-CD derivatives proceeded in a round-bottom glass flask using magnetic stirring and argon bubbling in an oil bath. β-CD-ethylenediamine (12CD) and β-CD-hexaethylenediamine (16CD) were utilized to modify PAA by attaching the amino group of CD derivatives to the carboxyl group of PAA using DCC and NMP [9]. The polymer was precipitated from the reaction media with 40% NaOH or diethyl ether. The precipitate was washed with NMP and methanol and dissolved in ultrapure water. Polymers were purified by dialysis and stored in a desiccant after being freeze-dried. The polymers were denoted as NaPA12CD and NaPA16CD (recovered in sodium hydroxide) and PAA12CD and PAA16CD (recovered in diethyl ether).

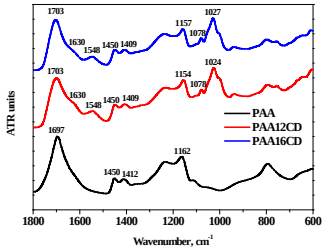

Figure 1. A. FTIR spectra of PAA, PAA12CD, PAA16CD.

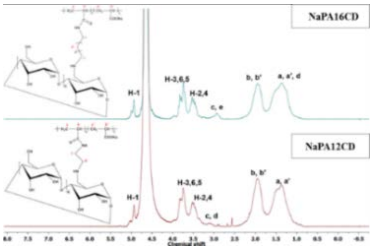

B. ^{1}H-NMR spectra of NaPA12CD and NaPA16CD.

The FTIR spectra (**Figure 1A**) exhibit bands at 1630 (shoulders on the carbonyl band – 1703 cm^{-1}) and 1548 cm^{-1}, which correspond to the vibrations of amide I and amide II. In addition, distinct absorption peaks in the spectra of the CD-functionalized polymers can be observed in the range of 1100 to 1000 cm^{-1}, indicating the presence of the glucopyranose ring of cyclodextrin [10]. The absence of these species within the spectrum of PAA serves as evidence for the effective

completion of the PAA reaction with CD derivatives. The ^{1}H-NMR spectra (Fig. 1B) were obtained by dissolving the sodium salt of the modified polymer in deuterium oxide. The ^{1}H-NMR confirmed the incorporation of the β-CD moieties in the PAA in both cases. The modified polymers with 12CD and 16CD displayed the characteristic peaks of the β-CD in the region 3–4 ppm as well as the signal corresponding to the methine and methylene protons of PAA at 1.92 ppm and 1.35 ppm, respectively.

Analysis of the interaction between CD-functionalized polyacrylates and spin moieties. EPR spectra of the CD-functionalized polymers (in the presence of RhB) were recorded using various spin probes (an example can be seen in **Figure 2**). Each experimental spectra was simulated in order to obtain the parameters of the free and complexed radical. Some of the values are presented in **Table 1** and they were used to estimate the binding constants.

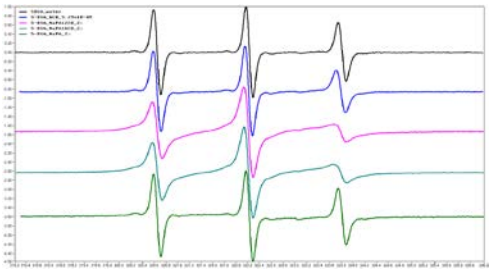

Figure 2. Some of the EPR experimental spectra for 5-DSA spin probe.

Table 1. Some of the spectral parameters using 5-DSA spin probe for the CD- functionalized polymers.

	Specia 1					Specia 2				
Sample	**aN (G)**	**aN (G)**	**aN (G)**	**tau**	**lg(tcorr)**	**aN (G)**	**aN (G)**	**aN (G)**	**tau**	**lg(tcorr)**
5- DSA water	15.74	15.91	15.87	1.02x10-^{10}s	-9.9889	-	-	-	-	-
5- DSA RhB β-CD 5.29 x 10^{-4}M	-	-	-	-	-	15.87	16.13	15.7	1.16x10^{-9}s	-8.9341
5- DSA RhB NaPA12CD 2%	15.62	16.00	15.97	1.02x10^{-10}s	-9.9875	14.74	15.82	15.86	1.57x10^{-10}s	-8.8035
5- DSA RhB NaPA16CD 2%	14.56	17.15	14.70	9.68x10^{-11}s	-10.0138	15.65	16.05	16.04	1.08x10^{-9}s	-8.7443
5-DSA RhB NaPA 2%	-	-	-	-	-	16.60	14.75	16.63	1.59x10^{-9}s	-8.8032

References

[1] Z. Mao, H. Rha, J. Kim, X. You, F. Zhang, W. Tao, J.S. Kim, *Adv. Sci.* 2023, 10(18), 2301177.
[2] T.L. Yusuf, B.O. Orimolade, D. Masekela, B. Mamba, N. Mabuba, *RSC Adv.* 2022, 12, 26176–26191.
[3] G. Stîngă, A. Băran, A. Iovescu, L. Aricov, D.F. Anghel, *J. Mol. Liq.* 2019, 273, 125–133.
[4] A. Băran, L. Aricov, G. Stîngă, A. Iovescu, A.R. Leontieș, V. V. Jerca, *J. Mol. Liq.* 2022, 346, 117103.
[5] H. Yan, Q. Jiang, J. Wang, S. Cao, Y. Qiu, H. Wang, Y. Liao, X. Xie, *Polymer* 2021, 221, 123617.
[6] M.G. Ortiz, M. A. Sanservino, A. Visintin, G. del C. Pizarro, M. V. Tundidor-Camba, E. Schott, A. Sepulveda, C. Zúniga, D. P. Oyarzún, R. Martin-Trasancos, *Carbohydr. Polym. Technol. Appl.* 2024, 7, 100414.
[7] I.C. Gîfu, M.E. Maxim, A. Iovescu, L. Aricov, E.L. Simion, A.R. Leontieș, M. Anastasescu, C. Munteanu, D. F. Anghel, *Appl. Surf. Sci.* 2017, 412, 489–496.
[8] L. Aricov, A. Băran, G. Stîngă, E. L. Simion, I.C. Gîfu, D. F. Anghel, V. Rădiţoiu, *Colloid. Polym. Sci.* 2017, 295(6), 1017–1038.
[9L. Aricov, A. Băran, E. L. Simion, I.C. Gîfu, D.F. Anghel, V.V. Jerca, D.M. Vuluga, *Colloid. Polym. Sci.* 2016, 294(4), 667–679.
[10] S. Demirci, S. Kinali-Demirci, B. Van Veller, *ACS Appl. Polym. Mater.* 2020, 2(2), 751–757.

Acknowledgment: ”Chemical host-guest molecule systems for health applications” (OMRI for identification of inflammatory pathologies), PNRR-III-C9-2023-I8-CF97, contract no. 760283/ 27.03.2024, project code CF97/ 31072023.

PP12. MISCIBILITY STUDY OF HYDROXYPROPYL CELLULOSE AND POLY(N-VINYLPYRROLIDONE) MIXTURES IN DILUTE SOLUTION

Alexandra Lupu*, Ioana-Alexandra Plugariu, Luiza Madalina Gradinaru, Maria Bercea
Petru Poni Institute of Macromolecular Chemistry, Romanian Academy, Iasi, Romania
**lupu.alexandra@icmpp.ro*

Hydroxypropyl cellulose (HPC) is a polysaccharide of high interest for pharmaceutical, cosmetic and food applications as thickener, emulsifier, pharmaceutical excipient, coating agent, binder or stabilizer [1–3]. Poly(N-vinylpyrrolidone) (PVP) is nontoxic and presents excellent biocompatibility and ability to form complexes and gels with both hydrophobic and hydrophilic polymers (including cellulose derivatives) and associated structures with numerous active substances [4,5]. The ability of PVP to form complexes allows the tailoring of the dissolution profiles of poor water-soluble polymers, inhibits precipitation, increases the bioavailability of poorly water-soluble drugs and controls their delivery. Recently, the viscosity of HPC/PVP mixtures in water was determined in the three domains of concentrations: dilute, semidilute and concentrated [6]. In the present study, the hydrodynamic properties of single polymer solutions and their mixtures were determined. The main interest was to investigate the miscibility between HPC and PVP in aqueous solution, according to various miscibility criteria given in literature.

HPC sample was supplied by Aqualon (Klucel) and PVP was purchased from Sigma-Aldrich. Stock solutions of HPC and PVP (concentration of 0.5 g/dL) were prepared at room temperature and then mixtures of HPC/PVP were achieved by mixing these solutions. w_{PVP} represents the weight fraction of PVP in the HPC/PVP mixture. The viscometric measurements were carried out at 25 °C by using an Ubbelohde viscometer, capillary type 0a (0.53 mm). The flow time for water, t_o, was 184.44 s.

The intrinsic viscosity, $[\eta]$, of HPC, PVP and HPC/PVP dilute solutions was determined according to the classical Huggins model:

$$\eta_{sp}/c = [\eta] + k_H[\eta]^2 c \qquad (1)$$

where η_{sp} is the specific viscosity, $\eta_{sp} = t/t_o - 1$, t and t_o represent the flow times of polymer solution and solvent, respectively, k_H is the Huggins constant, c is the solute concentration. In this study, c denotes the total concentration of dissolved macromolecules.

Figure 1(a) shows the Huggins plots for HPC/PVP mixtures in solution which allow the calculation of $[\eta]$ and k_H values. The intrinsic viscosity was plotted as a function of polymer mixture composition (**Figure 1(b)**) and a positive deviation from the additive rule was observed over the whole range of composition. This deviation is higher in the region of low PVP content ($w_{PVP} \leq 0.15$). The Huggins constant was higher than 0.5 for all HPC-containing systems, suggesting a tendency of aggregation due to favorable polymer-polymer intermolecular interactions. The viscometric data were further used to calculate two miscibility parameters: α and Δb.

The parameter, α, was proposed by Sun et al. [7] and it can be calculated as:

$$\alpha = k_m - \frac{k_1[\eta]_1^2 w_1^2 + k_2[\eta]_2^2 w_2^2 + 2\sqrt{k_1 k_2}[\eta]_1[\eta]_2 w_1 w_2}{([\eta]_1 w_1 + [\eta]_2 w_2)^2} \qquad (2)$$

where: k_1, k_2 and k_m are the Huggins coefficients for HPC, PVP and their mixture in solution.

According to Krigbaum and Wall [8], another compatibility parameter, Δb, can also be determined:

$$\Delta b = b_{12}^{exp} - b_{12}^{id}, \text{ where: } b_m^{exp} = b_{11}w_1^2 + b_{22}w_2^2 + 2b_{12}^{exp}w_1w_2 \text{ and } b_{12}^{id} = \sqrt{b_{11}b_{22}} \quad (3)$$

α and Δb > 0 suggest miscible polymers and α and Δb < 0 show that the polymers are immiscible.

According to the dependences shown in **Figure 2**, HPC/PVP mixtures are miscible over the whole composition range (α > 0 and α and Δb > 0). This might be the result of favorable intermolecular interactions between hydroxyl groups of HPC and carbonyl groups of PVP.

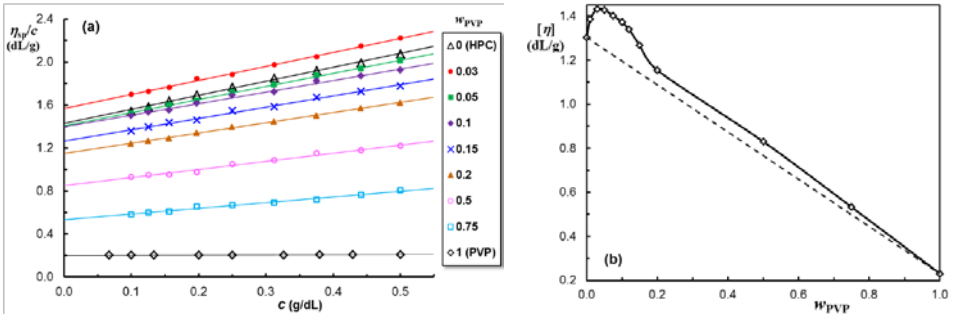

Figure 1. Huggins plots (a) and intrinsic viscosity as a function of HPC/PVP (b) [6].

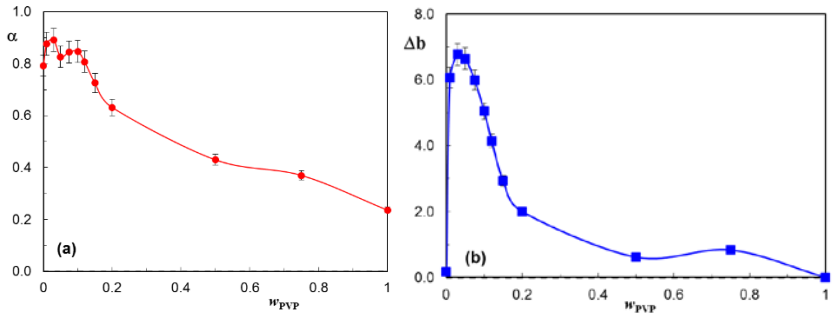

Figure 2. The miscibility parameters α (a) and Δb (b) for HPC/PVP mixtures in water at 25°C.

The preferred interactions between HPC and PVP macromolecules represent the driving force favoring the formation of mixed isolated coils with a more extended chain conformation [6], causing the increase of the viscosity. In addition, other intra- and intermolecular interactions between –OH groups of HPC can occur. The strong interactions between HPC and PVP were also evidenced in solid state, by using various techniques [9].

References

[1] D. Cholakova, K. Tsvetkova, V. Yordanova, K. Rusanova, N. Denkov, *Gels* 2025, 11, 113.
[2] Z. Shi, Y. Li, H. Duan, Y. Wang, X. Zhang, *Int. J. Biol. Macromol.* 2025, 318, 145223.
[3] I.A. Plugariu, L.M. Gradinaru, M. Avadanei, I. Rosca, L.E. Nita, C. Maxim, M. Bercea, *Pharm.* 2023, 16, 1510.
[4] A. R. D. Amaral, L. J. D. Danda, H. C. Rigonatto, *J. Drug Deliv. Sci. Technol*. 2025, 106, 106708.
[5] M. Teodorescu and M. Bercea, *Polym. Plast. Technol. Eng*. 2015, 54, 923–943.
[6] M. Bercea, A. Lupu, I.A. Plugariu, L.M. Gradinaru, P.Navard, *Cellulose Chem. Technol.* 2025, 59, 707-715.
[7] Z. Sun, W. Wang, Z. Feng, *Eur. Polym. J*. 1992, 28, 1259–1261.
[8] W.R. Krigbaum, F.T. Wall, *J. Polym. Sci.* 1950, 5, 505–514.
[9] K. Sudarsan Reddy, M. N. Prabhakar, V. Nagamaheswara Reddy, G. Sathyamaiah, *J. Appl. Polym. Sci*. 2012, 125, 2289–2296.

PP13. FATE OF PET MICROPLASTICS IN SOIL AND THEIR IMPACT ON SOIL PROPERTIES

Eliška Kameníková[1]*, Adéla Hrušková[1], Martin Brtnický[2], Lucie Šudomová[3], Jiří Kučerík[2]
[1]*Institute of Chemistry and Technology of Environmental Protection, Brno University of Technology, Faculty of Chemistry, Brno, Czech Republic*
[2] *Department of Agrochemistry, Soil Science, Microbiology and Plant Nutrition, Mendel University in Brno, Czech Republic*
[3]*rPET InWaste, s.r.o., 665 01 Rosice, Czech Republic*
**xckamenikova@vutbr.cz*

In recent years, microplastics, tiny plastic particles formed by the degradation of larger plastic products, have become one of the most discussed environmental issues of our time [1, 2]. These tiny plastic particles, smaller than 1 mm, are among the most common and persistent environmental contaminants [3]. They can enter ecosystems through the fragmentation of larger plastics or their intentional production, and subsequently accumulate in soil, water, the atmosphere, and living organisms. Their presence in soil is particularly significant because soil is a crucial medium for agriculture, nutrient cycles, and ecological balance [4]. Microplastics can alter the physical, chemical, and biological properties of soils – they can affect porosity, soil aggregation, and water retention, and can alter pH, conductivity, and nutrient content, thereby interfering with the processes that determine the fertility and ecological stability of soil systems [5]. At the same time, they act as carriers for other contaminants and microorganisms, which can have secondary effects on plants and soil microbiota [6]. This work focuses on studying the fate of PET microplastics in soil, their impact on the physical, chemical, and biological properties of soil, and their fluence on key soil processes. As part of the work, a series of laboratory experiments were carried out with seven different types of agricultural soils contaminated with PET particles of two different sizes. The results showed that PET microplastics affect both abiotic (e.g., field water capacity, thermal properties, aggregation) and biotic properties of soils (soil enzyme activity, respiration, and nitrogen compound concentration). In addition the microplastics and soils properties changed as a result to the expostion in the soil environment.

Seven types of agricultural soils of different properties were used to study the impact of PET microplastics on soil properties under laboratrory conditions. Soil samples were homogenized, contaminated with 1% PET particles of two sizes, and incubated for 12 months. During the incubation, subsamples were periodically collected to determine the physical, chemical, and biological properties of the soils. Soil parameters such as water field capacity (water retention of samples), particle size (sieving), thermogravimetric analysis (TGA) to identify potential changes in the thermal stability of soil after incubation, respiration of soil samples, and changes in the surface morphology of microplastics were observed by electron microscopy.

During the experiment, it was demonstrated that the presence of PET microplastics reduced the natural formation of larger soil aggregates and, conversely, stabilized smaller fractions, indicating a disruption of the natural soil structure. In terms of soil organic matter (SOM), no significant impact on the stable fraction was observed, except for a slight decrease in samples with larger particles.

A decrease in the thermolabile (easily degradable) SOM was observed in all samples, which corresponds to natural degradation processes during long-term incubation (**Figure 1A**). Soil respiratory activity was not significantly affected by the addition of microplastics, but a slight decreasing trend was observed with increasing PET particle size, which may indicate a reduction in the activity of aerobic microorganisms or impaired gas exchange. Electron microscopy (SEM) observations confirmed the rapid aging of PET particles in the soil environment. After three months of incubation, the first signs of physical degradation (cracks and surface damage) were already visible. After six to twelve months, the changes were more significant and were accompanied by local colonization by soil microorganisms. These findings confirm that the soil environment accelerates both the physical and biological aging of the polymer.

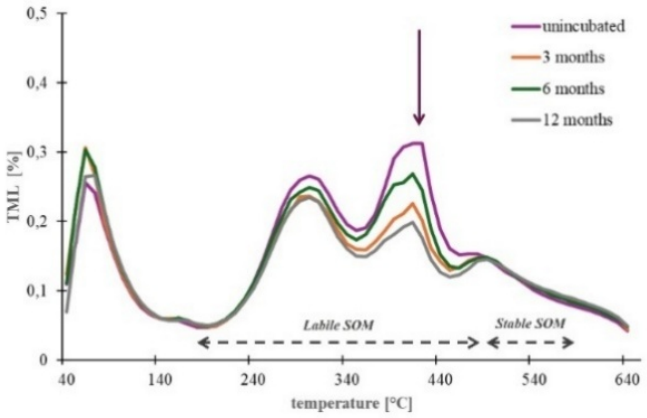

Figure 1. example of a soil sample (modal ranker) illustrating the effect of PET microplastics (< 63 um) on changes in soil organic matter (SOM) during incibation.

The results show that the presence of PET microplastics in soil affect its physical and biological properties. Microplastics alter the soil water dynamics, soil structure, and respiration processes, with the intensity of these changes depending on the soil type and particle size. Thermogravimetric and microscopic analysis confirmed that PET particles did not degrade completely during the incubation period, but show signs of surface morphology changes and interactions with soil biota.The study thus confirms that PET microplastics cannot be classified as inert microplastics in the soil environment. Their long-term presence can affect soil stability and functionality, and thus its ecological quality. The findings contribute to a better understanding of the fate of microplastics in terrestrial ecosystems and highlight the need for further monitoring under real field conditions.

References

[1] T. Montoto-Martínez, J.J. Hernández-Brito, M.D. Gelado-Caballero, *PLoS One* 2020, 15, e0232744.
[2] X. Zhu, *Front. Mar. Sci.* 2021, 7, 609243.
[3] L. Van Cauwenberghe, L. Devriese, F. Galgani, J. Robbens, C.R. Janssen, *Mar. Environ. Res.* 2015, 111, 5–17.
[4] T. Zhao, Y.M. Lozano, M.C. Rillig, *Front. Environ. Sci.* 2021, 9, 675803.
[5] E. Huerta Lwanga, T. Gertsen, H. Gooren, P. Peters, T. Salánki, M. van der Ploeg, E. Besseling, M.A. Koelmans, V. Geissen, *Environ. Pollut.* 2017, 220, 523–531.
[6] X. Zhang, Z. Wang, J. Zhang, H. Wu, Y. Sun, *J. Hazard. Mater.* 2021, 418, 126288.

Acknowledgment

The work was supported by the project FCH-S-25-8807 of the Ministry of Education, Youth and Sports of the Czech Republic.

PP14. HOW DOES MICROFLUIDICS ENABLE THE PRECISE AND REPRODUCIBLE FORMATION OF LIPOSOMES?

Razvan Ghiarasim*
Petru Poni Institute of Macromolecular Chemistry, Romanian Academy, Iasi, Romania.
**ghiarasim.razvan@icmpp.ro*

Liposomes are nanoscale vesicles composed of one or more phospholipid bilayers that can encapsulate both hydrophilic and hydrophobic compounds. Due to their biocompatibility, versatility, and ability to provide controlled release, liposomes have become key nanocarriers for drug delivery, imaging, and vaccine applications [1]. Traditionally, they are produced through bulk methods such as thin-film hydration, solvent evaporation, or ethanol injection [2]. While effective, these techniques generally lack precise control over vesicle size, yield broad size distributions, and show limited reproducibility. Additional post-processing steps like extrusion or sonication are often required, which lower lipid recovery and make scale-up challenging [2].

Microfluidic technology provides a practical solution to these limitations by allowing highly controlled lipid self-assembly under continuous-flow conditions. Within microfluidic channels, liposome formation is governed primarily by two experimental parameters: *Total Flow Rate (TFR)* and *Flow Rate Ratio (FRR)* between the aqueous and organic phases. By adjusting these parameters, it is possible to control the rate of solvent exchange and mixing intensity, thereby tuning the final vesicle size and uniformity with high reproducibility. Lower TFR and FRR values typically yield larger liposomes, while higher flow conditions promote rapid mixing and the formation of smaller, more homogeneous vesicles [3].

In this study, liposomes were prepared using a herringbone-structured microfluidic chip, which enhances mixing through chaotic advection. Two lipid compositions, DOPC/cholesterol and POPC/cholesterol, were used to obtain both *small unilamellar vesicles (SUVs)* and *large unilamellar vesicles (LUVs)*. The same formulations were also applied for doxorubicin (DOX) encapsulation, performed via both passive loading and active loading. The active loading followed the ammonium sulfate gradient method, in which a pH gradient drives DOX into pre-formed vesicles, leading to higher encapsulation and retention, an approach similar to that used for the FDA-approved liposomal drug Doxil (Doxorubicin Liposomal). The precise control over TFR and FRR allowed both encapsulation strategies to be optimized reproducibly within the same microfluidic platform.

After assembly, liposomal suspensions were purified by *tangential flow filtration (TFF)* to remove ethanol and non-encapsulated DOX, yielding stable and homogeneous dispersions. The systems were characterized by *dynamic light scattering (DLS)* to determine the hydrodynamic diameter and confirm SUV or LUV formation. Lipid quantification was performed using the Stewart assay to calculate the lipid recovery factor, while UV–Vis spectroscopy was employed to determine DOX content, encapsulation efficiency (EE%), and drug loading (DL%). Stability studies at 4 °C were carried out to evaluate vesicle integrity and encapsulation over time. All experiments were conducted in triplicate, confirming the reproducibility of the microfluidic process and the consistency of the results.

Overall, this study demonstrates that microfluidic-assisted assembly provides a reproducible, tunable, and scalable platform for liposome production. The ability to adjust vesicle size through control of TFR and FRR, together with the possibility of performing both passive and active drug loading under identical conditions, highlights the flexibility of microfluidic technology. These advantages make microfluidics a promising route for the scalable production of liposomal nanomedicines and next-generation lipid-based vaccines.

References

[1] R. Chelliah, R. Ramachandran, S. Vijayalakshmi, M. Karuvelan, K. Barathikannan, D.H. Oh, *Next Nanotechnology* 2025, 8, 100209.
[2] P. Liu, G. Chen, J. Zhang, *Molecules* 2022, 27, 1372.
[3] D. Carugo, J. Owen, E. Stride, N. Arkill, *Scientific Reports* 2016, 6, 25876.

Acknowledgment: This work was financially supported by a grant from the National Research Authority, project no. PNRR-III-C9-2023-I8-161, MultiPodGaN, contract no. 760285/27.03.2024, within the National Recovery and Resilience Plan.

PP15. OPTICAL AND STRUCTURAL CHARACTERIZATION OF Fe_3O_4 AEROMATERIAL

Catalin Creciunel[1,*], Tatiana Galatonova[1], Vadim Morari[2], Florica Doroftei[3], Andrei Dascalu[3], Laura Ursu[3], Vladimir Ciobanu[1]

[1]National Center for Materials Study and Testing, Technical University of Moldova, Chisinau, Republic of Moldova
[2]Institute of Electronic Engineering and Nanotechnologies "D. Ghitu", Technical University of Moldova, Chisinau, Republic of Moldova
[3]Petru Poni Institute of Macromolecular Chemistry, Romanian Academy, Iasi, Romania
**catalin.creciunel@cnstm.utm.md*

Recent developments in nanotechnology have introduced aeromaterials as a novel class of semiconductor architectures. Their ultralow density and porous structure enable unique properties, such as dual hydrophilic–hydrophobic behavior, enhanced light–matter interaction, and enhanced photocatalytic properties due to the high specific surface area [1,2].

In this work, we report on the fabrication of a Fe_3O_4 aeromaterial using two techniques namely spray pyrolysis and drop-infiltration. Fe_3O_4 was deposited initially on sacrificial ZnO microtetrapod templates with dimensions of 10 × 10 × 4 mm, with the density of 0.3 g/cm^3 [3]. A 0.15 M $FeCl_3$ alcohol-based solution was used as the precursor.

For the spray pyrolysis approach, a custom-built setup was used, with the substrate maintained at 480 °C and the deposition time being 3 minutes, yielding Fe_3O_4 thin films with an approximate thickness of 400 nm (**Figures 1a, c**). In the drop infiltration method, 300 µL of precursor solution was dropped onto the ZnO microtetrapods substrate at a rate of one drop per second, at room temperature, obtaining a sponge-like structure, with the thickness of deposited Fe_3O_4 of about 100 nm (**Figures 1 b, d**).

In both cases, the samples were subsequently annealed at 500 °C for one hour in air in order to improve the material's crystallinity and eliminate residual chlorine. The ultraporous Fe_3O_4 structure was obtained by selectively etching the ZnO template in 0.1 M citric acid for 24 h, followed by controlled drying in a lyophilizer system at −84 °C for 24 h.

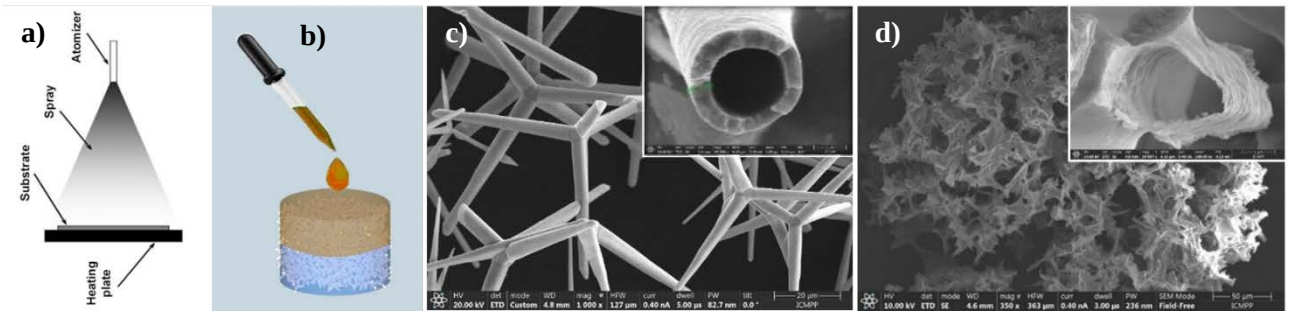

Figure 1. Schematics of the fabrication techniques and SEM images of the obtained aero-Fe_3O_4 by: a, c) spray pyrolysis; b, d) drop infiltration.

The synthesized aero-Fe_3O_4 was structurally and optically characterized using the X-ray Diffraction (XRD) and Raman Spectroscopy methods. The XRD pattern from **Figure 2a** displays characteristic reflections of the cubic inverse spinel structure of magnetite Fe_3O_4, highlighted by the intense (311) peak, with no evidence of residual ZnO, confirming high purity. The material exhibits a broad background signal, which, along with the subsequent Raman analysis, is indicative of its highly nanocrystalline and porous nature. The Raman spectrum from **Figure 2b** further validates the phase formation by showing the intense A_{1g} vibrational mode characteristic of Fe_3O_4 centered at approximately 660 cm^{-1}, with band broadening corroborating the small crystallite size. The photoelectrical characterization (**Figure 2c**) at 150 K and 300 K using a Nd:YAG (λ=325 nm) laser with a power density of 23 mJ/cm^2 has shown the presence of the photoremanent current, indicating that the photo-generated charge carriers become trapped in the material's defects or localized states within the crystal lattice.

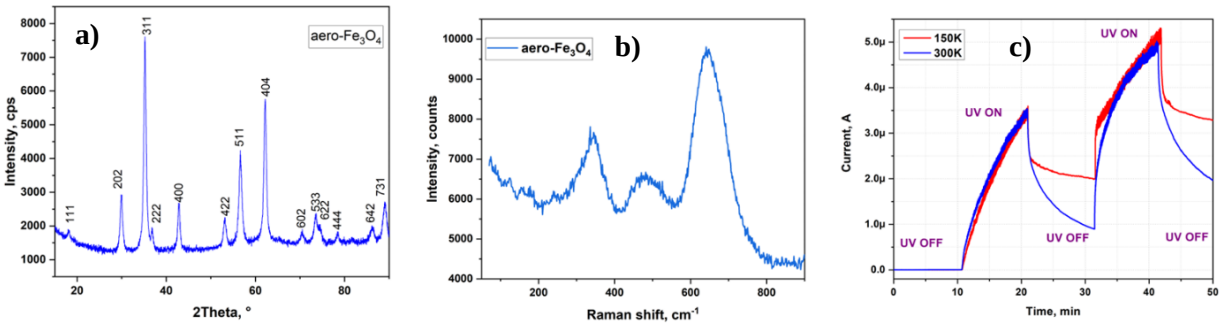

Figure 2. XRD pattern a), Raman spectrum b), and the photoelectric response at different temperatures upon excitation with UV laser c).

References

[1] I. M. Tiginyanu, O. Lupan, V.V. Ursaki, L. Chow, M. Enachi, *Scopus Export* 2011, 1-6, 396-479.

[2] I. Plesco, T. Braniste, N. Wolff, L. Gorceac, V. Duppel, B. Cinic, Y.K. Mishra, A. Sarua, R. Adelung, L. Kienle, I. Tiginyanu *APL Mater*.2020, 8, 061105.

[3] C. Creciunel, V. Ciobanu, E. V. Monaico, "Remote-controlled temperature setup designed for ZnO nanostructures fabrication," *International Colloquium "Physics of Materials" – PM 8*, 2024 p. 29.

Acknowledgment: The work was partially supported by the Young Researchers project #24.80012.5007.12TC and institutional subprogram #02.04.02 „Development of technologies and investigation of the properties of layered semiconductor compounds, hybrid nanostructures and laser sources".

PP16. TAILORING PULLULAN REACTIVITY THROUGH MULTI-ROUTE OXIDATION APPROACHES

Ioana-Sabina Trifan*, Raluca Ioana Baron, Gabriela Biliuta, Gabriela Liliana Ailiesei, Sergiu Coseri

Petru Poni Institute of Macromolecular Chemistry, Romanian Academy, Iasi, Romania
**trifan.sabina@icmpp.ro*

Oxidation is one of the most important ways to modify the physical and chemical properties of natural polymers to obtain materials with diversified functionality and new properties [1]. Furthermore, oxidation can lead to biologically active materials with applications in the medical field. It should be emphasized that oxidation is a chemical modification method of particular interest for functionalized polysaccharides. Mainly, oxidation reactions can occur at any of the hydroxyl groups in the sugar ring structure, and as a result of these reactions, carboxyl, aldehyde, or ketone groups are introduced. For a more intense modification of the properties, a high degree of oxidation is desirable, both in terms of the nature of the functional group and its position. There are various reagents used for oxidizing polysaccharides, but, unlike small-molecule organic chemistry, many of these cannot be used for natural polymers because the strongly acidic or basic environment required for the reaction leads to the degradation of the biopolymer.

In our study several oxidation protocols using two of the most selective oxidation reagents were performed to convert the primary and secondary OH groups of polysaccharides into carboxylic and/or carbonylic ones [2]. For this purpose, a water-soluble pullulan has been used as a model polysaccharide. Pullulan is a non-ionic water-soluble polysaccharide which is produced from starch by the yeast-like fungus *Aureobasidium pullulans*. Pullulan is known for its non-toxicity and biocompatibility. Most pullulan modifications are intended to reduce its water solubility or to introduce charged or reactive groups for functionality. In the pullulan structure, nine OH groups per repeating unit are available for substitution (**Figure 1**). The relative reactivity of these groups may vary greatly, depending on the solvents, reagents, and reaction conditions.

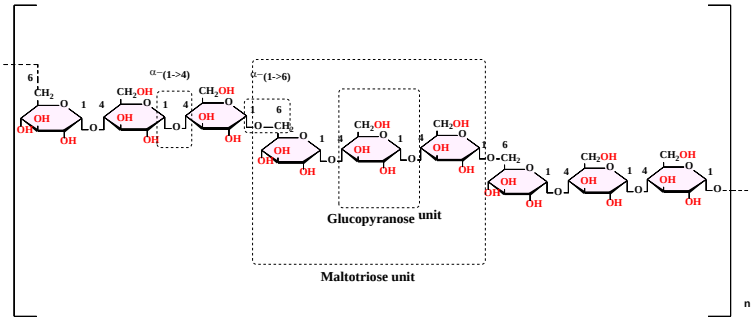

Figure 1. Chemical structure of pullulan.

Thus, in this work we propose the use of several pullulan oxidation routes, with the aim of investigating the influence of different oxidizing agents and reaction conditions on the degree of oxidation and on the final properties of the obtained product. Four distinct reaction mechanism were considered: (1) pullulan oxidation in the presence of the TEMPO reagent (2,2,6,6-tetramethylpiperidine-1-oxyl), a selective catalyst for the oxidation of primary hydroxyl groups to

carboxylic acids [3]; (2) oxidation with sodium periodate ($NaIO_4$), which acts by cleaving the bond between vicinal carbon atoms, thus generating aldehyde groups [4]; (3) a "one-pot" reaction, in which TEMPO and sodium periodate are used concurrently in a single step to simultaneously obtain carbonyl and carboxyl groups, combining the advantages of both oxidative mechanisms [5]; and (4) a two-step process, in which the initial oxidation with TEMPO is followed by a secondary oxidation with sodium periodate, to obtain a higher degree of functionalization and a more controlled distribution of carbonyl and carboxyl functional groups in the polymer structure. Depending on the chosen oxidation route, the reactions were carried out at room temperature, using water as a solvent, which provides a mild and environmentally friendly environment, suitable for preserving the integrity of the polymer chain. In the case of TEMPO oxidation, a classical catalytic system consisting of sodium hypochlorite (NaOCl) and sodium bromide (NaBr) was used, which regenerates the active form of the TEMPO radical, maintaining the efficiency of the oxidation process. In the reactions involving sodium periodate, it acted as the main oxidizing agent, capable of breaking the C–C bond between neighboring carbon atoms bearing hydroxyl groups, leading to the formation of dialdehydes. By combining these methods, the aim is to obtain a set of samples with different degrees of oxidation, which allows the correlation between the reaction conditions, the type of groups introduced and the structural and functional properties of the final product. The oxidation of pullulan was confirmed by advanced spectroscopic analyses, including Fourier transform infrared spectroscopy (FT-IR), proton nuclear magnetic resonance (^{1}H NMR) and carbon nuclear magnetic resonance (^{13}C NMR), which revealed the presence and nature of the carbonyl and carboxyl groups introduced into the polymer structure.

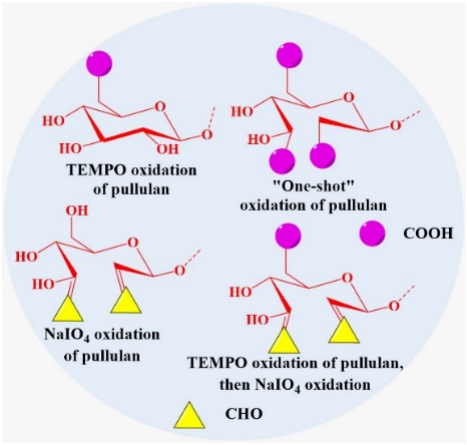

Figure 2. The general schematization of the nature of groups obtained after oxidation.

References

[1] R.I. Baron, G. Biliuta, A.M. Macsim, M.V. Dinu, S. Coseri, *Polymers* 2023, 15(19), 3930.
[2] M. Bercea, G. Biliuta, M. Avadanei, R.I. Baron, M. Butnaru, S. Coseri, *Carbohydr. Polym.* 2019, 206, 210-219.
[3] R.I. Baron, S. Coseri, *React. Funct. Polym.* 2020, 157, 104768.
[4] R.I. Baron, I.A. Duceac, S. Morariu, A.C. Bostănaru-Iliescu, S. Coseri, *Gels* 2022, 8, 726.
[5] R.I. Baron, G. Biliuta, A.M. Macsim, M.V. Dinu, S. Coseri, *Polymers* 2023, 15, 3930.

Acknowledgment: This work was supported by a grant of the Ministry of Research, Innovation and Digitization, CNCS-UEFISCDI, project number PN-IV-P2-2.1-TE-2023-1005, within PNCDI IV.

PP17. NOVEL PHTHALAZINO-ACETOPHENONE HYBRIDS: DESIGN, SYNTHESIS, AND STRUCTURAL CHARACTERIZATION

Marius Savu[1], Vasilichia Antoci[1], Dorina Amariucai-Mantu[1], Ramona Danac[1], Dumitrela Diaconu[1,2], Catalina Ciobanu[3], Ionel I. Mangalagiu[1,3*]

[1]*Faculty of Chemistry "Alexandru Ioan Cuza" University of Iasi, Iasi, Romania*
[2]*RECENT AIR Center,"Alexandru Ioan Cuza" University of Iasi, Iasi, Romania*
[3]*Institute of Interdisciplinary Research- CERNESIM "Alexandru Ioan Cuza" University of Iasi, Iasi, Romania*
**ionelm@uaic.ro*

Introduction

Phthalazine-based hybrid compounds attract considerable interest because of their wide range of biological activities, such as anticancer, antimicrobial, and anti-inflammatory [1]. The acetophenone scaffold is another highly versatile organic fragment, widely used in the synthesis of perfumes, flavors, dyes, plastics, agrochemicals, and pharmaceuticals. [2-3].

The main objective of this study was to design and synthesize novel hybrid molecules through the application of click chemistry. Our approach involved the combination of two distinct pharmacophoric units — a cycloadduct featuring a phthalazine core **1** and a diversely substituted phenacyl fragment containing an azide functional group **2** (Scheme 1). These two fragments were connected via a 1,2,3-triazole unit formed through a *click reaction* between the alkyne and azide components of the precursors. This synthetic strategy enabled the efficient preparation of new phthalazine–acetophenone hybrids, combining the structural diversity and biological potential of both scaffolds. The resulting compounds are promising candidates for further biological evaluation due to the presence of multiple pharmacophoric centers within a single molecular framework.

Experimental

The general synthetic route consists of three steps. In the first step, a quaternization reaction occurred between phthalazine and propargyl bromide, giving the corresponding quaternary salt. In the second step, a [3+2] dipolar cycloaddition was performed in the presence of 1,2-butylene oxide (acting as both solvent and base), and *N*-Phenylmaleimide as dipolarophile, when we obtained the target cycloadduct **1.** The third and final step, the *click reaction* was carried out using copper (II) sulfate as a catalyst and sodium ascorbate as a reducing agent in a THF-water (2:1, v:v) system. The reactions were performed between the cycloadduct **1**, obtained in the second step, and the diversely substituted phenacyl fragments **2a-d** bearing an azide functional group, leading to the desired hybrid compounds **3a-d** (**Scheme 1**).

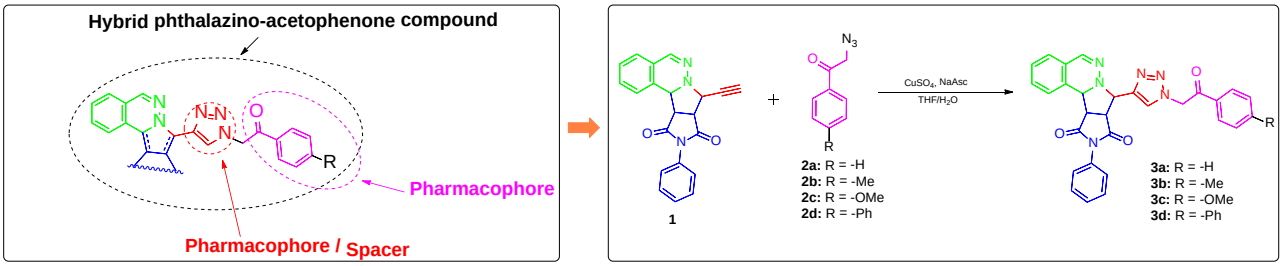

Scheme 1. Design and synthetic route of hybrid compounds 3a–d.

Results - Characterization

Table 1. Yields of the hybride compounds 6a-d.

Compound	Yield (%)	Reaction time (hours)
6a	62	6
6b	80	6
6c	82	6
6d	73	6

The structure of the newly synthesizes hybrid compounds were confirmed using: FT-IR and NMR (^{1}H, ^{13}C, 2D-correlations). In ^{1}H-NMR spectra, in the aliphatic region signals corresponding to the hydrogens from the tetrahydropyrrole ring are observed along with the signal corresponding to the methylene protons H_{24} (H_{24a} δ = 5.77 ppm, H_{24b} δ= 5.86 ppm). The most deshielded signals correspond to the hydrogens H_{27} (δ = 7.98 ppm), followed by the signal of the hydrogen H_{20} (δ = 7.85 ppm). In ^{13}C-NMR spectra, we observe in the aliphatic region the signals corresponding to the carbon atoms: C_{10}(δ = 49.4 ppm), C_{9}(δ = 50.85 ppm), C_{24}(δ = 55.4 ppm), C_{30}(δ = 55.8 ppm), C_{1}(δ = 59.5 ppm) and C_{11}(δ = 68.0 ppm). The most deshielded signals correspond to the carbon atom C_{25}(δ = 188.3 ppm), followed by the signals of the carbon atoms C_{14}(δ = 176.7 ppm) and C_{12} (δ = 174.7 ppm).

Conclusion and perspectives

Four new hybrid compounds containing a 1,2,3-triazole skeleton were synthesized in three steps, involving quaternization, cycloaddition, and click reactions. Structural confirmation of all newly synthesized hybrid compounds was carried out employing FT-IR and NMR (^{1}H-NMR, ^{13}C-NMR, 2D-correlation). Our aim is to test the new compounds regarding antitumoral activity, antimicrobial and antifungals properties.

References

[1] S. Zaib, I. Khan, *Bioorg. Chem.* 2020, 105, 104425.
[2] F.I. Zubkov, V.V. Kouznetsov, *Molecules* 2023, 28(1), 370.
[3] R. Rusu, A. Szumna, N. Rosu, C. Dumea, R. Danac, *Tetrahedron* 2015, 71-19, 2922-2926.

Acknowledgment: Acknowledgment is given to infrastructure support from (RECENT AIR) project, under grant agreement MySMIS no. 127324. Authors are also gratefully to CERNESIM center, for NMR experiments.

PP18. MODIFIED POLYHEDRAL OLIGOMERIC SILSESQUIOXANE: SYNTHESIS, CHARACTERIZATION AND POSSIBLE APPLICATIONS

Maria Medrihan[1]*, Bogdan-Constantin Condurache[1], Maria Ignat[1,2], Valeria Harabagiu[1]
[1]*Petru Poni Institute of Macromolecular Chemistry, Romanian Academy, Iasi, Romania*
[2]*Faculty of Chemistry, "Alexandru Ioan Cuza University of Iasi", Iasi, Romania*
**medrihan.maria@icmpp.ro*

All structures having the empirical formula $RSiO_{1.5}$, where R is hydrogen or any alkyl, alkylene, aryl, arylene, or organofunctional derivative of these groups, are referred to as silsesquioxane. As shown in **Scheme 1**, the silsesquioxanes form random structures, ladder, cage, and partial cage structures [1]. Because of their intriguing characteristics, including high physicochemical stability, porous character, low density, ease of preparation, low regeneration energy, and good thermal and chemical stabilities, the preparation of silsesquioxane oligomers has become a hot topic in both academic and industrial fields [2]. Light harvesting, chemical sensors, catalysis, iodine uptake, H_2 production from water, water treatment, optoelectronic devices [3], carbon dioxide reduction, nanofiltration, enantioseparation, energy storage, gas storage [4], and adsorption are just a few of the uses of these materials [5].

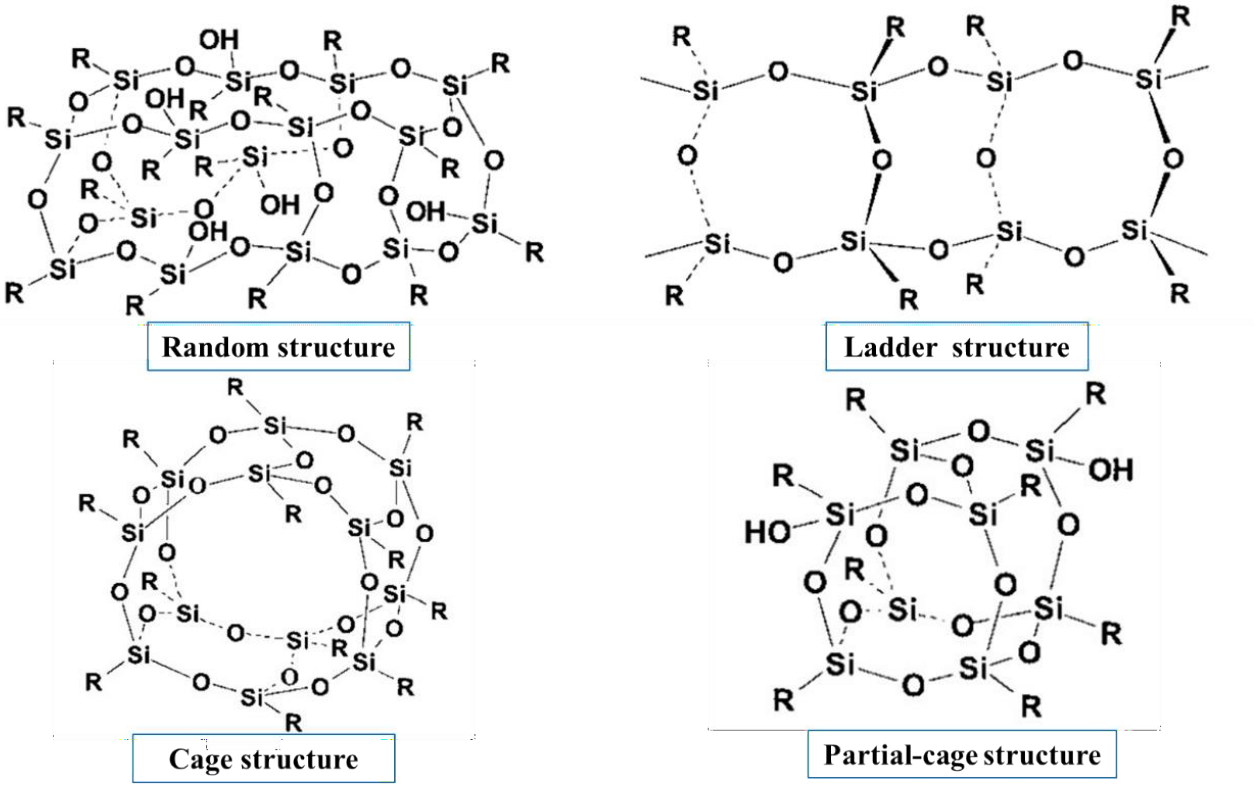

Scheme 1. Silsesquioxane usual structures [1].

The paper approaches the synthesis of a modified polyhedral oligomeric silsequioxane (POSS) and the characterization of the final product.

The synthesis consists of a two-step reaction, following the procedure described below:

1. First, octa (3-ammonium-propyl)POSS (OAPS) was prepared by reacting a mixture of (3- aminopropyl)triethoxysilane, methanol and concentrated hydrochloric acid into a flask equipped with a condenser and a magnetic stirrer, at 80°C, for 20 h, under vigorous stirring, using the refluxing method; after the reaction time has elapsed, the mixture was subjected for precipitation in THF and a white solid was obtained, then filtered and washed with cold methanol (yield of 41,5 %).
2. Secondly, the compound resulting in the first step was acylated with succinic anhydride to obtain the final product (octa-substituted carboxy-terminated POSS - OCPS). The reaction was performed in the presence of triethylamine, in methanol; the mixture was vigorously stirred at room temperature for 2 h. To afford a white powder, the solution was precipitated in $CHCl_3$, filtered, and washed with THF and $CHCl_3$ (yield of approximately 67 %).

The synthesized product was characterized by FTIR spectroscopy, SEM imaging with an integrated EDAX system, and ^{1}H-NMR technique. The SEM images reveal a compact morphology of the material that appears in different geometrical forms, as shown in **Figure 1**.

The resulting material`s characteristics recommend it for potential applications, such as catalysis, gas separation, and adsorption, which are considered for further investigations.

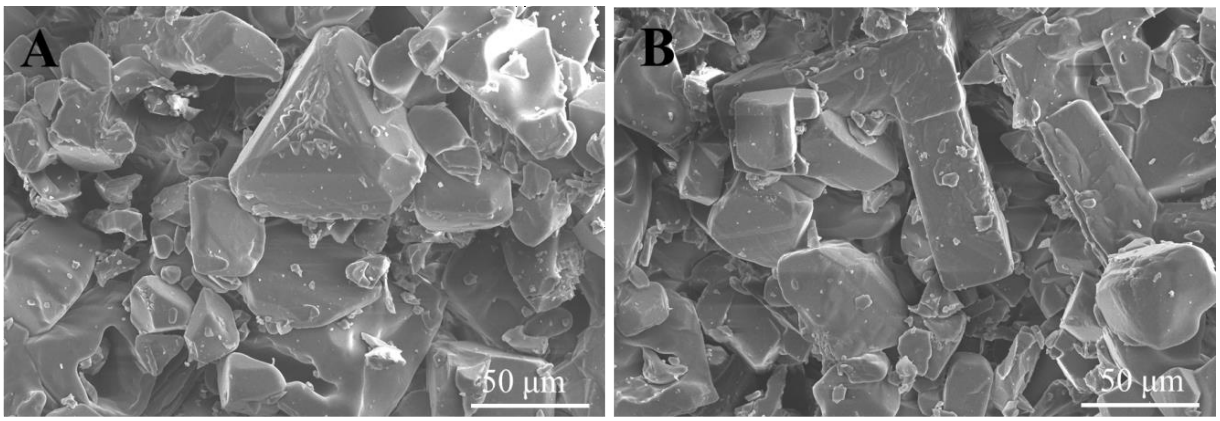

Figure 1. SEM images of OCPS (A and B).

References

[1] Z. Wen, X. Liu, W. Chen, R. Zhou, H. Wu, Y. Xia, L. Wu, *Polymers* 2024, 16, 846.
[2] M.G. Mohamed, M.-Y. Tsai, C.-F. Wang, C.-F. Huang, M. Danko, L. Dai, T. Chen, S.-W. Kuo, *Polymers*, 2021, 13(2), 221
[3] M.G. Mohamed, N.-Y. Liu, A.F.M. EL-Mahdy, S.-W. Kuo, *Microporous Mesoporous Mater.* 2021, 311, 110695.
[4] K. Cousins, R. Zhang, *Polymers* 2019, 11(4), 690.
[5] H. Furukawa, O.M. Yaghi, *J. Am. Chem. Soc.* 2009, 131(25), 8875–8883.

PP19. PREPARATION OF DEXTRAN–GUANOSINE–GOLD HYBRID MAGNETIC NANOPARTICLES AS SUBSTRATES FOR SURFACE-ENHANCED RAMAN SCATTERING

Tecla Dulgheriu*, Laura Ursu, Razvan Ghiarasim, Alexandru Rotaru, Mariana Pinteala
Petru Poni Institute of Macromolecular Chemistry, Romanian Academy, Iasi, Romania
**dulgheriu.tecla@icmpp.ro*

Magnetic nanoparticles have attracted significant attention in recent years due to their unique magnetic properties, biocompatibility, and versatility in biomedical and sensing applications [1]. To enhance stability and biocompatibility, polymer coatings such as dextran are commonly used [2]. Dextran provides a hydrophilic and biodegradable layer that improves colloidal stability and reduces cytotoxicity, while its abundant hydroxyl groups allow further functionalization with biomolecules or therapeutic agents [3].

The integration of magnetic nanoparticles with noble metals such as gold further enhances their functionality, enabling their use in plasmonic and surface-enhanced Raman scattering (SERS) platforms [4].

SERS has become a promising method for the detection of contaminants or biomolecules in aqueous media. [5] Magnetic nanoparticles functionalized with gold are capable of capturing target analytes, concentrating them locally, and generating specific electromagnetic hotspots, which collectively lead to significantly enhanced Raman signals. The low interference of water, the unique spectral fingerprint, and the development of portable and handheld equipment for *in situ* measurements contribute to the strong advantages of Raman-based techniques compared to other spectroscopic methods. Among the SERS nanoparticle substrates, those composed of plasmonic and magnetic components are prominent examples of versatility and efficiency [5,6].

Hybrid magnetic nanoparticles were synthesized by coating magnetite (Fe_3O_4) cores with dextran, [6] followed by functionalization with guanosine and benzene-1,4-diboronic acid in the presence of LiOH as base. Equimolar amounts of benzene-1,4-diboronic acid (a) and guanosine (b) were used to promote the formation of boronate ester linkages both with guanosine and the dextran shell, preventing exclusive binding to guanosine (**Figure 1**). Subsequently, the addition of $HAuCl_4$ led to gold deposition onto the functionalized nanoparticles. The deposition of gold resulted in a black coloration of the solution, indicating formation of branched gold nanoparticles [7].

The resulting hybrid materials were characterized by dynamic light scattering (DLS) for hydrodynamic size and colloidal stability, scanning electron microscopy (SEM) and scanning transmission electron microscopy (STEM) for morphological analysis, X-ray diffraction (XRD) for structural characterization, and UV-Vis spectroscopy to confirm the presence of gold and assess optical properties.

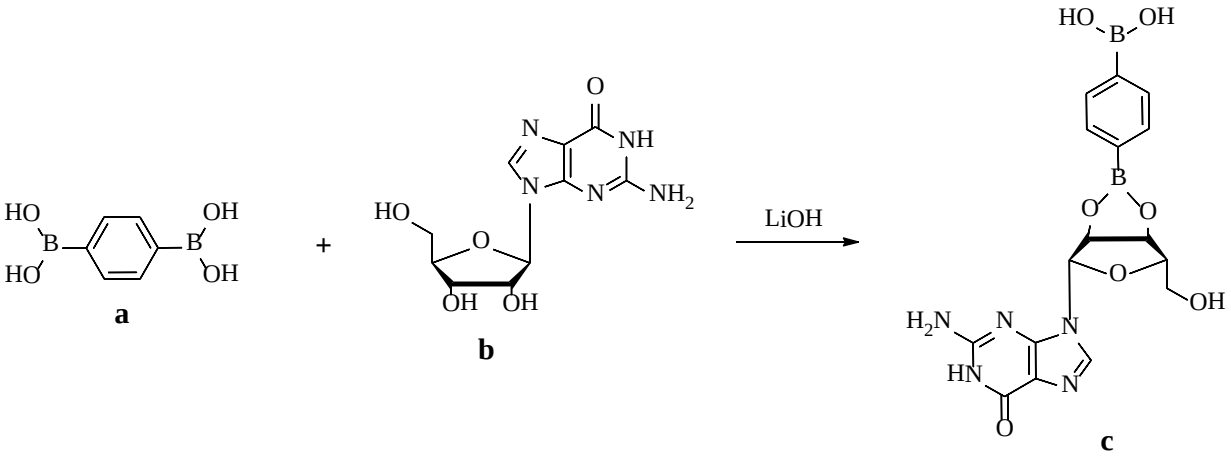

Figure 1. Synthesis of boronate ester (c) from benzene-1,4-diboronic acid (a) and guanosine (b) under basic conditions [8].

The results showed that the nanoparticles are relatively uniform, stable in suspension, and display clear plasmonic features, which suggests they could be promising candidates for SERS-based detection methods.

References:

[1] F. Bao, Yao, J.L. Yao, R.A. Gu, *Langmuir* 2009, 25(18), 10782–10787.
[2] L.B. Berganza, L. Litti, M. Meneghetti, S. Lanceros-Méndez, J. Reguera, *ACS omega* 2022, 7(49), 45493–45503.
[3] A.L. Rodriguez-Nieves, S. Shah, M.L. Taylor, M. Alle, X. Huang, *Nanomaterials* 2025, 15(4), 264.
[4] L.B. Berganza, L. Litti, M. Meneghetti, S. Lanceros-Méndez, J. Reguera, *ACS omega* 2022, 7(49), 45493–45503.
[5] D. Kim, Y. Zhang, J. Kehr, T. Klason, B. Bjelke, *J. Magn. Magn. Mater***.** 2001, 225, 256–261.
[6] S. Mornet, S. Vasseur, F. Grasset, E. Duguet, *J. Mater. Chem***.** 2004, 14, 2161–2175.
[7] K.H. Bae, M. Park, M.J. Do, T. Hyeon, *ACS Nano* 2012, 6, 5266–5273
[8] M.C. Sardaru, S. Morariu, O.E. Carp, E.L. Ursu, A. Rotaru, M. Barboiu, *Chem. Commun.* 2023, 59, 3134-3137

Acknowledgment:

This work was financially supported by a grant from the National Research Authority, project no. PNRR-III-C9-2023-I8-161, MultiPodGaN, contract no. 760285/27.03.2024, within the National Recovery and Resilience Plan.